UNIVERSITÉ DE TOURS

ÉCOLE DOCTORALE : « Santé, Sciences Biologiques et Chimie du Vivant »

ÉQUIPE de RECHERCHE : « EA6295 Nanomédicaments et Nanosondes »

THÈSE présentée par :

Iveta VILÍMOVÁ

soutenue le : **14 Décembre 2022**

pour obtenir le grade de : **Docteur de l'université de Tours**
Discipline/ Spécialité : Chimie

Développement de nanosondes pour la détection de miARN dans des fluides biologiques

THÈSE dirigée par :

Mme HERVÉ-AUBERT Katel	Maître de conférences, HDR, Université de Tours
M. CHOURPA Igor	Professeur, Université de Tours

RAPPORTEURS :

Mme MÉNAGER Christine	Professeur, Sorbonne Université
M. SANDRE Olivier	Directeur de recherche, Université de Bordeaux

---

JURY :

Mme HERVÉ-AUBERT Katel	Maître de conférences, HDR, Université de Tours
M. CHOURPA Igor	Professeur, Université de Tours
Mme MÉNAGER Christine	Professeur, Sorbonne Université
M. SANDRE Olivier	Directeur de recherche, Université de Bordeaux
M. LARTIGUE Lénaïc	Maître de conférences, Université de Nantes
Mme GOUILLEUX-GRUART Valérie	Maître de conférences, Praticien hospitalier, Université de Tours

MEMBRE INVITE :

M. RAOUL William	Chargé de recherche, Université de Tours

Acknowledgements - Poděkování

On these pages, it is my pleasure to thank everyone who kept me company during the last three years (in person or in your/mine thoughts). All of you remained firm in saying I can do it, (even when I doubted a lot), and without you, this all would be infinitely harder. I was lucky to have you on this journey with me, and I am grateful for your presence in my life.

So without further ado, I would like to express my deepest thanks to:

Igor Chourpa, the leader of the lab unit EA6295 Nanomédicaments at Nanosondes, who welcomed me to the team, and as my co-supervisor was always ready to give me advice and find time to discuss any problems, with empathetic and understanding everyday approach.

Katel Hervé-Aubert, my supervisor, who was always supportive and compassionate, and who is also one of the main reasons I persevered and, in the end, prevailed with this PhD effort. Thank you for always having an open door (literally) to answer my questions, and for being unwaveringly kind even when both of us were stressed up to our ears.

Stéphanie David, for sharing expertise in everything pertaining to the electrophoresis room;
Martin Soucé, for always being ready to help with and discuss the intricacies of HPLC;
And all the other members of the team; Emilie Munnier, Emilie Allard-Vannier, Frank Bonnier, Xavier Pers, Jean-François Fouquenet; who were always willing to answer questions or offer help.

Daiva, our daily chats ranging from musings about the weather, to complaints about the life of PhD were indispensable. It was a pleasure to share the office (and our everyday work life) with you, and I will miss our talks and walks.

Similarly, I can't forget the other people I shared the office with, who graciously helped me to settle into my new PhD life when I first arrived: Louise, who was always ready to have bueno with me, Sahar, with complete understanding for all my struggles and Vinh, with an unruffled attitude about absolutely everything.

And to other people from the lab, who it was always a pleasure to meet, in the corridors, in the lab, in the meeting room, and exchange commiserating and encouraging words: Hichem and Ayyoub, who were always ready to poke fun; Suha, with her calm patience; Yoann, and his gentle help not only with qRT-PCR; Malika, Emmanuel, Alaa, Amanda, Valentina, who all always found few minutes for idle chit-chat, and all the students that I met while they did

their internship in the lab and everyone else I forgot to mention (because despite my best efforts I probably did forget someone, and in that case, I apologize!).

To Karolína Šišková, the supervisor of my master thesis, who always patiently answered all my clueless questions and who set me on this French patch towards PhD. Díky Kájo!

I am glad I had the chance to work with all of you and learn from you. Thank you!

To my friends:

Valeria and Magda (and Herbie), for helping me survive the first year in Tours. I am incredibly happy I met you, and your company got me through the worst stages of settling in and starting to live in a completely different country. Vale, our walks made even the confinement pleasant, and Magda, our biking trips were always adventures. And funnily enough, your friendships gave me the strength to stay in Tours, even when you both didn't. I hope to see you soon!

Ana and Anton, for keeping me company in the arguably hellish third year, with beer, fun, food, and occasional Benedictine (and lately the updates about Nacho the kitten). You always cheered me up, even when I felt like a walking thundercloud.

Antoine, for our occasional walks and for detailed updates (and photos) of your puppy, whose fluffy, fluffy early stages brought me great joy.

Lucie, for the initial encouragement and matter-of-fact acceptance that I was really going off to study France, and all the support after.

Viktorie and Anežka, my friends from Olomouc studies, who I hope to see again soon at some point.

Radek and Veronika, for making my (very stressful) month pass even faster, by taking my mind off my worries and being always ready to chat and go for lunch or crepe together. It was great fun hearing the Czech language in the corridors of our French lab!

Fra, our almost daily exchanges about nothing important in particular, or about things that currently frustrated us the most were always a surefire way to make me smile and kept me going. You were my to-go person to complain or to share joy, and I appreciate you (and your hugs, when we see each other) very much. Looking forward to see where we go next! :)

All the best, Ivet

Tak, a teď v češtině: Je mi opravdovým potěšením na těchto stránkách poděkovat vám všem co jste mi v posledních třech letech dělali společnost, ať už osobně nebo jenom v myšlenkách (mých či vašich). Všichni jste (alespoň navenek :) nepochybovali že to zvládnu, (i když já jsem občas pochybovala hodně), a dodávali jste mi potřebnou sílu a motivaci to nevzdat (bez vás by tahle (třijazyčná) epika asi nevznikla). Jsem moc ráda že vás mám ve svém životě.

Děkuji vzdálenější rodině, sestřenicím, bratrancům, (zdravím malého pra-bratrance), tetám a strýcům které jsem za poslední roky nevídala moc často, protože nebylo úplně jednoduché najít datum kdy se potkat. Dědovi Zdeňkovi a babičce Míle, která ve mně malého vědce podporovala odmalička. Dědovi Joškovi a babičce Martě, za jejich nezřízený optimismus a dobrou náladu při našich telefonních hovorech (které byly občas překaženy kvůli těm zatraceným internetům), tetě Miri a strejdovi Petrovi za všeobecnou připravenost rozptýlit mé francouzské chmury.

Staršímu bratrovi: Honzi, pořád spolu nemluvíme zrovna často, nicméně si tvé (možná místy lehce potměšilé, protože sis tím sám prošel) podpory zpovzdálí cením taky. I když myslím, že o opičení už nemůže být řeč, uznávám, že jsi mi ukázal, že to jde: sebrat se, jít žít do zahraničí, a (u)dělat tam doktorát.

Rodičům: Mami, Tati, co si budeme vykládat, rozhodně bych se nedostala tak daleko bez vaší od malička neutuchající podpory a povzbuzení. Naše hovory jsou nejen příjemné rozptýlení a vzpruha, ale i něžná připomínka, že ono to nějak půjde. Nesmírně si vážím že jste tu pro mě vždy byli, i když jsem zrovna nacházela doslova tisíc mil daleko, a že jste mi vždycky poskytli útočiště a bezpečný přístav kam se vrátit. Děkuji.

- S láskou, Ivča

"Not all those who wander are lost – Ne každý, kdo bloudí, je ztracený."

-J.R.R. Tolkien

Résumé

Ces travaux de thèse de doctorat portent sur le « Développement de nanosondes pour la détection de miARN dans des fluides biologiques », décrivant la préparation de nanosondes magnétiques qui permettraient l'amélioration de la détection des miARN par n'importe quelle technique analytique. Les travaux sont organisés selon deux principaux objectifs: i) formulation et caractérisation de nanosondes conçues pour capter des miARN cibles: TmiR-155, un biomarqueur du cancer du sein et TmiR-484, un biomarqueur du cancer colorectal, et ii) validation des protocoles de capture médiée par les nanosondes de TmiR-484 dans des échantillons biologiques. Les nanosondes sont à base de nanoparticules d'oxyde de fer superparamagnétiques - SPIONs, avec une couche de polyéthylène glycol (PEG) liée de façon covalente et portant à leur extrémité un groupement biotine. Par l'utilisation de SPIONs PEGylées comme précurseur, les nanosondes ont été formulées en deux étapes: i) modification de la surface des SPIONs PEGylées avec de la streptavidine, et ii) fonctionnalisation avec une séquence de nucléotides biotinylés, CmiR-155 ou cDNA-484, qui sont complémentaires aux miRs cibles, TmiR-155 ou TmiR-484 respectivement. Le tri magnétique a été utilisé comme méthode de purification, séparant les nanosondes de divers milieux et permettant leur reconcentration. La stabilité colloïdale a été évaluée en mesurant leur diamètre hydrodynamique (DH) et leur potentiel zêta (ZP). La principale méthode d'analyse utilisée pour suivre les étapes de formulation et la concentration de miR greffé est la chromatographie liquide haute performance par exclusion de taille (SE HPLC). Le nombre estimé de séquences nucléotidiques greffées par nanosonde est de 22 pour CmiR-155 et de 17 pour l'ADNc-484. Les nanosondes résultantes ont une taille d'environ 70 nm et un ZP proche de la neutralité. Les nanosondes sont restées colloïdalement stables après incubation dans des échantillons de sérum humain pendant 12 heures. Les nanosondes ont été testées pour leur efficacité de capture des deux TmiR dans une solution modèle à différentes concentrations, et le TmiR-484 a également été capté dans des échantillons de sérum humain de volontaires adultes sains, résultats confirmés par une analyse qRT-PCR. Dans l'ensemble, le potentiel de capture des miARN cibles dans des échantillons biologiques encourage l'utilisation future des nanosondes pour améliorer la détection d'une expression dérégulée des miARN.

Mots clés: nanosondes, miARN, conjugaison, fonctionnalisation, isolation de miR, sérum humain

Abstract

This PhD thesis is focused on the "Development of nanoprobes for detection of miRNA in biofluids", addressing the sample preparation of magnetic nanoprobes that would enable the improvement of miRNA detection by any analytical technique. The work is organized following the two main objectives: i) formulation and characterization of nanoprobes designed to capture target miRNA, TmiR-155, a biomarker of breast cancer, and TmiR-484, a biomarker for colorectal cancer, and ii) validation of protocols for nanoprobes-mediated capture of TmiR-484 in biological samples. The nanoprobes were based on Superparamagnetic Iron Oxide Nanoparticles - SPIONs, with a shell of covalently bound polyethylene glycol (PEG) carrying biotin at the opposite terminal group. Using the PEGylated SPIONs as a precursor, the nanoprobes were formulated in two steps: i) surface modification of the PEGylated SPIONs with streptavidin, and ii) functionalization with a biotinylated nucleotide sequence, either CmiR-155 or cDNA-484, which are complementary to the target miR, TmiR-155 or TmiR-484 respectively. Magnetic sorting was used as a purification method, separating nanoprobes from various media and allowing their reconcentration. The colloidal stability was assessed by measuring their hydrodynamic diameter (D_H) and zeta potential (ZP). The main analytical method used for monitoring the formulation steps and the miR concentration was Size Exclusion High-Performance Liquid Chromatography (SE HPLC). The estimated number of nucleotide sequences grafted per nanoprobe was 22 for CmiR-155, and 17 for cDNA-484. The resulting nanoprobes had a size of about 70 nm and nearly neutral ZP. The nanoprobes remained colloidally stable after incubation in human serum samples for 12 hours. The nanoprobes were tested for their capture efficiency of both TmiRs in model solution at different concentrations, and TmiR-484 was also captured in human serum samples from healthy adult volunteers, which was confirmed by qRT-PCR analysis. Altogether, the potential to capture target miRNA in biological samples is encouraging the future use of nanoprobes to enhance the sensing of dysregulated levels of miRNA expression.

Keywords: nanoprobes, miRNA, conjugation, functionalization, miR isolation, human serum

Table of contents

Acknowledgements - Poděkování 2

Résumé 5

Abstract 6

Table of contents 7

Abbreviations 9

INTRODUCTION 10

1. miR biogenesis 10

2. MiRs as biomarkers 11

3. MiR and cancer 13

4. MiR in biofluids 14

4.1 Isolation of miR from biofluids 14

5. Established detection methods 15

6. Detection methods based on nanomaterials 17

6.1 Nanomaterials as detection platforms 18

6.2 Magnetic nanoparticles for miR sensing 19

OBJECTIVES OF THE THESIS 21

OBJECTIFS DE LA THESE 23

Literature 25

PART I - Development and characterization of nanoprobes 33

Publication 1: Formation of miRNA nanoprobes – conjugation approaches leading to the functionalization 34

Préambule de la Publication 1 35

Publication 2: Two-step formulation of magnetic nanoprobes for microRNA capture 52

Préambule de la Publication 2 53

Part II - Development of protocols for nanoprobe-mediated TmiR isolation from biological samples 64

Publication 3: Magnetic nanoprobes for miRNA-484 capture in human serum 65
Préambule de la Publication 3 66
GENERAL DISCUSSION 88
CONCLUSIONS AND PERSPECTIVES 95
CONCLUSIONS ET PERSPECTIVES 99
Literature 103
CURRICULUM VITAE 108

List of figures

Figure 1 – miR biogenesis 11
Figure 2 – Dysregulation of miR expression influencing the tumour development 12
Figure 3 – Schematic representation of possible approaches in TmiR sensing 17

Abbreviations

AAS	Atomic Absorption Spectrophotometry
BC	Breast cancer
CRC	Colorectal cancer
cDNA	Complementary DNA
CmiR	Complementary miR
Ct	Cycle threshold
DLS	Dynamic Light Scattering
DH	Hydrodynamic diameter
HS	Human serum
PEG	Polyethylene glycol
LPRS	Localized Surface Plasmon Resonance
miR, miRNA	microRNA
MNPs	Metal Oxide Nanoparticles
mRNA	messenger RNA
MS	Magnetic separation
NPR	Nanoprobes
NPs	Nanoparticles
PCR	Polymerase Chain Reaction
PDI	Polydispersity index
QDs	Quantum dots
qRT-PCR	Quantitative Reverse Transcription Polymerase Chain Reaction
RISC	RNA Inducing Silencing Complex
RT	Reverse Transcription
SE HPLC	Size Exclusion High-Performance Liquid Chromatography
SERS	Surface-enhanced Raman Scattering
siRNA	small interfering RNAs
SPIONs	Superparamagnetic Iron Oxide Nanoparticles
STR	Streptavidin
TmiR	target miR
tRNA	transfer RNA
XPS	X-ray photoelectron spectroscopy
ZP	Zeta potential

INTRODUCTION

A major part of human genome transcriptions consists of non-coding RNA molecules, which act as regulators of gene expression and protein function at both transcriptional and post-transcriptional levels in biological processes. Depending on the size of the transcription, non-coding RNAs can be categorized as long non-coding RNAs and small non-coding RNAs. Long non-coding RNAs have more than 200 nucleotides in length, and small non-coding RNAs are of various lengths while being shorter than 200 nucleotides, such as small interfering RNAs (siRNA), transfer RNA (tRNA), and microRNAs (miRNAs, miRs) [1].

MiRs are small, non-coding RNAs, with the length generally settled in the interval from 17 to 25 nucleotides. MiRs target specific mRNA (messenger RNA, carrying information to the ribosome from DNA) resulting in the regulation of post-transcriptional gene expression. Single miR can be bound to several targeted mRNAs while regulating their function, and vice versa single mRNA can be bound and targeted by several miRs. The differing complementarity between miRs and their mRNA targets influences the mechanisms of protein expressions [2]. The more common partial complementarity results in protein translational suppression or inhibition, and as such, in the human genome miRs are estimated to modulate up to 60% of protein-coding genes at the post-translational level [3].

1. miR biogenesis

Typically, miRNA genes are transcribed in the nucleus by RNA polymerase II or III (gene transcribing protein complexes) [4] as primary transcripts (pri-microRNAs, pri-miRs), usually with a length of several thousand nucleotides with local stem-loop structures, a poly-A tail (a long chain of adenine nucleotides) and a 5'-cap (an altered nucleotide at the end of primary transcript). Pri-miRs are then cleaved in the nucleus by the Drosha enzyme, resulting in precursor transcripts (pre-microRNA, pre-miR) with a length of approximately 70 nucleotides [5]. Afterwards, pre-miRs are transferred to the cytoplasm where the loops of pre-miR are cleaved by RNAse enzyme called Dicer [6], resulting in mature miR duplex of the length around 20 nucleotides, which then becomes a part of Argonaute protein

subfamily [7]. These are then incorporated into RNA Inducing Silencing Complex (RISC, multi-protein complex with one strand of either miRNA or siRNA) and the miR duplexes are separated by RNA helicases (enzymes capable of rearranging RNA structure) [8]. MiR strands then either remain attached to RISC or degrade, and the mature miR in the RISC can be bound to the 3' untranslated region (3'UTR, a section of mRNA after nucleotide triplet which signals the end of the translation) of the target mRNA, causing either translational repression or degradation of mRNA [9] (Figure1).

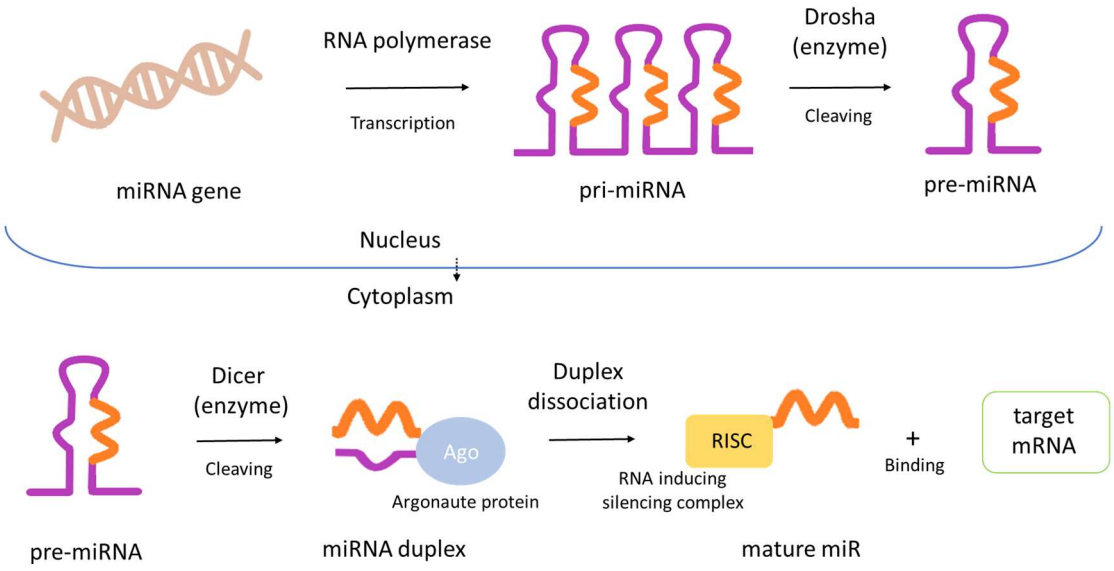

Figure 1 – MiR biogenesis. Transcription in the nucleus by RNA polymerase into pri-miRNA, which is processed by the Drosha enzyme into pre-miRNA, which is transferred to the cytoplasm to be cleaved by the Dicer enzyme. The generated duplex of RNA is attached to the argonaute protein, and becomes a part of the RNA Inducing Silencing Complex, where the duplex is separated by RNA helicases into two single-stranded miRs, a mature strand that remains bound to the RISC complex and a passenger strand that degrades. The mature miR binds with the target messenger RNA.

2. MiRs as biomarkers

The first example of mature miR was the identification of two small RNA transcript products of the lin-4 gene in the nematode (roundworm) Caenorhabditis elegans. Since the

initial discovery in 1993 [10], more than 2600 miRs sequences have been published and identified in the human genome [11] and various other organisms [12]. MiRs play a crucial role in assorted biological processes, such as metabolism, organ development, embryogenesis, apoptosis, homeostasis, and more. On that account, the field of miR biology is rapidly evolving, and miRs are currently being developed as novel biomarkers for therapeutics and diagnostics of many diseases [13,14].

Dysregulated expression levels of miRs can be detected in viral infections, neurological disorders, muscle degenerative diseases, cardiovascular disorders, diabetes, and cancer. In each disease, the expression levels of multiple miRs are either decreased or increased, varying more or less significantly in comparison to healthy tissue. This can be similarly detected during the progress of the disease, although in some cases the difference of expression can be very small. Thus, the low miR detection limits of the methods are crucial, since the detection of miRs in bodyfluids can be affected by the presence of other interfering biomolecules, high viscosity, and pH influence, in addition to the overall low quantity of target miRs [13,15].

The related research is in larger part focused on different types of cancer, as the miRs play a major role in cellular processes, and their atypical expression often leads to the onset, development, and metastasis of cancer. From their altered expression, miRs can be described as oncogenes or tumour suppressors [16]. Oncogenic miRs are present with increased expression in cancer cells, inhibiting tumour suppressor genes and leading to malignancy and tumour genesis. Inversely, tumour-suppressing miRs down-regulate the expression of oncogenes (Figure 2). The disrupted balance between these two types of miRs, namely their respective down-regulation and up-regulation, influences various cellular processes leading to cancer development, such as replicative immortality, anti-apoptotic response, angiogenesis, and more [9].

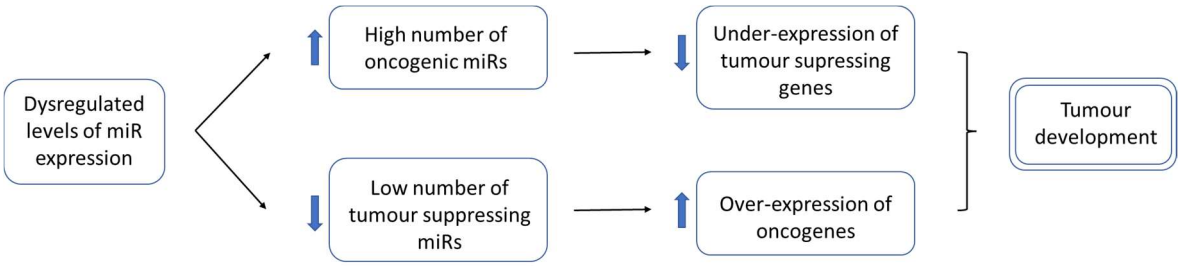

Figure 2 – Dysregulation of miR expression influencing the tumour development.

3. MiR and cancer

The first suggestion of the role of miR in cancer progression was shown in 2002 when a cluster of miR-15 and miR-16 was detected in the genomic region which is frequently deleted in chronic lymphocytic leukemia [17]. Since then, miRs have been linked to numerous pathologies and the majority of all known cancers. As previously mentioned, miRs can function as either oncogenic miRs or tumour-suppressing miRs, depending on their target gene. Similarly, alterations in genes responsible for cancer progression are also linked to miR dysregulation [18].

Many miR profiling studies have been performed over the years, noting the differences of miR expression through the state of health to the late stage of the disease [19]. MiR-21 is one of the most predominantly upregulated in various cancers, affecting cell reproduction (proliferation), apoptosis, and angiogenesis, all of which lead to the origin and progress of cancer. However, its over-expression is not specific to one particular disease, which makes it inconvenient for a biomarker function [20]. MiR-9, abundantly found in the brain, was confirmed to target protein-coding genes directly in glioma cells [21]. The same miR-9 was found to be down-regulated in oral cancer [22].

Breast cancer (BC), a complex and heterogeneous disease, is the most common cancer globally diagnosed. The malignancy occurs upon disruption or dysregulation of cellular and molecular signalling pathways in mammary cells [23]. Numerous miRs have been identified in BC, both tumour-suppressors such as miR-16 [24] and miR-497 [25], or oncogenic miRs like miR-130b [26] and miR-1297 [27], are only a couple of examples out of many [9]. Often mentioned regarding BC is miR-155, noted to be over-expressed in breast cancer cells, resulting in genomic instability and fragility of telomere (ending part of a chromosome) [28].

Lung cancer is the second most common cancer, one with the highest morbidity. The most investigated miRs among a wide spectrum of others [29] are for example miR-34 [30], and miR-145 [31], both of which target signalling pathways of EGFR (epidermal growth factor receptor).

The third most common is colorectal cancer (CRC), exceedingly problematic particularly due to its largely asymptomatic progression which delays the crucial early diagnosis and treatment [32]. There is an abundance of miR sequences connected to CRC [33], such as miR-92a, an oncogenic miR promoting tumour growth [34] and showing increased levels in exosomes in the early stages of CRC [35]. Similarly, miR-484 was

determined to be closely related to the development of CRC and had shown notably increased levels in the later stages of CRC [36].

Altogether, the assessment of miRs as cancer biomarkers is an ongoing effort, both to identify and validate the expression of chosen miR. Connected to that is the issue with a large variety of miR sequences with small differences and at times opposing expression levels depending on the stage of the disease. Similarly, plenty of the same miRs are observed in different diseases, creating overlap that is necessary to untangle in the interest of the highest accuracy required for cancer diagnosis.

4. MiR in biofluids

MiRs remain stable in microparticles (microvesicles, apoptotic bodies, exosomes), but most importantly they are present in circulating cell-free form in biofluids such as saliva, tears, urine, and blood, more specifically plasma and serum [13,37]. Body fluids are accessible through non-invasive (urine, sweat, tears, vaginal secret, menstruation blood, etc.) or invasive means (whole blood, plasma, serum, cerebrospinal fluid, etc.), both of which are less stressful for the body than biopsies and support repeated acquisition for follow-up studies [15].

Free miRNAs are released by cells through exosomes or extracellular vesicles with various other molecules, such as proteins and RNA. Generally, miRs are associated with RNA-binding proteins, which lend them stability in body fluids [38].

The expression of miRs in various body fluids varies not only according to the type of the disease and its stage but is also dependent on the specific aspects related to the patient like diet, medications, and age. Additionally, the correlation of miR levels differs across respective body fluids, showing higher levels in one body fluid while significantly lower amounts are present in the other [39].

4.1 Isolation of miR from biofluids

For most of the established detection methods, it is necessary to isolate miR from body fluid samples. This presents an interesting challenge due to the overall small amount of miRs in body fluids, and the presence of various proteins (such as lipoproteins and RNA-protein complexes) and other inhibiting agents which cause interference in the isolation process. Similarly, hemolysis (destruction of red blood cells) and cell residue may influence

the yield from blood samples and subsequently from plasma and serum [40,41]. Commercially available kits are generally used, specializing in the miR extraction from respective sample types. However, different extraction kits often yield different results, influencing the yield and the reproducibility [42].

5. Established detection methods

To this day, the methods generally used for miRNA analysis are microarrays, next-generation sequencing, Northern blotting, in-situ hybridization, and quantitative reverse transcription Polymerase Chain Reaction (qRT-PCR). These current detection methods analyse the comparison of the miR expression profiles in the healthy state and at the stage of disease [43]. The distinction between the methods can be made depending on the range of their detection. A screening assay for the identification of a large spectrum of dysregulated miRs can be done by microarray assays or next-generation sequencing. Microarray assays allow comprehensive profiling of target genes of differentially expressed miRs [44], while having the disadvantage of low consistency between the differential expressions, along with low specificity, sensitivity, and reproducibility [45]. Next-generation sequencing is generally used for analysis and classification using sequencing libraries allowing the sift through a considerable part of genetic information [46]. However, the data analysis is complex and requires specialized equipment, along with the disadvantage of high cost and long processing time [47]. Both of these methods are often combined with qRT-PCR for a more precise confirmation [48,49].

Conversely, other methods are focused on the detection of known individual miR and their expression and regulation. One such method is Northern blot, based on gel electrophoresis and molecular hybridization, leading to size-selective separation of miR [11,50]. However, it is not possible to distinguish miRs with different sequences and the same molecular weight [47]. In-situ hybridization allows the visualization of the target sequence directly in tissues and cell lines [51]. The target DNA or RNA sequences are visualized with specific (usually commercial) probes (either fluorescent or chromogen, based on the same principle), but the consistency of this method is poor for low levels of miR expression [52].

The arguably most common method is qRT-PCR, a well-established method for miR analysis. Target miR is transformed into complementary DNA (cDNA) in reverse

transcription (RT), which is used as a template for amplification in a polymerase chain reaction (PCR). The linear amplification of the starting cDNA results in a fluorescence signal which can be quantified and monitored in real-time [53]. The reverse transcription can be universal, by adding either polyA tails or both polyA tails and 5′ adapter sequence and to 3′ end of miR, in both cases followed by reverse transcription with a poly T primer with a universal sequence (Tag) appended at the 3′ end. The addition of polyA tails enhances the cost-effectivity and is advantageous for the analysis of different miRs in a small initial amount of material, however, the differentiation between pre-miRNAs is not achievable. The other possibility is a case of specific reverse transcription, which can be done by miR-specific stem-loop primer, followed by qPCR with a miR-specific probe. While more expensive, this approach can help with the differentiation between pri-miRNA, pre-miRNA, and mature miR [54]. The quantification of miR with qRT-PCR can be divided into absolute and relative approaches; absolute quantification uses a calibration curve generated during the analysis from known standards (such as plasmids, synthetic miRNA, etc.). The relative quantification compares measured levels of miR which are normalized to a reference gene with known expression levels. While relative quantification is considered more reliable, the choice of the reference gene must be independently validated [53]. The variations in qRT-PCR analysis can be caused by deviation in the extraction of miR [55], slight differences in the chosen fluorophore such as SYBR green [56] (that emits stronger fluorescence signal in direct proportion to the amount of double-stranded DNA present in the sample), and the qRT-PCR instrument itself [57].

Overall, none of these methods is void of limitations – the major ones being low selectivity, imperfect reproducibility, inadequate sensitivity, and interferences caused by cross-hybridization. Connected to that are requirements for expensive instruments, specialized skills, time-consuming steps, and in some cases a large amount of sample is necessary. There are varying limits of detection sensitivity, and the theoretical capability of detecting single RNA molecules is not always accomplished in reality [47]. For successful assays, the required quantity of genetic material is typically in the range from hundreds of nanograms (qRT-PCR) to micrograms (Northern blotting), with a need for purification of miRNA along with its conversion to complementary DNA for amplification by polymerase reactions. For methods based on exponential amplification (qRT-PCR), the errors of detection are also amplified, posing a challenge along with possible contamination and false positives [13].

6. Detection methods based on nanomaterials

Detection methods based on nanomaterials (or on nanotechnologies in general) present a path for a more straightforward detection process. Many of these methods are based on signal amplifications (electro-chemical, fluorescent, colorimetric, etc.); such as exponential amplification [58], target recycling amplification, enzyme-based [59] and enzyme-free [60] amplifications, catalytic hairpin assembly reaction [61], strand displacement and hybridization cascade amplification [62], etc. The overall advantage of these approaches would be the possibility of a direct (in-situ) detection in the solution and the avoidance of the complicated extraction process to obtain miR from biofluids, which is necessary for established methods such as qRT-PCR, Northern blot, and others (Figure 3).

However, even though reported limits of detection can reach very low levels in the model solutions, the detection directly in the biofluid is challenging due to the presence of other biomolecules, varying viscosity, and pH. Because of the relative novelty of nanomaterial-based methods, there are many questions left to answer regarding the standardization, optimization, and normalization of such methods, followed by their reproducibility and data processing. Oftentimes, it is possible to combine nanomaterial-based detection with conventional methods like qRT-PCR, both in the interest of verification and possible enhancement [63].

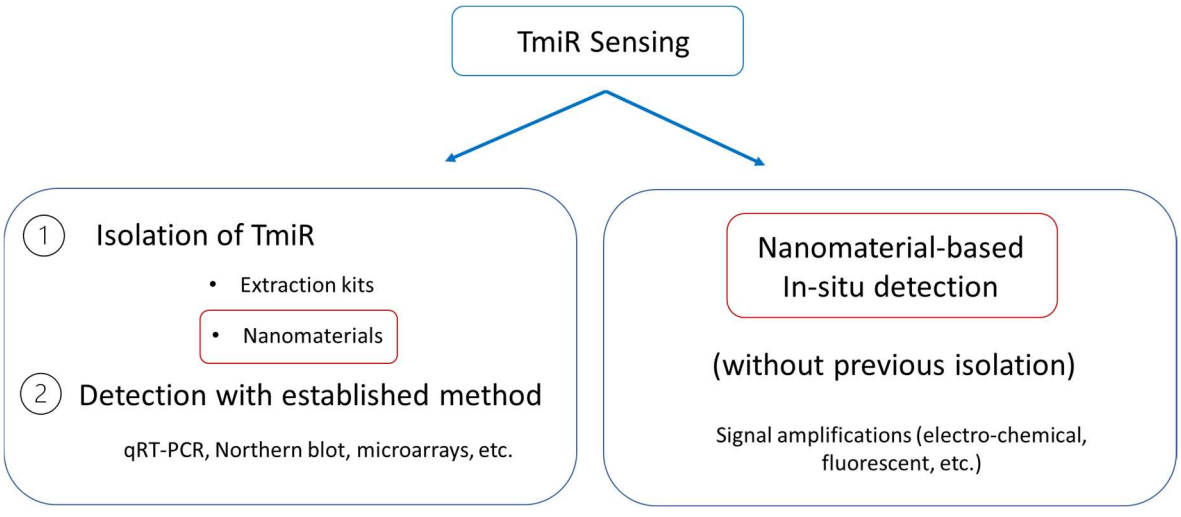

Figure 3 – Schematic representation of possible approaches in TmiR sensing.

6.1 Nanomaterials as detection platforms

Nanomaterials can be characterized by various attributes: size (the interval generally agreed on is from 1 to 100 nm), shape (e.g., sphere, wire, rod, cube, star, etc.), material (e.g., metal, semiconductor, dielectric, etc.), form (e.g., colloidal suspensions, fixed nanostructures, etc.) and configuration (the manner of combining the different materials). Due to their minuscule size, inorganic nanomaterials differ in properties from their corresponding counterparts in bulk [64,65].

The most well-known and employable of these properties are the high surface energy and surface-to-volume ratio, the tunable optical (absorption/emission, photothermal conversion), and magnetic (superparamagnetism, magnetic hyperthermia) properties. High surface energy makes nanomaterials (particularly in the form of colloidal suspension) predisposed to be coated with organic shells, but also can lead to their aggregation and precipitation and thus calls for electrostatic and/or steric stabilization. A high surface-area-to-volume ratio means a large number of surface atoms are available for reaction, offering higher catalytic activity. Magnetic and optical properties, along with biocompatibility, vary depending on the material, the size, and the surface state [64,66].

Due to the inorganic material confinement within a small volume, the iron oxide nanoparticles below 20 nm are superparamagnetic (SPIONs) [67], while gold nanoparticles (AuNPs) and semiconductor nanoparticles (quantum dots, QDs) of size comprised within the range of 2-10 nm are luminescent, with emission wavelength being correlated to their size [68,69]. In addition, noble metal NPs (Au, Ag) exhibit the plasmonic effect (plasmons being collective oscillations of surface electrons) and their interaction with the light of resonant wavelength depends not only on their size but also on their surface state [70]. The surface state can be affected by the NP interaction with other particles (aggregation, assembly) and/or with organic molecules (coating) [71,72]. As a result, one observes the plasmonic absorption bands (called localized surface plasmon resonance, LSPR bands) for which the maxima are occurring in a wide range of the spectrum, from visible to near-infrared (NIR) [62,73].

Undoubtedly, the development of a method and protocol which would allow the capture and the detection of target miR is crucial to obtain a working mechanism for disease diagnosis. With all their properties, nanomaterials have been explored in recent years for miR sensing and have become prime tools in related research. Quite often, two or more types of nanomaterial can be combined in an effort to bring together several of their advantageous

properties, such as fluorescence and magnetism. In the case of miR detection (and overall nucleic acid detection), nanomaterials are generally functionalized with oligonucleotides complementary to the target sequence. The presence of target miR can be for example detected by the occurrence and amplification of a binding event [74].

Nanoparticles (NPs) in particular exhibit advantageous qualities for surface modification and functionalization, presenting plenty of active chemical groups on their surface (such as hydroxyl groups on metal oxide NPs). Since most miR sensing strategies are based on forming a heteroduplex between the target miR and a complementary sequence of oligonucleotides, choosing the conjugation approach for the functionalization with the complementary sequence is a fundamental step. While selecting the conjugation variant, it is good to keep in mind the available reactive groups on the surface of the nanomaterial and the conjugated ligand, the chemical and mechanical stability of the final product, and the simplicity of the procedure.

6.2 Magnetic nanoparticles for miR sensing

Regarding magnetic nanomaterials and NPs, metal oxide NPs (MNPs) are easily the most popular in the research, with coprecipitation being a widely used method of synthesis. The metal precursors (for instance Fe^{2+} and Fe^{3+} chlorides) are dissolved in an acidic solution, followed by the addition of a strong base. This results in a large amount of MNPs dispersed in the aqueous medium. To control morphology and size distribution on MNPs, the attention is focused on optimizing and improving the synthesis [75,76].

To take advantage of additional beneficial properties, MNPs can be combined with noble metal (Au, Ag) NPs. As such, various composites with MNPs were documented: magnetic core-shell Fe_3O_4−AuNPs modified with peptide nucleic acids and used for miR-21 detection [77]; DNA-modified monodisperse iron oxide NPs with the amount of target miR-149 determined by measurement of the fluorescent intensity of fluorescent spots [59]; Fe_3O_4 NPs coated with polydopamine in combination with carbon dots for miR-167 fluorescence determination [78]; core-shell Au-Ag NPs attached to Fe_3O_4-SiO_2 MNPs for SERS detection of miR-21 [79] and many others [15].

NPs with strong magnetic signals can easily aggregate, while superparamagnetic NPs are colloidally stable, with a slower magnetic response. The solution to the challenge of obtaining a stronger magnetic signal while attaining colloidal stability was proposed by

coating multiple small superparamagnetic NPs with silica, creating a conglomerate that is possible to coat with Au shell, for detection of miR-21 [80].

Concerning the detection from biofluids, using MNPs offers an incentive for fast sensitive, and selective extraction of targeted TmiR, however, only a small number of studies focused on detection in complex media full of interfering biomolecules. The most commonly investigated body fluids are urine [81], blood [82], and serum [83].

Overall, miR detection with MNPs is a varied field, with many diverse approaches. Current challenges lie mainly in the demonstration of the capture and detection ability not only in model solutions but most importantly in real biological samples.

OBJECTIVES OF THE THESIS

This thesis is focused on the "Development of nanoprobes for detection of miRNA in biofluids". In this work, we describe a protocol for the generation of magnetic nanoprobes which can capture chosen target miR (TmiR) and we demonstrate their capture ability both in model solutions and in a biofluid.

The nanoprobes have a core of Superparamagnetic Iron Oxide Nanoparticles (SPIONs), an optimized nano-platform previously established by our team [84]. SPIONs are usually in the form of colloidally stable aqueous suspensions called ferrofluids and are already commonly utilized in biomedical applications [85]. The surface of the SPIONs is first silanized with 3-aminopropyltrimethoxysilane (APS), then PEGylated with NHS-PEG_{5000}-biotin. The attachment of hydrophilic PEG chains to the surface of SPIONs improves their colloidal stability in aqueous media of neutral pH due to the steric hindrance. Biotin moiety at the end of the PEG chain provides a high affinity for binding with the protein streptavidin. Using PEGylated SPIONs (NP) as nanoprobe precursors, the nanoprobes are formulated in two steps: surface modification with streptavidin (NP-STR) and subsequent functionalization with the sequence of oligonucleotides complimentary to the TmiR. Two complementary sequences of nucleotides were studied here, of RNA (Complementary miR – CmiR) or DNA nature (complementary DNA – cDNA). The final nanoprobes were thus in the form of NP-STR-CmiR for targeting miR-155 or NP-STR-cDNA for targeting miR-484. The TmiR-155 is considered over-expressed in breast cancer [9,28], shaping it as a possible biomarker for early detection in pathology. TmiR-484 is dysregulated in colorectal cancer, where the levels of TmiR-484 in human serum are lower in the early stage of the disease and over-expressed in advanced stages [86].

The objectives of the thesis were the following: i) Development and characterization of the nanoprobes, and ii) Development of protocols for nanoprobe-mediated TmiR isolation from biological samples.

The first objective of the development of nanoprobes using streptavidin-biotin interactions included both the two-step formulation and its quantitative monitoring with Size-Exclusion High-Performance Liquid Chromatography (SE HPLC). The colloidal stability of the developed NP-STR-CmiR-155 and NP-STR-cDNA-484 was studied first in the model solution of PBS 1X and then in the serum. The functionalized nanoprobes were

able to capture their intended TmiRs with sufficient efficiency in the model solution, leading to their use in biofluids.

The second objective was reached with nanoprobes NP-STR-cDNA-484 which were first incubated in human serum (HS, from 3 healthy patients) and then isolated from the HS by magnetic sorting. The miR levels in HS samples before and after their incubation with NPs were measured with qRT-PCR, allowing to differentiate even between very low concentrations of TmiR.

Following the **General introduction** and the chapter **Objectives of the thesis**, this work is presented in two parts:

- **Part I – Development and characterization of nanoprobes.** This part is set forth with a review focused on the most common conjugation approaches used in the formulation of miRNA nanoprobes, explaining both the choice of the nanomaterial and the advantages and disadvantages present in respective conjugation approaches leading to functionalization. Following is the first experimental article, detailing the protocol for the formulation of nanoprobes with close monitoring of the process, their characterization, stability, and capture ability of TmiR-155.
- **Part II – Development of protocols for nanoprobe-mediated TmiR isolation from HS**. The second experimental article is focused on the formulation and application of nanoprobes for the isolation of TmiR-484 in combination with the qRT-PCR analysis.

Afterwards, the implications and significance of the results are discussed in the **General discussion**, followed by the **Conclusions and perspectives**.

OBJECTIFS DE LA THESE

Cette thèse porte sur le « Développement de nanosondes pour la détection de miARN dans des fluides biologiques». Dans ce travail, nous décrivons, dans un premier temps, un protocole de génération de nanosondes magnétiques capables de capturer des miRs cibles (TmiR). Puis, dans un second temps, les capacités de capture de ces nanosondes sont démontrées à la fois dans des solutions modèles et dans des fluides biologiques.

Les nanosondes ont un cœur de nanoparticules d'oxyde de fer superparamagnétiques (SPIONs), une nano-plateforme optimisée précédemment développée par notre équipe [84]. Les SPIONs se présentent généralement sous la forme d'une suspension aqueuse colloïdalement stable appelée ferrofluide, et sont déjà couramment utilisées dans des applications biomédicales [85]. La surface des SPIONs est d'abord silanisée avec du 3-aminopropyltriméthoxysilane (APS), puis PEGylée avec du NHS –PEG_{5000} –biotine. Le greffage des chaînes PEG hydrophiles à la surface des SPIONs améliore leur stabilité colloïdale en milieu physiologique en raison de l'encombrement stérique. Les groupements biotines à l'extrémité de la chaîne PEG, fournit une haute affinité pour la liaison avec la protéine streptavidine. En utilisant des SPIONs PEGylées (NP) comme précurseurs, les nanosondes sont formulées en deux étapes : modification de surface avec de la streptavidine (NP-STR) et fonctionnalisation ultérieure avec la séquence d'oligonucléotides complémentaires au TmiR. Deux séquences complémentaires de nucléotides ont ici été étudiées, de nature ARN (Complementary miR – CmiR) ou de nature ADN (Complementary DNA – cDNA). Les nanosondes finales se présentent ainsi sous la forme de NP-STR-CmiR pour cibler miR-155 ou NP-STR-cDNA pour cibler miR-484. Le TmiR-155 est connu pour être surexprimé dans les cancers du sein [9,28], ce qui en fait un biomarqueur possible pour une détection précoce de la pathologie. Le TmiR-484 est, quant à lui, dérégulé dans le cancer colorectal, où les taux de TmiR-484, dans le sérum humain sont plus faibles au stade précoce de la maladie et surexprimés aux stades avancés [86].

Les objectifs de la thèse étaient les suivants : i) développement et caractérisation des nanosondes, et ii) développement de protocoles pour l'isolement de TmiR à l'aide de nanosondes à partir d'échantillons biologiques.

Le premier objectif du développement de nanosondes utilisant des interactions streptavidine-biotine comprenait à la fois la formulation en deux étapes et son suivi quantitatif par chromatographie liquide à haute performance par exclusion de taille (SE HPLC). La stabilité colloïdale des NP-STR-CmiR-155 et NP-STR-cDNA-484 a d'abord été étudiée dans des solutions modèles de PBS 1X puis dans du sérum. Les nanosondes fonctionnalisées ont pu capturer les TmiR choisis avec une efficacité suffisante dans des solutions modèles, conduisant à leur utilisation dans des fluides biologiques.

Le deuxième objectif a été atteint avec les NP-STR-cDNA-484 qui ont d'abord été incubés dans du sérum humain (HS, de 3 patients sains), puis isolés du HS par tri magnétique. Les niveaux de miR dans les échantillons sériques, avant et après leur incubation avec des nanosondes, ont été mesurés par qRT-PCR, technique capable de différencier de très faibles concentrations de TmiR.

Suite à l'**Introduction générale** et aux **Objectifs de la thèse**, ce travail est présenté en deux parties:

- **Partie I** – **Développement et caractérisation des nanosondes**. Cette partie débute par une revue axée sur les approches de conjugaison les plus utilisées dans la formulation de nanosondes miARN, en expliquant à la fois le choix du nanomatériau et les avantages et inconvénients présents dans les approches de conjugaison respectives conduisant à la fonctionnalisation. Ensuite, le premier article expérimental est présenté. Cet article détaille le protocole de formulation des nanosondes avec le suivi analytique du procédé, leur caractérisation, leur stabilité et leur capacité de capture du TmiR-155.
- **Partie II** - **Développement de protocoles pour isoler des TmiR du sérum humain à l'aide des nanosondes**. Le deuxième article expérimental est axé sur la formulation et l'application des nanosondes pour l'isolement et la quantification du TmiR-484 en combinaison avec l'analyse qRT-PCR.

Ensuite, les implications et la signification des résultats sont présentées dans la **Discussion générale**, suivie de la **Conclusion** et des **perspectives** de ce travail de thèse.

Literature

1. Masud, M.K.; Umer, M.; Hossain, M.S.A.; Yamauchi, Y.; Nguyen, N.T.; Shiddiky, M.J.A. Nanoarchitecture Frameworks for Electrochemical MiRNA Detection. *Trends Biochem. Sci.* **2019**, *44*, 433–452, doi:10.1016/j.tibs.2018.11.012.

2. Wightman, F.F.; Giono, L.E.; Fededa, J.P.; Mata, M. De Target RNAs Strike Back on MicroRNAs. *Front. Genet.* **2018**, *9*, 1–21, doi:10.3389/fgene.2018.00435.

3. Catalanotto, C.; Cogoni, C.; Zardo, G. MicroRNA in Control of Gene Expression : An Overview of Nuclear Functions. *Int. J. Mol. Sci. Rev.* **2016**, *17*, doi:10.3390/ijms17101712.

4. Arimbasseri, A.G.; Rijal, K.; Maraia, R.J. Comparative Overview of RNA Polymerase II and III Transcription Cycles , with Focus on RNA Polymerase III Termination and Reinitiation. *Landes Biosci.* **2013**, 1–13, doi:http://dx.doi.org/10.4161/trns.27369.

5. Schanen, B.C.; Li, X. Transcriptional Regulation of Mammalian MiRNA Genes. *Genomics* **2012**, *97*, 1–6, doi:10.1016/j.ygeno.2010.10.005.Transcriptional.

6. Pong, S.K.; Gullerova, M. Noncanonical Functions of MicroRNA Pathway Enzymes – Drosha , DGCR8 , Dicer and Ago Proteins. *FEBS Lett.* **2018**, *592*, 2973–2986, doi:10.1002/1873-3468.13196.

7. Yang, J.; Cho, W.C.; Zheng, Y. Argonaute Proteins : Structural Features , Functions and Emerging Roles. *J. Adv. Res.* **2020**, *24*, 317–324, doi:10.1016/j.jare.2020.04.017.

8. Owttrim, G.W.; Rna, K. Diverse Roles in Prokaryotic Response to Abiotic Stress RNA Helicases. *Landes Biosci.* **2013**, *10*, 96–110, doi:http://dx.doi.org/10.4161/rna.22638.

9. Loh, H.-Y.; Norman, B.P.; Lai, K.-S.; Rahman, N.M.A.N.A.; Alitheen, N.B.M.; Osman, M.A. The Regulatory Role of MicroRNAs in Breast Cancer. *Int. J. Mol. Sci.* **2019**, *20*, 4940, doi:10.3390/ijms20194940.

10. Lee, R.C. The C . Elegans Heterochronic Gene Lin-4 Encodes Small RNAs with Antisense Complementarity to & II-14. *Cell* **1993**, *75*, 843–854, doi:10.1016/0092-8674(93)90529-y.

11. Alles, J.; Fehlmann, T.; Fischer, U.; Backes, C.; Galata, V.; Minet, M.; Hart, M.; Abu-Halima, M.; Grässer, F.A.; Lenhof, H.P.; et al. An Estimate of the Total Number of True Human MiRNAs. *Nucleic Acids Res.* **2019**, *47*, 3353–3364, doi:10.1093/nar/gkz097.

12. Kozomara, A.; Birgaoanu, M.; Griffiths-jones, S. MiRBase : From MicroRNA Sequences to Function. *Nucleic Acid Res.* **2019**, *47*, 155–162, doi:10.1093/nar/gky1141.

13. Chandrasekaran, A.R.; Punnoose, J.A.; Zhou, L.; Dey, P.; Dey, B.K.; Halvorsen, K. DNA Nanotechnology Approaches for MicroRNA Detection and Diagnosis. *Nucleic Acids Res.* **2019**, 1–17, doi:10.1093/nar/gkz580.

14. Lo, P.K.; Wolfson, B.; Zhou, X.; Duru, N.; Gernapudi, R.; Zhou, Q. Noncoding RNAs in Breast Cancer. *Brief. Funct. Genomics* **2016**, *15*, 200–221, doi:10.1093/bfgp/elv055.

15. Gessner, I.; Fries, J.W.U.; Brune, V.; Mathur, S. Magnetic Nanoparticle-Based Amplification of MicroRNA Detection in Body Fluids for Early Disease Diagnosis. *J. Mater. Chem. B* **2021**, *9*, 9–22, doi:10.1039/d0tb02165b.

16. Svoronos, A.A.; Engelman, D.M.; Slack, F.J. OncomiR or Tumor Suppressor? The Duplicity of MicroRNAs in Cancer. *Cancer Res.* **2016**, *76*, 3666–3670, doi:10.1158/0008-5472.CAN-16-0359.

17. Calin, G.A.; Dumitru, C.D.; Shimizu, M.; Bichi, R.; Zupo, S.; Noch, E.; Aldler, H.; Rattan, S.; Keating, M.; Rai, K.; et al. Frequent Deletions and Down-Regulation of Micro- RNA Genes MiR15 and MiR16 at 13q14 in Chronic Lymphocytic Leukemia. *PNAS* **2002**, *99*, 13–18, doi:10.1073/pnas.242606799.

18. He, B.; Zhao, Z.; Cai, Q.; Zhang, Y.; Zhang, P.; Shi, S.; Xie, H. MiRNA-Based Biomarkers , Therapies , and Resistance in Cancer. *Int. J. Biol. Sci.* **2020**, *16*, doi:10.7150/ijbs.47203.

19. Segal, M.; Slack, F.J. Challenges Identifying Efficacious MiRNA Therapeutics for Cancer Challenges Identifying Efficacious MiRNA Therapeutics for Cancer. *Expert Opin. Drug Discov.* **2020**, *15*, 987–992, doi:10.1080/17460441.2020.1765770.

20. Jenike, A.E.; Halushka, M.K. MiR-21 : A Non - Specific Biomarker of All Maladies. *Biomark. Res.* **2021**, *1*, 1–7, doi:10.1186/s40364-021-00272-1.

21. Chen, X.; Yang, F.; Zhang, T.; Wang, W.; Xi, W.; Li, Y.; Zhang, D.; Huo, Y.; Zhang, J.; Yang, A.; et al. MiR-9 Promotes Tumorigenesis and Angiogenesis and Is Activated by MYC and OCT4 in Human Glioma. *J. Exp. Clin. Cancer Res.* **2019**, *2*, 1–16, doi:10.1186/s13046-019-1078-2.

22. Shang, A.; Lu, W.; Yang, M.; Zhou, C.; Zhang, H.; Wang, W.; Wang, W.; Wu, G. MiR-9 Induces Cell Arrest and Apoptosis of Oral Squamous Cell Carcinoma via CDK 4 / 6 Pathway. *Artif. Cells, Nanomedicine, Biotechnol.* **2018**, *46*, 1754–1762, doi:10.1080/21691401.2017.1391825.

23. Fouad, Y.A.; Aanei, C. Revisiting the Hallmarks of Cancer. *Cancer Res* **2017**, *7*, 1016–1036.

24. Guo, X.; Connick, M.C.; Vanderhoof, J.; Ishak, M.; Hartley, R.S. MicroRNA-16 Modulates HuR Regulation of Cyclin E1 in Breast Cancer Cells. *Int. J. Mol. Sci.* **2015**, *16*, 7112–7132, doi:10.3390/ijms16047112.

25. Luo, Q.; Li, X.; Gao, Y.; Long, Y.; Chen, L.; Huang, Y.; Fang, L. MiRNA-497 Regulates Cell Growth and Invasion by Targeting Cyclin E1 in Breast Cancer. *Cancer Cell Int.* **2013**, *13*, 1–8, doi:10.1186/1475-2867-13-95.

26. Mi, Y.; Wei, Z.; Li, N.; Zhen, S.; Lifen, Z.; Huimin, Z.; Ji, L. MicroRNA-130b Targets PTEN to Mediate Drug Resistance and Proliferation of Breast Cancer Cells via the PI3K / Akt Signaling Pathway. *Sci. Rep.* **2017**, 1–12, doi:10.1038/srep41942.

27. Liu, C.; Liu, Z.; Li, X.; Tang, X.; He, J.; Lu, S. MicroRNA-1297 Contributes to Tumor Growth of Human Breast Cancer by Targeting PTEN / PI3K / AKT Signaling. *Oncol. Rep.* **2017**, *38*, 2435–2443, doi:10.3892/or.2017.5884.

28. Dinami, R.; Ercolani, C.; Petti, E.; Piazza, S.; Ciani, Y.; Sestito, R.; Sacconi, A.; Biagioni, F.; Sage, C.; Agami, R.; et al. MiR-155 Drives Telomere Fragility in Human Breast Cancer by Targeting TRF1. *Cancer Res.* **2014**, *74*, 4145–4156, doi:10.1158/0008-5472.CAN-13-2038.

29. Wu, K.; Tsai, Y.; Lien, C.; Kuo, P. The Roles of MicroRNA in Lung Cancer. *Int. J. Mol. Sci.* **2019**, *20*, 1–25, doi:10.3390/ijms20071611.

30. Zhang, L.; Liao, Y.; Tang, L. MicroRNA-34 Family : A Potential Tumor Suppressor and Therapeutic Candidate in Cancer. *J. Exp. Clin. Cancer Res.* **2019**, *5*, 1–13, doi:10.1186/s13046-019-1059-5.

31. Xu, W.; Liu, Z.; Deng, F.; Wang, D.; Li, X.; Tian, T.; Zhang, J. MiR-145 : A Potential Biomarker of Cancer Migration and Invasion. *Am J Transl Res* **2019**, *11*, 6739–6753.

32. Ren, A.; Dong, Y.; Tsoi, H.; Yu, J. Detection of MiRNA as Non-Invasive Biomarkers of Colorectal Cancer. *Int. J. Mol. Sci.* **2015**, *16*, 2810–2823, doi:10.3390/ijms16022810.

33. Niu, L.; Yang, W.; Duan, L.; Wang, X.; Li, Y.; Xu, C.; Liu, C.; Zhang, Y.; Zhou, W.; Liu, J.; et al. Biological Implications and Clinical Potential of Metastasis-Related MiRNA in Colorectal Cancer. *Mol. Ther. Nucleic Acid* **2021**, *23*, 42–54, doi:10.1016/j.omtn.2020.10.030.

34. Chen, E.; Li, Q.; Wang, H.; Yang, F.; Min, L.; Yang, J. Biomedicine & Pharmacotherapy MiR-92a Promotes Tumorigenesis of Colorectal Cancer , a Transcriptomic and Functional Based Study. *Biomed. Pharmacother.* **2018**, *106*, 1370–1377, doi:10.1016/j.biopha.2018.07.098.

35. Fu, F.; Jiang, W.; Zhou, L. Circulating Exosomal MiR-17-5p and MiR-92a-3p Predict Pathologic Stage and Grade of Colorectal Cancer. *Transl. Oncol.* **2018**, *11*, 221–232, doi:10.1016/j.tranon.2017.12.012.

36. Jia, Y.Z.; Liu, J.; Wang, G.Q.; Song, Z.F. MiR-484: A Potential Biomarker in Health and Disease. *Front. Oncol.* **2022**, *12*, 1–22, doi:10.3389/fonc.2022.830420.

37. Cui, C.; Cui, Q. The Relationship of Human Tissue MicroRNAs with Those from Body Fluids. *Sci. Rep.* **2020**, *10*, 1–7, doi:10.1038/s41598-020-62534-6.

38. Junqueira-Neto, S.; Batista, I.A.; Costa, J.L.; Melo, S.A. Liquid Biopsy beyond Circulating Tumor Cells and Cell-Free DNA. *Acta Cytol.* **2019**, *63*, 479–488, doi:10.1159/000493969.

39. Loeser, H.; Brandenstein, M. Von; Burst, V.; Richter, C.; Buettner, R.; Kurschat, C. In Glomerular Disease , Urinary MicroRNA15a Is A Biomarker for Inflammatory Signaling Mediated by Protein and Endothelin-1. *J. Mol. Med. Clin. Appl. 2*, 1–10, doi:10.16966/2575-0305.110.

40. Kirschner, M.B.; Kao, S.C.; Edelman, J.J.; Armstrong, N.J.; Vallely, M.P.; Zandwijk, N. Van; Reid, G. Haemolysis during Sample Preparation Alters MicroRNA Content of Plasma. *PLoS One* **2011**, *6*, doi:10.1371/journal.pone.0024145.

41. McDonald, J.S.; Milosevic, D.; Reddi, H. V; Grebe, S.K.; Algeciras-schimnich, A. Analysis of Circulating MicroRNA : Preanalytical and Analytical Challenges. *Clin. Chem.* **2011**, *840*, 833–840, doi:10.1373/clinchem.2010.157198.

42. Brown, R.A.M.; Epis, M.R.; Horsham, J.L.; Kabir, T.D.; Richardson, K.L.; Leedman, P.J. Total RNA Extraction from Tissues for MicroRNA and Target Gene Expression Analysis : Not All Kits Are Created Equal. *BMC Biotechnol.* **2018**, 1–11, doi:10.1186/s12896-018-0421-6.

43. Yaylak, B.; Akgül, B. Experimental MicroRNA Detection Methods. In *miRNomics: MicroRNA Biology and Computational Analysis*; Allmer, J., Yousef, M., Eds.; Springer US: New York, NY, 2022; pp. 33–55 ISBN 978-1-0716-1170-8.

44. Ideozu, J.E.; Zhang, X.; Rangaraj, V.; McColley, S.; Levy, H. Microarray Profiling Identifies Extracellular Circulating MiRNAs Dysregulated in Cystic Fibrosis. *Sci. Rep.* **2019**, *9*, 1–11, doi:10.1038/s41598-019-51890-7.

45. Mestdagh, P.; Hartmann, N.; Baeriswyl, L.; Andreasen, D.; Bernard, N.; Chen, C.; Cheo, D.; D'Andrade, P.; DeMayo, M.; Dennis, L.; et al. Evaluation of Quantitative MiRNA Expression Platforms in the MicroRNA Quality Control (MiRQC) Study. *Nat. Methods* **2014**, *11*, 809–815, doi:10.1038/nmeth.3014.

46. Martinez-Gutierrez, A.D.; Catalan, O.M.; Vázquez-Romo, R.; Reyes, F.I.P.; Alvarado-Miranda, A.; Medina, F.L.; Bargallo-Rocha, J.E.; Moreno, L.T.O.; de León, D.C.; Herrera, L.A.; et al. MiRNA Profile Obtained by Next-generation Sequencing in Metastatic Breast Cancer Patients Is Able to Predict the Response to Systemic Treatments. *Int. J. Mol. Med.* **2019**, *44*, 1267–1280, doi:10.3892/ijmm.2019.4292.

47. Ouyang, T.; Liu, Z.; Han, Z.; Ge, Q. MicroRNA Detection Specificity: Recent Advances and Future Perspective. *Anal. Chem.* **2019**, *91*, 3179–3186, doi:10.1021/acs.analchem.8b05909.

48. Rusek, M.; Michalska-Jakubus, M.; Kowal, M.; Bełtowski, J.; Krasowska, D. A Novel MiRNA-4484 Is up-Regulated on Microarray and Associated with Increased MMP-21 Expression in Serum of Systemic Sclerosis Patients. *Sci. Rep.* **2019**, *9*, 1–13, doi:10.1038/s41598-019-50695-y.

49. Galluzzo, A.; Gallo, S.; Pardini, B.; Birolo, G.; Fariselli, P.; Boretto, P.; Vitacolonna, A.; Peraldo-neia, C.; Spilinga, M.; Volpe, A.; et al. Identification of Novel Circulating MicroRNAs in Advanced Heart Failure by Next-Generation Sequencing. *ESC Hear. Fail.* **2021**, *8*, 2907–2919, doi:10.1002/ehf2.13371.

50. Várallyay, É.; Burgyán, J.; Havelda, Z. MicroRNA Detection by Northern Blotting Using Locked Nucleic Acid Probes. *Nat. Protoc.* **2008**, *3*, 190–196, doi:10.1038/nprot.2007.528.

51. Moukengue, B.; Amiaud, J.; Jacques, C.; Charrier, C.; Ory, B.; Lamoureux, F. Analysis of MRNA, MiRNA, and DNA in Bone Cells by RT-QPCR and in Situ Hybridization. *Methods Mol. Biol.* **2019**, *1914*, 169–196, doi:10.1007/978-1-4939-8997-3_9.

52. Veselinyová, D.; Mašlanková, J.; Kalinová, K.; Helena, M.; Mária, M.; Rabajdová, M. Selected In Situ Hybridization Methods : Principles and Application. *Molecules* **2021**, *26*, 3874, doi:10.3390/molecules26133874.

53. Degliangeli, F.; Pompa, P.P.; Fiammengo, R. Nanotechnology-Based Strategies for the Detection and Quantification of MicroRNA. *Chem. - A Eur. J.* **2014**, *20*, 9476–9492, doi:10.1002/chem.201402649.

54. Lu, T.X.; Rothenberg, M.E. Fundamentals of Allergy and Immunology MicroRNA. **2018**, *limi*, 1202–1207, doi:10.1016/j.jaci.2017.08.034.

55. Ban, E.; Song, E.J. Considerations and Suggestions for the Reliable Analysis of MiRNA in Plasma Using QRT-PCR. *Genes (Basel).* **2022**, *13*, 328, doi:10.3390/genes13020328.

56. Tajadini, M.; Panjehpour, M.; Javanmard, S. Comparison of SYBR Green and TaqMan Methods in Quantitative Real-Time Polymerase Chain Reaction Analysis of Four Adenosine Receptor Subtypes. *Adv. Biomed. Res.* **2014**, *3*, 85, doi:10.4103/2277-9175.127998.

57. Fauth, M.; Saul, M.J. Validation of Extracellular MiRNA Quantification in Blood Samples Using RT - QPCR. *FASEB Bio Adv.* **2019**, *1*, 481–492, doi:10.1096/fba.2019-00018.

58. Wei, S.; Chen, G.; Jia, X.; Mao, X.; Chen, T.; Mao, D.; Zhang, W.; Xiong, W. Exponential Amplification Reaction and Triplex DNA Mediated Aggregation of Gold Nanoparticles for Sensitive Colorimetric Detection of MicroRNA. *Anal. Chim. Acta* **2020**, *1095*, 179–184, doi:10.1016/j.aca.2019.10.020.

59. Chan, H.N.; Ho, S.L.; He, D.; Li, H.W. Direct and Sensitive Detection of Circulating MiRNA in Human Serum by Ligase-Mediated Amplification. *Talanta* **2020**, *206*, 120217, doi:10.1016/j.talanta.2019.120217.

60. Cheng, W.; Ma, J.; Cao, P.; Zhang, Y.; Xu, C.; Yi, Y.; Li, J. Enzyme-Free Electrochemical Biosensor Based on Double Signal Amplification Strategy for the Ultra-Sensitive Detection of Exosomal MicroRNAs in Biological Samples. *Talanta* **2020**, *219*, 121242, doi:10.1016/j.talanta.2020.121242.

61. Ma, X.; Ma, Y.; Ejeromedoghene, O.; Kandawa-schulz, M.; Song, W.; Wang, Y. Dual-Mode Corroborative Detection of MiRNA-21 Based on Catalytic Hairpin Assembly Reaction and Oxygen Reduction Reaction Combined Strategy for the Signal Amplification. *Sensors Actuators B. Chem.* **2022**, *364*, 131924, doi:10.1016/j.snb.2022.131924.

62. Li, M.; Cheng, J.; Yuan, Z.; Shen, Q.; Fan, Q. DNAzyme-Catalyzed Etching Process of Au/Ag Nanocages Visualized via Dark-Field Imaging with Time Elapse for Ultrasensitive Detection of MicroRNA. *Sensors Actuators, B Chem.* **2021**, *330*, 129347, doi:10.1016/j.snb.2020.129347.

63. Jet, T.; Gines, G.; Rondelez, Y. Advances in Multiplexed Techniques for the Detection and Quantification of MicroRNAs. *Chem. Soc. Rev.* **2021**, 4141–4161, doi:10.1039/d0cs00609b.

64. Christian, P.; Von Der Kammer, F.; Baalousha, M.; Hofmann, T. Nanoparticles: Structure, Properties, Preparation and Behaviour in Environmental Media. *Ecotoxicology* **2008**, *17*, 326–343, doi:10.1007/s10646-008-0213-1.

65. Khan, I.; Saeed, K.; Khan, I. Nanoparticles: Properties, Applications and Toxicities. *Arab. J. Chem.* **2019**, *12*, 908–931, doi:10.1016/j.arabjc.2017.05.011.

66. Nasrabadi, H.T.; Abbasi, E.; Davaran, S.; Kouhi, M.; Akbarzadeh, A. Bimetallic Nanoparticles: Preparation, Properties, and Biomedical Applications. *Artif. Cells, Nanomedicine Biotechnol.* **2016**, *44*, 376–380, doi:10.3109/21691401.2014.953632.

67. Xiao, Y. Superparamagnetic Nanoparticles for Biomedical Applications. *J. Mater. Chem. B* **2020**, *8*, 354–367, doi:10.1039/c9tb01955c.

68. Dong, L. *Optical Properties of Nanoparticles in Composite Materials*; 2012; ISBN 9789175015002.

69. Das, S.; Mitra, S.; Khurana, S.M.P.; Debnath, N. Nanomaterials for Biomedical Applications. *Front. Life Sci.* **2013**, *7*, 90–98, doi:10.1080/21553769.2013.869510.

70. Coutinho, C.; Somoza, Á. MicroRNA Sensors Based on Gold Nanoparticles. *Anal. Bioanal. Chem.* **2019**, *411*, 1807–1824, doi:10.1007/s00216-018-1450-7.

71. González-Rubio, G.; De Oliveira, T.M.; Altantzis, T.; La Porta, A.; Guerrero-Martínez, A.; Bals, S.; Scarabelli, L.; Liz-Marzán, L.M. Disentangling the Effect of Seed Size and Crystal Habit on Gold Nanoparticle Seeded Growth. *Chem. Commun.* **2017**, *53*, 11360–11363, doi:10.1039/c7cc06854a.

72. Fischer, A.; Thuenemann, A.F.; Emmerling, F.; Rademann, K.; Kraehnert, R.; Polte, J.; Tuaev, X.; Wuithschick, M. Formation Mechanism of Colloidal Silver Nanoparticles: Analogies and Differences to the Growth of Gold Nanoparticles. *ACS Nano* **2012**, *6*, 5791–5802, doi:10.1021/nn301724z.

73. Lee, T.; Mohammadniaei, M.; Zhang, H.; Yoon, J.; Choi, H.K.; Guo, S.; Guo, P.; Choi, J.W. Single Functionalized PRNA/Gold Nanoparticle for Ultrasensitive MicroRNA Detection Using Electrochemical Surface-Enhanced Raman Spectroscopy. *Adv. Sci.* **2020**, *7*, doi:10.1002/advs.201902477.

74. Wang, M.; Chen, W.; Tang, L.; Yan, R.; Miao, P. Duplex-Specific Nuclease Assisted MiRNA Assay Based on Gold and Silver Nanoparticles Co-Decorated on Electrode Interface. *Anal. Chim. Acta* **2020**, *1107*, 23–29, doi:10.1016/j.aca.2020.01.041.

75. Guo, T.; Lin, M.; Huang, J.; Zhou, C.; Tian, W.; Yu, H.; Jiang, X.; Ye, J.; Shi, Y.; Xiao, Y.; et al. The Recent Advances of Magnetic Nanoparticles in Medicine. *J. Nanomater.* **2018**, *2018*, doi:10.1155/2018/7805147.

76. Alonso, J.; Barandiarán, J.M.; Fernández Barquín, L.; García-Arribas, A. *Magnetic Nanoparticles, Synthesis, Properties, and Applications*; 2018; ISBN 9780128139059.

77. Wang, H.; Tang, H.; Yang, C.; Li, Y. Selective Single Molecule Nanopore Sensing of MicroRNA Using PNA Functionalized Magnetic Core-Shell Fe3O4-Au Nanoparticles. *Anal. Chem.* **2019**, *91*, 7965–7970, doi:10.1021/acs.analchem.9b02025.

78. Cao, X.; Zhang, K.; Yan, W.; Xia, Z.; He, S.; Xu, X.; Ye, Y. Calcium Ion Assisted Fluorescence Determination of MicroRNA-167 Using Carbon Dots – Labeled Probe DNA and Polydopamine-Coated Fe3O4 Nanoparticles. *Microchim. Acta* **2020**, *187*, doi:10.1007/s00604-020-4209-8.

79. Li, M.; Li, J.; Zhang, X.; Yao, M.; Li, P.; Xu, W. Simultaneous Detection of Tumor-Related MRNA and MiRNA in Cancer Cells with Magnetic SERS Nanotags. *Talanta* **2021**, *232*, 122432, doi:10.1016/j.talanta.2021.122432.

80. Mehdipour, M.; Gloag, L.; Bennett, D.T.; Hoque, S.; Pardehkhorram, R.; Bakthavathsalam, P.; Gonçales, V.R.; Tilley, R.D.; Gooding, J.J. Synthesis of Gold-Coated Magnetic Conglomerate Nanoparticles with a Fast Magnetic Response for Bio-Sensing. *J. Mater. Chem. C* **2021**, *9*, 1034–1043, doi:10.1039/d0tc04702c.

81. Lu, W.; Chen, Y.; Liu, Z.; Tang, W.; Feng, Q.; Sun, J.; Jiang, X. Quantitative Detection of MicroRNA in One Step via Next Generation Magnetic Relaxation. *Asc Nano* **2016**, *10*, 6685–6692, doi:10.1021/acsnano.6b01903.

82. Zhang, N.; Shi, X.; Guo, H.; Zhao, X.; Zhao, W.; Xu, J.; Chen, H. Gold Nanoparticle Couples with Entropy-Driven Toehold-Mediated DNA Strand Displacement Reaction on Magnetic Beads: Toward Ultrasensitive Energy-Transfer-Based Photoelectrochemical Detection of MiRNA-141 in Real Blood Sample. *Anal. Chem.* **2018**, *90*, 11892–11898, doi:10.1021/acs.analchem.8b01966.

83. Shen, Z.; He, L.; Wang, W.; Tan, L.; Gan, N. Highly Sensitive and Simultaneous Detection of MicroRNAs in Serum Using Stir-Bar Assisted Magnetic DNA Nanospheres-Encoded Probes. *Biosens. Bioelectron.* **2020**, *148*, 111831, doi:10.1016/j.bios.2019.111831.

84. Hervé, K.; Douziech-Eyrolles, L.; Munnier, E.; Cohen-Jonathan, S.; Soucé, M.; Marchais, H.; Limelette, P.; Warmont, F.; Saboungi, M.L.; Dubois, P.; et al. The Development of Stable Aqueous Suspensions of PEGylated SPIONs for Biomedical Applications. *Nanotechnology* **2008**, *19*, doi:10.1088/0957-4484/19/46/465608.

85. Janko, C.; Ratschker, T.; Nguyen, K.; Zschiesche, L.; Tietze, R.; Lyer, S.; Alexiou, C. Functionalized Superparamagnetic Iron Oxide Nanoparticles (SPIONs) as Platform for the Targeted Multimodal Tumor Therapy. *Front. Oncol.* **2019**, *9*, 1–9, doi:10.3389/fonc.2019.00059.

86. Lu, X.; Lu, J. The Significance of Detection of Serum MiR-423-5p and MiR-484 for Diagnosis of Colorectal Cancer. *Clin. Lab.* **2015**, *61*, 187–190, doi:10.7754/clin.lab.2014.140625.

PART I

Development and characterization of nanoprobes

Publication 1:

Formation of miRNA nanoprobes – conjugation approaches leading to the functionalization

Accepted in “Molecules”, December 2022

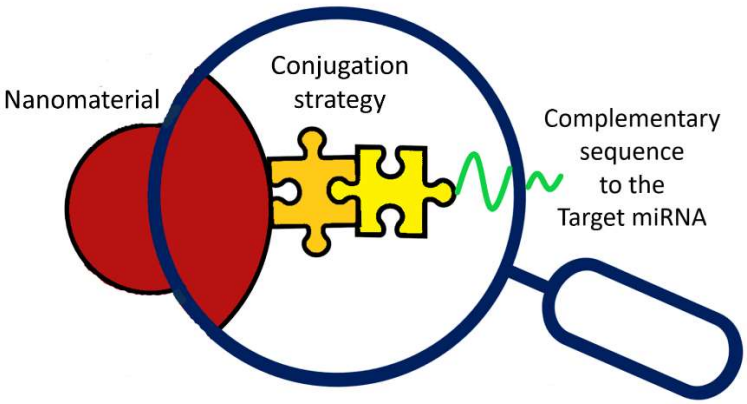

Préambule de la Publication 1

Récemment, les microARN (miARN) ont suscité un grand intérêt en tant que nouveaux biomarqueurs diagnostiques et pronostiques, grâce à leur intéressant potentiel pour diagnostiquer précocement de nombreuses pathologies. Les miARN, étant de courtes séquences d'ARN non codantes, la sensibilité et la sélectivité de leur détection restent un véritable challenge dans la recherche scientifique. Ainsi, des méthodes basées sur les nanomatériaux ont émergé dans l'espoir de développer de nouvelles approches pour une détection rapide et facile. Au cœur des méthodes de détection basées sur les nanotechnologies se trouvent les nanosondes et autres nanomatériaux fonctionnalisés. La capture des miARN cibles est généralement basée sur leur hybridation avec leur séquence d'oligonucléotides complémentaires. Ainsi, la séquence complémentaire doit être attachée au nanomatériau avec une stratégie de conjugaison spécifique. Comme chaque nanomatériau a ses propriétés uniques et que chaque approche de conjugaison présente ses inconvénients et ses avantages, cette revue offre un aperçu des principales approches de conjugaison dans la détection de miARN à base de nanomatériaux. Commençant par un bref récapitulatif des propriétés et caractéristiques spécifiques des nanomatériaux pouvant être utilisés comme substrat, l'accent est ensuite mis sur la chimie de liaisons covalentes et non covalentes conduisant à la fonctionnalisation des nanomatériaux, les plus couramment utilisés dans la détection des miARN.

molecules

MDPI

Review

Formation of miRNA Nanoprobes—Conjugation Approaches Leading to the Functionalization

Iveta Vilímová, Katel Hervé-Aubert * and Igor Chourpa

EA6295 Nanomédicaments et Nanosondes, Université de Tours, 37200 Tours, France
* Correspondence: katel.herve@univ-tours.fr; Tel.: +33-247-367-157

Abstract: Recently, microRNAs (miRNA) captured the interest as novel diagnostic and prognostic biomarkers, with their potential for early indication of numerous pathologies. Since miRNA is a short, non-coding RNA sequence, the sensitivity and selectivity of their detection remain a cornerstone of scientific research. As such, methods based on nanomaterials have emerged in hopes of developing fast and facile approaches. At the core of the detection method based on nanotechnology lie nanoprobes and other functionalized nanomaterials. Since miRNA sensing and detection are generally rooted in the capture of target miRNA with the complementary sequence of oligonucleotides, the sequence needs to be attached to the nanomaterial with a specific conjugation strategy. As each nanomaterial has its unique properties, and each conjugation approach presents its drawbacks and advantages, this review offers a condensed overview of the conjugation approaches in nanomaterial-based miRNA sensing. Starting with a brief recapitulation of specific properties and characteristics of nanomaterials that can be used as a substrate, the focus is then centered on covalent and non-covalent bonding chemistry, leading to the functionalization of the nanomaterials, which are the most commonly used in miRNA sensing methods.

Keywords: miRNA; conjugation strategy; covalent bonding; non-covalent bonding; nanomaterial

check for updates

Citation: Vilímová, I.; Hervé-Aubert, K.; Chourpa, I. Formation of miRNA Nanoprobes—Conjugation Approaches Leading to the Functionalization. *Molecules* **2022**, *27*, 8428. https://doi.org/10.3390/molecules27238428

Academic Editor: Jahir Orozco Holguín

Received: 27 September 2022
Accepted: 25 November 2022
Published: 2 December 2022

Publisher's Note: MDPI stays neutral with regard to jurisdictional claims in published maps and institutional affiliations.

Copyright: © 2022 by the authors. Licensee MDPI, Basel, Switzerland. This article is an open access article distributed under the terms and conditions of the Creative Commons Attribution (CC BY) license (https://creativecommons.org/licenses/by/4.0/).

1. Introduction

The detection of miRNAs (short, non-coding RNA sequences of approximately 19 to 25 nucleotides) has tremendous potential for early diagnosis of varying disorders, most notably life-threatening and unpredictable diseases such as cancer. Their function as circulating biomarkers is however hindered by their sparseness in body fluids, small size, and minor differences between the types of miRNAs. Thus, their detection in a short time with high accuracy in biological samples remains a challenge. Body fluids affect large spectra of detecting systems due to their high viscosity, the pH influence, the presence of other interfering biomolecules, and as previously mentioned, low amounts of target miRNA [1].

The miRNA expression spectrum in respective body fluids can differ not only depending on the disease type and pathological conditions but also on other aspects related to the patient (e.g., medication, diet, age, etc.) The body fluids in which miRNAs are detected can be obtained by either invasive or non-invasive procedures. Currently, the research is more often focused on the detection in body fluids obtained by non-invasive or weakly invasive means, such as urine, whole blood, and serum. For the miRNA capture, the body fluid is typically mixed with nanoprobe suspension [1,2].

Methods and approaches of miRNA detection based on nanotechnologies offer an alternative path to a faster and less complicated detection process, nevertheless also with specific challenges, including reproducibility, standardization, optimization, normalization, and data processing. The techniques vary in utilized material (organic, inorganic, or hybrid), nanostructures (nanorods, nanowires, nanosheets, etc.), and the strategy of the

hybrid), nanostructures (nanorods, nanowires, nanosheets, etc.), and the strategy of the complementary DNA application (hairpin conjugates, molecular beacons, catalytic self-assembly, spherical nucleic acids, etc.) [3–5].

As such, hybrid NPs are particularly interesting since they combine the unique physical properties of the inorganic core (especially useful for their detection/quantification) with the biocompatibility/biospecificity of the organic shell.

After the selection of the nanomaterial as the substrate, for example, for the nanoprobe, the next step is the functionalization via an appropriate conjugation strategy, generally in the form of the attachment of an oligonucleotide sequence. The cornerstone of miRNA targeting approaches is antisense technology based on hybridizing the target miRNA with a complementary oligonucleotide sequence, leading to the formation of a duplex with higher stability. Usually, a complementary miRNA of the same length as the target miRNA is used, since such molecules are widely commercially available along with a wide range of modifications. Other possibilities, such as single- or double-stranded DNA, various hairpin probes, and molecular beacons, depend on the chosen approach and subsequent detection technique. The form of the target miRNA depends on the chosen media of miRNA detection—for validation of a method in model solutions, it is possible to use commercially produced sequences mimicking the naturally occurring miRNA, whose detection in biofluids can be hindered by other biomolecules and proteins present [6].

The preparation of the functionalized material can be, at times, less scrutinized on the road to miRNA detection, the reports often understandably focused on achieving the lowest detection limits [7]. The review articles regarding miRNA detection methods analyze new developments and novel experimental techniques [5,8] or are devoted to some particular nanomaterial [9] or functionalized ligands [10]. However, to the best of our knowledge, none of those reviews is focused on the general strategy of functionalization and on its validation, in particular on the important details of the experimental protocol. In view of this situation, we suggest this review as an attempt to gain a deeper insight in the conjugation strategies and methods (Figure 1). In particular, this review is focused on the most common conjugation approaches applied to connect the nanomaterial and complementary sequences that are used to target specific miRNA. Since each nanomaterial presents its own unique properties and characteristics beyond those common to all, they are briefly outlined in the first part, along with the suggestion of potential characterization techniques. The following section describes the choice of conjugation approaches, divided into covalent and non-covalent ones, with drawbacks and advantages presented for each.

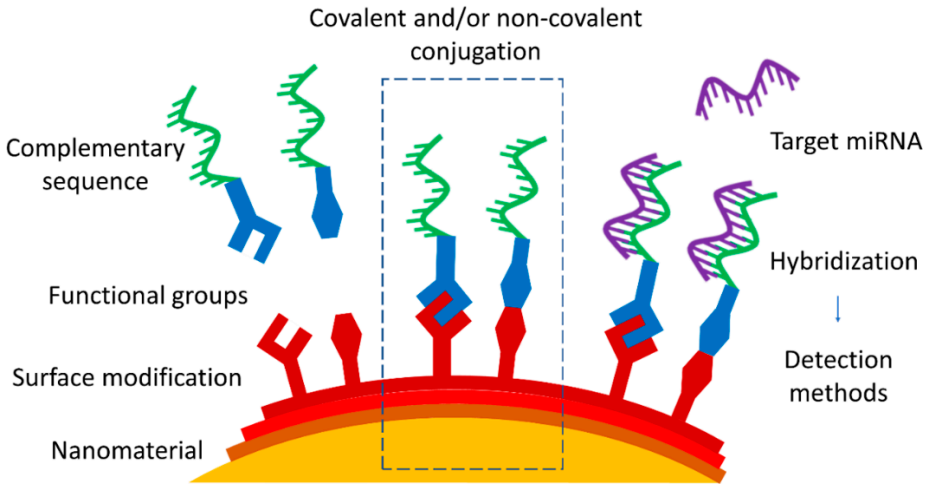

Figure 1. Position of the focus of this review, i.e., approaches of nanomaterial functionalization by covalent or non-covalent conjugation with complementary miRNA or DNA sequence as a part of the strategy of miRNA nanoprobe development.

2. Nanomaterials Used as Substrates

All nanomaterials mentioned in this brief overview have high surface energy and a high surface-to-volume ratio, leading to a higher catalytical activity. Their more specific properties vary depending on the nanomaterial, which oftentimes leads to a combination of two or more types of nanomaterials to take better advantage of their strengths (Table 1).

2.1. Gold Nanoparticles

Gold nanoparticles (AuNPs) have excellent catalytic and electrical properties and unique optical properties, which are extensively studied for signal amplification with the aim of reaching highly sensitive biosensing. Their optical properties are rooted in the localized surface plasmon resonance (LSPR) phenomenon, and additionally, the plasmonic surface can quench the fluorescence. With the increase of their size and/or upon aggregation of the AuNPs in aqueous suspensions (colloids), their LSPR band shifts are detected by means of a UV-Vis spectrometer or seen with a naked eye as a color change [11].

AuNPs are biocompatible due to their chemical stability in biological fluids. Possible toxicity concerns are connected to their long-term retention in the body. On the other hand, AuNPs can be easily modified with miRNA molecules, particularly due to the gold surface affinity to the thiol group [12]. Used as electrochemical or optical sensors in fluorescence, surface-enhanced Raman scattering (SERS), surface plasmon resonance (SPR), or colorimetry-based detection approaches, AuNPs can either be dispersed in the aqueous media [13] or immobilized on solid support [14]. The enhancement of AuNPs is widely used in the applications of biosensors in miRNA detection, achieving higher selectivity and sensitivity starting from sub-nanomolar levels [11].

2.2. Silver Nanoparticles

Compared with AuNPs, the LSPR band of silver nanoparticles (AgNPs) has a shorter position (approximately 400 nm instead of 535 nm). Nevertheless, both the monodispersity and reproducibility are more difficult to control with AgNPs compared with AuNPs. This leads to a frequent combination of AgNPs with other metals, such as gold, for example, in the form of core–shell nanoparticles [15–17].

AgNPs have found application as sensors in electrochemical and optical detection due to their high extinction coefficient, high scattering-to-extinction ratio, and high field enhancement. AgNPs show distinct amplified signals [18] along with strong Raman and fluorescence enhancement. Successful approaches are based on plasmonic properties of AgNPs implemented in platforms applying SERS [19], LSPR [20], or fluorescence readouts for detecting miRNA [21]. Similar to other metal nanoparticles, AgNPs also need a compatible organic coating before their use in biological systems to positively influence their stability and possible cytotoxicity [22,23].

2.3. Magnetic Nanoparticles

The term "magnetic nanoparticles" (MNPs) generally encompasses metal (e.g., iron, nickel platinum, and cobalt), metal oxide (e.g., iron oxides Fe_3O_4, γ-Fe_2O_3, and ferrites), and metal alloy NPs (e.g., FePt and FeCo). MNPs present several advantages enabling their application in biomedicine, since after proper modification, MNPs are non-toxic and biocompatible and can be utilized as nanovectors for specific targeting. Their magnetic properties allow the use of magnetic separation for the binding and detection of biomolecules [24,25]. MNPs are often combined with other nanomaterial types to unite the specific advantages [26].

Considering that miRNAs are generally present in very low concentrations in body fluids, the possibility to reconcentrate the miRNAs captured by MNPs via magnetic separation or extraction presents an enticing enhancement in the detection process. The miRNA extraction from a larger volume sample also represents insight into a larger population of the molecules and provides simpler handling procedures. However, the magnetic separa-

tion can be hampered if the viscous drag of body fluids overwhelms the magnetophoretic force [27].

2.4. Quantum Dots

Quantum dots (QDs) are luminescent semiconductor nanocrystals with the possibility to tune the maximum wavelength of their light emission spectra. Stable QDs can be obtained by an easy one-pot and/or one-step synthesis directly in a water medium [28]. Aqueous suspensions of QDs have a high photoluminescent quantum yield and resistance to photobleaching [29]. These qualities prompted their advancing application as optical, electrochemical, and chemiluminescent biosensors [4].

Due to high surface reactivity, QDs can serve as a nanoscale scaffold for further functionalization with common conjugation chemistry.

All in all, QDs are useful in miRNA detection due to their strong fluorescence provided by high quantum yield, narrow emission, and broad absorption spectra which provide multicolor labels with one light source and a strongly active surface for conjugations. Interactions on the surface of QDs lead to the activation or quenching of the fluorescence signal, allowing miRNA detection in complex media, such as body fluids.

2.5. Carbon Nanomaterials

Various carbon nanomaterials offer different characteristics (higher surface area, biocompatibility, and non-toxicity) useful for biosensing. Generally, carbon nanoparticles have strong and adjustable photoluminescence [30].

Carbon nanomaterials for miRNA detection can be in the form of carbon nanoparticles [31], carbon nanotubes [32], nanofibers [33], quantum dots [34], fullerenes [35], graphene nanosheets [36], and graphene oxide [37].

The good electrical conductivity and sensitivity of carbon nanomaterials are applied for the design and construction of electrochemical biosensors, particularly for electrode surface modification and for the preparation of modified electrodes [30,38–40].

Table 1. Types of nanomaterials used as substrates for miRNA nanoprobes.

Nanomaterial	Advantages	Disadvantages	References
Gold	• easy synthesis and modification • chemical stability • affinity to a variety of ligands • plasmonic properties	• poor degradability • possible long-term toxicity	[11,14,41]
Silver	• electrochemical detection • plasmonic properties stronger than with gold	• poor degradability • possible cytotoxicity	[18,20,42]
Magnetic	• superparamagnetism • magnet-based purification andseparation	• in larger size prone to magnetic aggregation	[1,43,44]
Quantum dots	• strong and stable fluorescence • high surface reactivity • high electron transfer	• stabilizers and surfactants needed on the surface	[28,45,46]
Carbon	• widely available carbon sources • fluorescence properties • electrocatalytic activity	• few in vivo studies performed	[30,37,47]

2.6. Characterization of Properties of the Nanomaterial before and after Conjugations

The determination of the physico-chemical properties of the chosen nanomaterial goes hand in hand with the need for monitoring their changes, both before and after the successful conjugation of a biomolecule. Some characterization techniques are more popular than others; however, as a rule, there is usually a combination of two or more methods used to cover possible inaccuracies and weak spots of the measurements.

Dynamic light scattering (DLS) measurements remain crucial in the confirmation of the size distribution of nanoparticles in aqueous dispersion and their colloidal stability [43]. The determination of the hydrodynamic diameter (DH) is usually joined by the evaluation of the zeta potential representative of the surface charges since the change of this parameter is often used to confirm the surface modification of the nanomaterial [48,49]. However, with small biomolecules such as miRNA, the changes in DH and zeta potential are generally too small to be reliable proof of conjugation. Although DLS and zetametry measurements are very common and can be found in the majority of performed studies, they are also necessarily joined by other complementary techniques which allow for more accurate confirmations [50].

Gel electrophoresis (of both the agarose and the polyacrylamide types) can be used to determine whether the conjugation between the nanomaterial and the ligand, or between two ligands, occurred. The migration of the unattached ligands is noticeably different compared with the migration of the conjugated ones, allowing for the separation of both. As a control, samples of NPs conjugated to a nucleotide sequence complementary to target miRNA, the non-conjugated NPs [44,51], and the solutions of free sequences are often used [52,53]. However, when it comes to confirmation of the binding of a large number of biomolecules, it is necessary to have a reliable purification technique to eliminate the excess of free ligands.

Structural and elemental analyses with X-ray diffraction (XRD) and X-ray photoelectron spectroscopy are often combined [38] and are generally used as a precise way to study the composition and bulk properties of a nanomaterial, including the presence of biomolecules on its surface. XRD provides information about the structural properties of a nanomaterial [44], including crystallinity and phase, while it can also give a rough idea of the average size of the NPs. XPS is the most sensitive spatially resolved technique enabling the determination of the bonding nature and elemental ratio in the nanomaterial, data from which the composition of the layers can be deduced [35]. Both techniques are less efficient with very small NPs, with smaller precision in structural measurements, and with amorphous NPs, where different atomic lengths can affect the measurement.

Thermogravimetric analysis (TGA) is centered on the weight loss of a sample as a function of increased temperature. Due to the organic content, the characteristic weight loss profile before and after the conjugation is investigated [12,14]. Generally, TGA is useful to confirm the presence of organic molecules conjugated to the inorganic nanomaterial, as is also the case with spectroscopic techniques.

Fourier transform infrared (FT-IR) spectroscopy is based on the detection of certain functional groups present on the surface of the nanomaterial in the event of successful conjugation and is considered acceptable for the detection of biological ligands onto inorganic nanomaterial [34,54,55]. Nevertheless, FT-IR is not always sensitive enough. Additionally, non-reacted components need to be removed with the appropriate purification method prior to FT-IR measurements.

Fluorescence spectroscopy is quite favored for confirmation of both the successful functionalization of the nanomaterial and the subsequent hybridization of target miRNA. The strategies are based on either the quenching of the fluorescence signal [56] or its increase after the binding event [34]. It can be the nanomaterial itself that has fluorescent properties, such as QDs, or a complementary sequence to the target miRNA modified with fluorescent dye. Therefore, in the case of using fluorescent components, the characterization of the nanoprobe and the detection of the target miRNA capture are closely entwined. Notably, it is important to have an efficient strategy of sample purification or a reliable way to distinguish the signals, as the non-conjugated fluorescence components can easily interfere with the accuracy of the measurements.

3. Conjugation Strategies Leading to Functionalization

The coating of the nanomaterial, more specifically of nanoparticles, improves the chemical and colloidal stability, provides surface modification available for further functionalization, and can alter the properties of NPs [57].

Selection of the conjugation method is influenced by: (i) available reactive groups on the surface of the nanomaterial and on the ligands intended to be conjugated; (ii) chemical and mechanical stability of both precursors and final product; and (iii) simplicity and reproducibility of the synthetic procedure, along with its cost-effectiveness [58].

Nanomaterials can be conjugated with various targeting biomolecules (such as proteins, nucleic acids, antibodies, and small drug molecules) via covalent or non-covalent assembly, which is more or less stable, respectively. Covalent conjugation is possible to achieve through the direct conjugation method, click chemistry, cross-linking strategies, etc. Non-covalent conjugation relies on physical interactions, such as hydrogen bonds, and interactions by electrostatic attraction or hydrophobic behavior. It should be noted that experimental approaches for formulating miRNA nanoprobes often combine covalent and non-covalent attachment to better exploit the advantages of both strategies, summarized in Table 2. Similarly, the most common approaches mentioned in the text are put into focus in Figure 2.

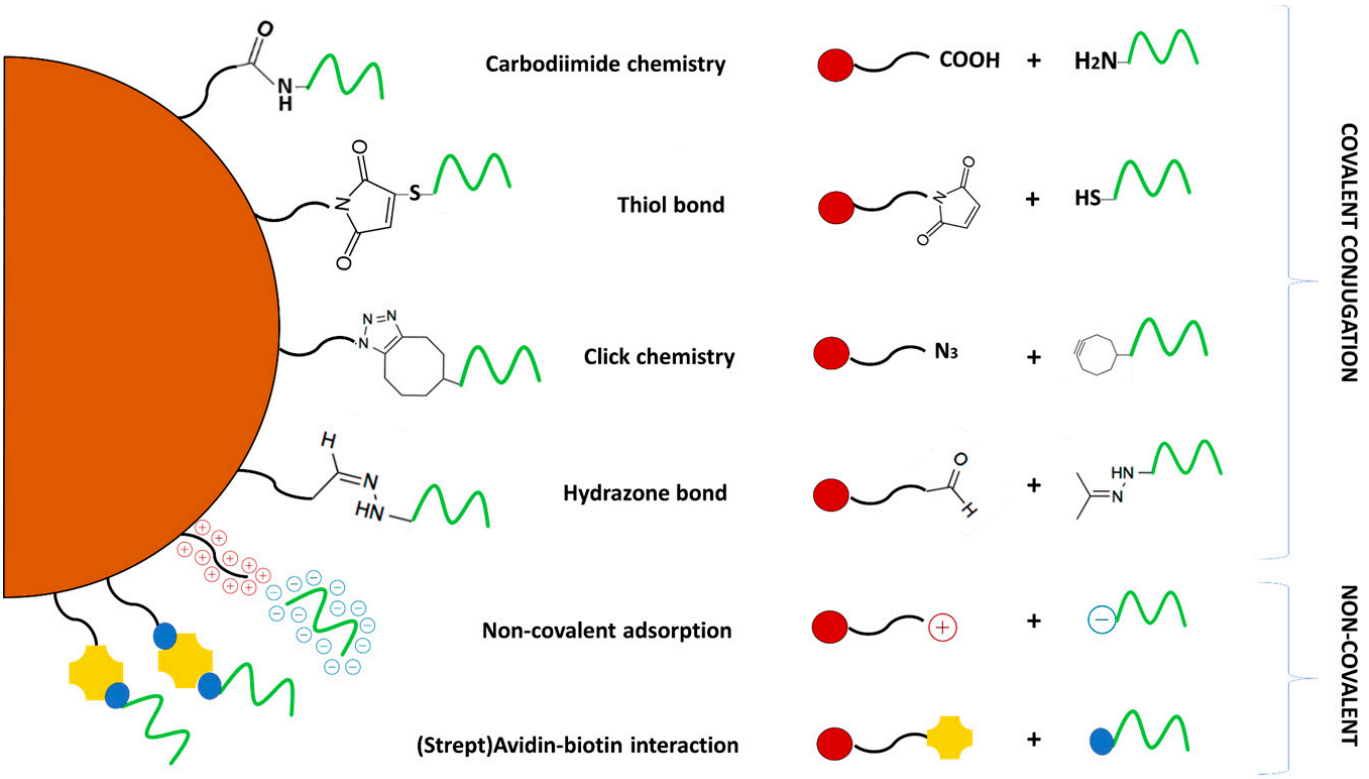

Figure 2. Schematic representations of covalent and non-covalent conjugation approaches.

3.1. Covalent Conjugation

Covalent conjugation offers high stability and reaction efficiency. Several functional groups can form a covalent bond on the surface of nanomaterial and ligand, such as carboxyl (-COOH), amine (-NH2), aldehyde (-CHO), and thiol (-SH, sulfhydryl). In the case of the absence of a reactive group on some biomolecules and drugs, modification is possible before the conjugation [58]. The most popular covalent conjugations are carbodiimide chemistry and thiol bond, with widespread application.

3.1.1. Carboxylic Acid–Amine Bond

Amines, a general label for compounds with a nitrogen atom with a free electron pair, are reactive due to their nucleophilic ability (donating the free electron pair to form a bond). This is especially the case for primary amines, making them ideal participants in conjugation with reactive groups. Amines are also widely used for the modification of biomolecules. For example, nearly all proteins have free amine at the N-terminus. The ending parts of proteins (C-terminus) often contain carboxyl groups which are also found on the side chains of amino acids (e.g., glutamate and aspartate). Carboxylic acids are very potent for fast reactions with nucleophilic compounds, where the hydrogen from acid is removed to form an anion, which is unsusceptible to additional reactions with a second nucleophilic compound [59].

One of the most widely used types of links is the amide bonds formed by the reaction of the amine group with N-hydroxysuccinimidyl (NHS)-activated carboxylic compound. In this method, the carboxylic compound has a first reaction with 1-ethyl-3-(3-dimethylaminopropyl)carbodiimide (EDC) and NHS to form an acyl amino ester, followed by a subsequent reaction with an amine to create the amide bond of exceptional stability. EDC is a universal cross-linking agent; however, after the reaction with the carboxyl group, some unstable intermediate is formed with a very short life in aqueous solutions, hence, the addition of NHS acts as a stabilizing agent [9].

In miRNA detection, NHS can be used for activation of carboxyl-modified nanomaterials, such as magnetic beads [60,61], and subsequent attachment of NH_2-modified miRNA antisense strain. For example, the carboxylic acid group can be attached to the surface magnetic nanoparticles with silica coating [55]. Alternatively, a single-stranded DNA probe with COOH− group on one end can be covalently bound to amino-modified magnetic iron oxide nanoparticles [62].

A similar principle was utilized by Mahani et al., with a molecular beacon in a hairpin structure with a fluorescent quencher at one end and the NH_2 group at the other. Carbon QD with the carboxyl groups on the surface formed an amide link with a molecular beacon, and only weak fluorescence was observed for the whole complex. In the presence of target miRNA-21, the hybridization of the hairpin structure led to the opening of the molecular beacon loop. The change in the distance between the quencher and the QD led to a change and increase of the fluorescent signal [63].

Amination, a reductive reaction where the amine group is combined with an organic molecule by transforming a carbonyl group (such as the carboxylic group), was used by Salimi et al. for the functionalization of graphene oxide. Graphene oxide is suitable for reduction and functionalization, and after functionalization with amine, the resulting graphene presents acceptable material for the attachment of biomolecules. Salimi et al. used this fact in the fabrication of an electrochemical biosensor for the selective detection of miRNA. Amino-functionalized reduced graphene oxide was assembled on the surface of a glassy carbon electrode with glutaraldehyde as a cross-linking agent, and a special sequence of miRNA-containing terminal amino group was attached for the detection of target miRNA [64].

Horny et al. utilized magnetic hyperthermia, with superparamagnetic core–shell γ-Fe_2O_3–SiO_2 NPs working as nanoheaters. Maghemite cores were slightly pre-aggregated before coating with a silica shell, the elongated shape proposing suitable properties for magnetic hyperthermia. Since silica-coated core–shell nanoparticles with a maghemite γ-Fe_2O_3 core had -NH_2 groups present on the surface, it allowed for the attachment of carboxyl-modified DNA probes [65].

Gao et al. combined carbon dots with graphene oxide. Carbon dots were linked with the amine-modified complementary DNA, and this complex was adsorbed on the surface of graphene oxide, quenching the fluorescence signal of the carbon dots. In the presence of target miRNA, the DNA desorbed from the surface of graphene oxide, hybridizing with the target miRNA and renewing the fluorescence signal, in proportion to the concentration of target miRNA [34].

Notably, amine modification of complementary oligonucleotide sequences continues to be the popular approach. Yao et al. conjugated iodide-modified magnetic beads with carboxyl groups on the surface and amine-modified DNA probes [42]. Xu et al. linked an amine-modified DNA probe with core–shell Au–Ag NPs covered with 5,5′-dithiobis (2-nitrobenzoic acid) [53]. Yazdanparast et al. synthesized magnetic core–shell Fe_3O_4–Ag NPs with carboxylic groups on the surface and joined them with amine-modified C-miRNA, applying the complex on a magnetic bar carbon paste electrode [54].

Carbodiimide chemistry is one of the most common approaches to binding miRNA to the nanomaterial. The reaction can be performed in an aqueous medium with no need for a complex solvent system, leading to a widespread application. However, the best efficiency is achieved in acidic pH, and it is necessary to perform it in buffers without additional amine and carboxylic groups. Depending on the nanomaterial, the challenge is presented in the form of the alignment of ligands and their binding orientation on the surface of the nanomaterial with multiple amine groups present. Moreover, the presence of additional amine and carboxylic groups (in ligands, on the nanomaterial, and in biological fluids) can also lead to a lower selectivity of the reaction [58,66].

3.1.2. Thiol Bond

Thiol is a compound with the -SH pair linked to single carbon or a carbon-containing group of atoms. Thiols play a large role in biological systems, as they maintain suitable levels of oxidation and reduction state of cells, proteins, and organisms. It is also possible to link thiol and amine groups covalently (using a heterobifunctional coupling agent with one sulfhydryl-reactive and one amine-reactive group) or to link thiol and alcohol groups (similarly with an agent containing a hydroxyl reactive site). Alternatively, a biomolecule can be attached directly to the surface of the nanomaterial, using a dative (coordination) bond, generally formed by the biomolecule donating two electrons from a single atom. This usually happens with metal affinity coordination and thiol interactions. The formed bond is longer than the covalent bond, with higher energy and sensitivity to oxidation and change in pH. Metal-affinity bonds are formed between cationic metal on the surface of the nanomaterial and, for example, imidazole ring present at histidine residues. Affinity is increased with a larger number of histidine amino acids [9].

The high affinity of thiol groups for gold results in a self-assembled monolayer on the gold surface, or simply in the Au–S bond (which is more stable than a self-assembled monolayer), making it quite popular and gaining it widespread application. The strength of the bond between isolated thiols and gold depends on the properties of the gold surface, interaction time, and the pH of the solution. Coordinate Au–SH bond shifts to a covalent nature of the Au–S bond with higher pH. The reaction offers better efficiency at neutral pH and is suitable for nanomaterials or ligands that are less stable at acidic pH [67]. In many cases, thiolated capture probes with complementary sequences to target miRNA are used in some combination with AuNPs [21]. For example, Al Mubarak et al. covalently bound a hairpin probe of complementary DNA to the surface localized AuNPs on a gold substrate by using 1,4-benzenedithiol (a benzene core with two -SH groups in opposite places) [68].

M. Wang et al. obtained a strong electrochemical response of AgNPs in combination with AuNPs on a glassy carbon electrode for miRNA detection. AgNPs were adsorbed on the electrode subsequently after AuNPs with a clearly detectable silver peak. When AuNPs functionalized with thiolated complementary DNA were present on the electrode, steric hindrance and electrostatic repulsion prevented the adsorption of AgNPs, decreasing the signal response of AgNPs. In the presence of target miRNA, the complementary DNA was hybridized on the surface of AuNPs, forming a duplex. Duplex-specific nuclease, an enzyme able to disrupt the bond between the nucleotides in the duplex, leads to the elimination of the duplex from the surface of AuNPs. AgNPs could be then adsorbed on the electrode, providing detectable signal amplification and leading to the determination of the amount of target miRNA [39].

A similar approach of AuNPs (combined with polypyrrole-reduced graphene oxide) deposited on a glassy carbon electrode enabled the immobilization of thiolated capture probes, permitting the further formation of hairpin probes [52]. In the same vein, the self-assembly of thiolated capture probes and their subsequent immobilization on a pencil graphite electrode, modified with carbon black material and AuNPs, allowed the capture of the target miRNA [40].

A complementary DNA probe modified with SH can be covalently bonded to the AuNP surface [14,29,41], and similarly, the same type of modification can be used for a conjugation on AgNPs [18,69], core–shell Au–Ag NPs [26], Au–Ag nanocages [20], AuNP–peptide nanotube composites [12], Au-coated conglomerates of superparamagnetic NPs [43], citrate-capped AuNPs electrostatically adsorbed to Fe_3O_4 NPs [70], Ag nanoclusters on Au electrode [71], and hollow Au–Ag nanospheres [72].

The maleimide chemistry, along with the carbodiimide chemistry, is a very common strategy in miRNA adsorption to the nanomaterial. The functional groups of the reaction are less common in biological fluids, leading to better selectivity and ligand orientation. However, the thiolation of ligands can lead to a change in their chemical structure, negatively influencing the binding affinity. The presence of proteins containing thiol groups (such as in serums) can also lead to a less selective reaction [10].

3.1.3. Click Chemistry and Hydrazone Bond

As miRNA capture and detection can still be considered a new branch of scientific research, many of the covalent conjugation strategies that are regularly used for binding targeting biomolecules or ligands to nanomaterials [9,10] have not yet been applied for miRNA, or only rarely. Two such examples are presented here, namely click chemistry and hydrazone bond.

In the variety of conjugation strategies with biomolecules exists the problem of undesired side reactions, due to the vast number of reactive sites and functional groups. While this is partially managed with specific coupling agents, they also may react with other functional groups (one such example is NHS, able to react with sulfhydryl and hydroxyl groups). This led to the development of bio-orthogonal chemistry, where reagents are stable (not prone to oxidization or hydrolyzation process) and have a reactive site that reacts only with a specific functional group.

These types of reactions are often referred to as click chemistry with their concept lying in a reaction that occurs quickly, under moderate conditions, and leads to a specific product (possibly with an easily removed by-product). Leading advancements of click chemistry were the developments of copper-catalyzed click chemistry followed by the copper-free approach, Diels–Alder cycloadditions, or Thiol–Michael click reactions. Click chemistry is also very popular in gene therapeutics, for easy conjugation of RNA, mRNA, and siRNA with, for example, fluorescent molecules [9,73].

Lu et al. used aggregation of AuNPs amplified by click chemistry for the detection of plant miRNA by DLS. Two probes, probe A, modified with dibenzocyclooctyne, and probe B, modified with azide, were synthesized to form a complementary sequence to target miRNA together. Hybridization with target miRNA leads to the close vicinity of both functional groups, forming a complex. Similarly, two types of AuNPs, with two sequences complementary to probe A and probe B, led to the respective attachment of both probes, and when in the presence of target miRNA, allowed the formation of bigger aggregates of AuNPs [74].

L. Zhou et al. employed click chemistry, i.e., the copper (I)-catalyzed azide–alkyne cycloaddition to combine two nucleic acid strands containing G-quadruplex DNA sequences. Alkyne-modified hairpin strand and azide-modified strand were bound by click chemistry reaction, forming complementary DNA capture probes, which were deposited on a Au electrode modified with fullerene nanoparticles [35].

Another type of bio-orthogonal conjugation method has a basis in reductive amination reaction (amine group is combined with organic molecule), where a hydrazone bond is

formed by a reaction between aldehydes and hydrazide groups. The synthetic procedure is straightforward with good reproducibility, and the unique advantage is the pH sensitivity of the resulting bond—the bond is stable at neutral pH but becomes easily affected at acidic pH [58].

Ye Wang applied hydrazone coupling chemistry catalyzed by aniline to conjugate a specific hexahistidine peptide to amine-functionalized DNA, which led to this complex being self-assembled onto the hydrophilic surface of fluorescent quantum dots [75].

These strategies are less commonly applied for the nano-conjugation of complementary miRNA sequences to the nanomaterial, due to a relatively recent focus on the conjugation via click chemistry, combined with even more recent interest in miRNA-related functionalization. Nevertheless, there is significant potential for more studies in this field.

3.2. Non-Covalent Conjugation

The formation of macromolecules through non-covalent bonding is very common in nature, using for example, hydrophobic effects, coordination chemistry, hydrogen bonding, and dipole interactions (electrostatic and weaker dispersion forces). Along with covalent attachment, thiolated molecules can be also used for non-covalent conjugation (generally depending on the pH of the solvent). If the biomolecule has available thiol residue, the sulfhydryl group can form a dative bond on the surface of the nanomaterial.

The method of non-covalent bonding presents several advantages, such as fast formulation, avoidance of complex bonding, and the possibility of a quick release in target sites while minimizing cytotoxicity. This results in simple and cost-effective synthesis requiring fewer chemical reagents, allowing for industrial production and clinical applications. Nevertheless, compared with the covalent bonds, non-covalent linking is weaker and more prone to dissolution out of specific conditions. Often the stability of such bonds is weak in biofluids, presenting a challenge to overcome for in vivo applications.

3.2.1. Non-Covalent Adsorption—Electrostatic and Hydrophobic/Hydrophilic Interactions

Electrostatic and hydrophobic/hydrophilic interactions are very well-known, their attractiveness being in the rapid binding process with no further chemical modification steps necessary. However, this type of passive adsorption results in a non-specific bond between the nanomaterial and the biomolecule, leading to reduced stability in biological fluids, and complicating the in vivo applications and the characterization of the functionalized nanomaterial.

Electrostatic interaction and subsequent adsorption on the surface of the nanomaterial originate from the attraction of two opposite charges. This interaction is non-specific, relying on the strength of the respective charges of the two interacting parts, and is susceptible to changes in experimental conditions (such as temperature, pH, and ionic strength). There is also a possibility of electrostatic complex dissociation due to the presence of other competing biomolecules and the following exchange [9].

As miRNA molecules are negatively charged, the high positive charge of polyethylenimine-capped AuNPs is suitable for the concentration of target miRNA-155. Hakimian et al. mixed the resulting complex with citrate-capped AuNPs covalently attached to a thiolated hairpin DNA probe. Both types of AuNPs formed cross-linking aggregates due to probe–target attachment, allowing detectable aggregation of AuNPs [49].

Ajgaonkar et al. used graphene quantum dots doped with nitrogen as a slightly positively charged nanoplatform, non-covalently bonding the single-stranded DNA capture probe. The electrostatic binding of the capture probe and the $\pi-\pi$ stacking onto the surface of the graphene-QDs altered their intrinsic fluorescence [76].

Despite the potential of non-covalent adsorption, the application remains limited due to the challenging and often weak stability presented by such bonds.

3.2.2. Streptavidin–Biotin

A well-known example of affinity interactions is the (strept)avidin–biotin interaction, which is irreversible and stable (unaffected by variations of temperature, pH, organic solvents, or denaturing agents). The natural high-affinity interaction occurring between (strept)avidin and biotin is similar to the interaction between enzyme and substrate (or receptor and ligand), and the resulting bond is approaching the strength of the covalent bonding.

Streptavidin is similar to avidin (glycoprotein consisting of four identical subunits), and as a biotin-binding protein, it possesses four binding sites to biotin, one for each subunit. Compared with avidin, it has a lower charge with a smaller possibility of electrostatic interaction with other biomolecules (or cell membranes), which also makes the protein less soluble in an aqueous medium. Furthermore, streptavidin is a non-glycosylated protein (without carbohydrate residues), making the likelihood of a non-specific bond to other molecules via carbohydrate receptors significantly smaller. It is possible to insert biotin (vitamin B7) into biomolecules without affecting their properties or activity. Carboxylic acid in this small molecule also allows covalent conjugation [77].

Both the nanomaterial and/or the biomolecule can be biotinylated, making it a very popular conjugation of choice. Likewise, streptavidin and biotin modifications are widely commercially available, allowing for easy use (one such example is pre-prepared streptavidin-modified magnetic nanoparticles, e.g., magnetic beads [78,79], QDs [75], biotin-modified RNA [13], or biotinylated DNA sequences [78]).

Streptavidin modification of NPs can be also performed with a cross-linking agent, such as presented by Chan et al. concerning silica-coated iron oxide NPs. After the amino-functionalization of the NPs, streptavidin was bonded to the surface with glutaraldehyde acting as a cross-linking agent. The biotinylated DNA was then linked to the streptavidin-coated NPs, and the resulting nanoprobes were used for the capture of a complex formed by target miRNA and molecular beacon containing target miRNA sequence [80].

In our previous publication, we modified the surface of PEGylated SPOINs with streptavidin. Biotin at the end of the PEG chain allowed close coverage of streptavidin, and the creation of the sufficient streptavidin layer of available biotin-binding spots enabled the functionalization with biotinylated complementary miRNA sequences, leading to the formation of nanoprobes with the ability to capture the target miRNA [50].

As was already mentioned, the combination of two or more conjugation approaches is very common. Cheng et al. deposited a thiolated hairpin probe on the surface of a gold electrode via the Au–S bond, and its loop structure was opened with the hybridization of target miRNA. The second hairpin probe modified with biotin lost the loop structure in the presence of the open first probe, leaving the biotinylated end to bind with AgNPs modified with streptavidin. The addition of more biotinylated AgNPs led to the aggregation of AgNPs and a stronger electrochemical signal [81].

A drawback in the extremely popular streptavidin–biotin conjugation is the large structure of the final complex, as streptavidin is a protein, and biotin itself is usually linked to the respective nanomaterial (or biomolecule) using a spacer (such as PEG chain) or cross-linking agent, adding to the final size and potentially affecting the binding rate [9].

Table 2. Covalent and non-covalent strategies for the functionalization of nanomaterials.

	Conjugation Strategy	Advantages	Disadvantages	References
Covalent conjugation	Carboxylic acid—amine bond	+ high stability; + high conjugation efficiency; + no chemical modification on the ligands	– low selectivity; – absence of control over ligand orientation; – reactions in acidic and water-free media	[42,54,65]
	Thiol bond	+ fast and selective reactions; + neutral pH media that avoid NP aggregation	– thiolation may hinder the biological activities of ligands; – non-selective in media containing thiol groups	[14,26,52]
	Click chemistry	+ site-specific conjugation; + higher yield; + control of ligand orientation; + mild conditions	– relatively new and more complicated than other methods; – possible toxicity with Cu(I) catalysts	[33,74]
	Hydrazone bond	+ stable at neutral pH	– easily affected by acidic pH	[75]
Non-covalent conjugation	Non-covalent adsorption: Electrostatic and hydrophobic/hydrophilic interactions	+ fast and easy formulation; + reduced toxicity due to high charges of NPs	– weak interactions and poor stability – harder to characterize	[49,76,82]
	(Strept)avidin–biotin	+ specific interaction + irreversible and stable + good orientation of conjugated ligands	– the large structure of the final complex – the potentially lower binding rate	[13,80,81]

4. Conclusions

Since the recognition of miRNAs as novel prognostic biomarkers, their accurate sensing and detection became crucial, especially in non-invasively obtained biofluids. As such, methods based on nanomaterials present several advantages stemming from unique properties (e.g., optical, magnetic, and electrochemical) depending on the chosen nanomaterial. Quite often, two or more types of nanomaterial can be combined in an effort to bring together several of their advantageous properties.

Covalent conjugations (carbodiimide bond, thiol bond, click chemistry, and hydrazone bond) form a stable covalent bond, while non-covalent conjugations (non-covalent adsorption, electrostatic, hydrophobic/hydrophobic interactions, and streptavidin–biotin interaction) rely on physical interactions between the ligand and the nanomaterial. Covalent conjugation often offers high stability, yield, and efficiency, at the cost of sensitivity to the medium of the reaction and pH, with, at times, lower selectivity. Similarly, non-covalent conjugation shows fast and easy formulation with the avoidance of complex chemical modification; however, the interactions are often weak and harder to characterize.

The mentioned limitations present interesting challenges in the functionalization of the nanomaterial, with the procedure generally expected to be simple, fast, and efficient. First, functionalization is often difficult to determine and requires a combination of two or more analytical techniques. Second, the overall stability and longevity of a nanoprobe or functionalized nanomaterial have to be controlled. Third, the binding affinity of the chosen nanoplatform connected to the subsequent miRNA capture, and its sensitivity to the media, pH, and composition needs to be better determined. On the other hand, the biomolecules naturally present in the biological samples can interfere with the functionalized nanoplatforms and lead to decreased selectivity and/or sensitivity. This issue depends on the experimental design of the capture and still needs to be studied in depth.

Considering the relatively young research field of miRNA detection, some of the conjugation approaches, which were successfully applied for ligands and biomolecules other than RNA sequences and their variations, have yet to be used. This fact leaves ample space for presenting novel applications on the road to functionalization with the goal of miRNA sensing.

Author Contributions: Conceptualization, K.H.-A., I.C. and I.V.; investigation, I.V.; data curation, I.V.; writing—original draft preparation, I.V.; writing—review and editing, K.H.-A. and I.C.; visualization, I.V.; supervision, K.H.-A. and I.C.; project administration, K.H.-A.; funding acquisition, K.H.-A. All authors have read and agreed to the published version of the manuscript.

Funding: This research was funded by "Ligue Nationale contre le Cancer" (the local committees 37, 53 and 56), in the project NANOmiR.

Institutional Review Board Statement: Not applicable.

Informed Consent Statement: Not applicable.

Data Availability Statement: No new data were created or analyzed in this study. Data sharing is not applicable to this article.

Conflicts of Interest: The authors declare no conflict of interest.

References

1. Gessner, I.; Fries, J.W.U.; Brune, V.; Mathur, S. Magnetic Nanoparticle-Based Amplification of MicroRNA Detection in Body Fluids for Early Disease Diagnosis. *J. Mater. Chem. B* **2021**, *9*, 9–22. [CrossRef] [PubMed]
2. Junqueira-Neto, S.; Batista, I.A.; Costa, J.L.; Melo, S.A. Liquid Biopsy beyond Circulating Tumor Cells and Cell-Free DNA. *Acta Cytol.* **2019**, *63*, 479–488. [CrossRef] [PubMed]
3. Chandrasekaran, A.R.; Punnoose, J.A.; Zhou, L.; Dey, P.; Dey, B.K.; Halvorsen, K. DNA Nanotechnology Approaches for MicroRNA Detection and Diagnosis. *Nucleic Acids Res.* **2019**, *47*, 10489–10505. [CrossRef]
4. Masud, M.K.; Umer, M.; Hossain, M.S.A.; Yamauchi, Y.; Nguyen, N.T.; Shiddiky, M.J.A. Nanoarchitecture Frameworks for Electrochemical MiRNA Detection. *Trends Biochem. Sci.* **2019**, *44*, 433–452. [CrossRef] [PubMed]
5. Jet, T.; Gines, G.; Rondelez, Y. Advances in Multiplexed Techniques for the Detection and Quantification of MicroRNAs. *Chem. Soc. Rev.* **2021**, *50*, 4141–4161. [CrossRef]
6. Grijalvo, S.; Alagia, A.; Jorge, A.F.; Eritja, R. Covalent Strategies for Targeting Messenger and Non-Coding RNAs: An Updated Review on SiRNA, MiRNA and AntimiR Conjugates. *Genes* **2018**, *9*, 74. [CrossRef]
7. Shen, Z.; He, L.; Wang, W.; Tan, L.; Gan, N. Highly Sensitive and Simultaneous Detection of MicroRNAs in Serum Using Stir-Bar Assisted Magnetic DNA Nanospheres-Encoded Probes. *Biosens. Bioelectron.* **2020**, *148*, 111831. [CrossRef]
8. Khashayar, P.; Al-Madhagi, S.; Azimzadeh, M.; Scognamiglio, V.; Arduini, F. New Frontiers in Microfluidics Devices for MiRNA Analysis. *TrAC Trends Anal. Chem.* **2022**, *156*, 116706. [CrossRef]
9. Pereira, G.; Monteiro, C.A.P.; Albuquerque, G.M.; Pereira, M.I.A.; Cabrera, M.P.; Cabral Filho, P.E.; Pereira, G.A.L.; Fontesa, A.; Santos, B.S. (Bio)Conjugation Strategies Applied to Fluorescent Semiconductor Quantum Dots. *J. Braz. Chem. Soc.* **2019**, *30*, 2536–2560. [CrossRef]
10. Nguyen, P.V.; Allard-vannier, E.; Chourpa, I.; Herv, K. Nanomedicines Functionalized with Anti-EGFR Ligands for Active Targeting in Cancer Therapy: Biological Strategy, Design and Quality Control. *Int. J. Pharm.* **2021**, *605*, 120795. [CrossRef]
11. Coutinho, C.; Somoza, Á. MicroRNA Sensors Based on Gold Nanoparticles. *Anal. Bioanal. Chem.* **2019**, *411*, 1807–1824. [CrossRef] [PubMed]
12. Yaman, Y.T.; Vural, O.A.; Bolat, G.; Abaci, S. One-Pot Synthesized Gold Nanoparticle-Peptide Nanotube Modified Disposable Sensor for Impedimetric Recognition of MiRNA 410. *Sens. Actuators B Chem.* **2020**, *320*, 128343. [CrossRef]
13. Lee, T.; Mohammadniaei, M.; Zhang, H.; Yoon, J.; Choi, H.K.; Guo, S.; Guo, P.; Choi, J.W. Single Functionalized PRNA/Gold Nanoparticle for Ultrasensitive MicroRNA Detection Using Electrochemical Surface-Enhanced Raman Spectroscopy. *Adv. Sci.* **2020**, *7*, 1902477. [CrossRef] [PubMed]
14. Akbal Vural, O.; Yaman, Y.T.; Bolat, G.; Abaci, S. Human Serum Albumin−Gold Nanoparticle Based Impedimetric Sensor for Sensitive Detection of MiRNA-200c. *Electroanalysis* **2021**, *33*, 925–935. [CrossRef]
15. González-Rubio, G.; De Oliveira, T.M.; Altantzis, T.; La Porta, A.; Guerrero-Martínez, A.; Bals, S.; Scarabelli, L.; Liz-Marzán, L.M. Disentangling the Effect of Seed Size and Crystal Habit on Gold Nanoparticle Seeded Growth. *Chem. Commun.* **2017**, *53*, 11360–11363. [CrossRef] [PubMed]
16. Polte, J. Fundamental Growth Principles of Colloidal Metal Nanoparticles—A New Perspective. *CrystEngComm* **2015**, *17*, 6809–6830. [CrossRef]

17. Fischer, A.; Thuenemann, A.F.; Emmerling, F.; Rademann, K.; Kraehnert, R.; Polte, J.; Tuaev, X.; Wuithschick, M. Formation Mechanism of Colloidal Silver Nanoparticles: Analogies and Differences to the Growth of Gold Nanoparticles. *ACS Nano* **2012**, *6*, 5791–5802. [CrossRef]
18. Li, H.; Cai, Q.; Yan, X.; Jie, G.; Jie, G. Ratiometric Electrochemical Biosensor Based on Silver Nanoparticles Coupled with Walker Amplification for Sensitive Detection of MicroRNA. *Sens. Actuators B Chem.* **2022**, *353*, 131115. [CrossRef]
19. Pang, Y.; Wang, C.; Wang, J.; Sun, Z.; Xiao, R.; Wang, S. Fe3O4@Ag Magnetic Nanoparticles for MicroRNA Capture and Duplex-Specific Nuclease Signal Amplification Based SERS Detection in Cancer Cells. *Biosens. Bioelectron.* **2016**, *79*, 574–580. [CrossRef]
20. Li, M.; Cheng, J.; Yuan, Z.; Shen, Q.; Fan, Q. DNAzyme-Catalyzed Etching Process of Au/Ag Nanocages Visualized via Dark-Field Imaging with Time Elapse for Ultrasensitive Detection of MicroRNA. *Sens. Actuators B Chem.* **2021**, *330*, 129347. [CrossRef]
21. Zhou, W.; Tian, Y.F.; Yin, B.C.; Ye, B.C. Simultaneous Surface-Enhanced Raman Spectroscopy Detection of Multiplexed MicroRNA Biomarkers. *Anal. Chem.* **2017**, *89*, 6120–6128. [CrossRef] [PubMed]
22. Sharma, V.K.; Siskova, K.M.; Zboril, R.; Gardea-Torresdey, J.L. Organic-Coated Silver Nanoparticles in Biological and Environmental Conditions: Fate, Stability and Toxicity. *Adv. Colloid Interface Sci.* **2014**, *204*, 15–34. [CrossRef] [PubMed]
23. Panáček, A.; Kvítek, L.; Smékalová, M.; Večeřová, R.; Kolář, M.; Röderová, M.; Dyčka, F.; Šebela, M.; Prucek, R.; Tomanec, O.; et al. Bacterial Resistance to Silver Nanoparticles and How to Overcome It. *Nat. Nanotechnol.* **2018**, *13*, 65–71. [CrossRef] [PubMed]
24. Knežević, N.; Gadjanski, I.; Durand, J.O. Magnetic Nanoarchitectures for Cancer Sensing, Imaging and Therapy. *J. Mater. Chem. B* **2019**, *7*, 9–23. [CrossRef]
25. Janko, C.; Ratschker, T.; Nguyen, K.; Zschiesche, L.; Tietze, R.; Lyer, S.; Alexiou, C. Functionalized Superparamagnetic Iron Oxide Nanoparticles (SPIONs) as Platform for the Targeted Multimodal Tumor Therapy. *Front. Oncol.* **2019**, *9*, 59. [CrossRef]
26. Li, M.; Li, J.; Zhang, X.; Yao, M.; Li, P.; Xu, W. Simultaneous Detection of Tumor-Related MRNA and MiRNA in Cancer Cells with Magnetic SERS Nanotags. *Talanta* **2021**, *232*, 122432. [CrossRef]
27. Leong, S.S.; Yeap, S.P.; Lim, J.K. Working Principle and Application of Magnetic Separation for Biomedical Diagnostic at High- and Low-Field Gradients. *Interface Focus* **2016**, *6*, 20160048. [CrossRef]
28. Goryacheva, O.A.; Novikova, A.S.; Drozd, D.D.; Pidenko, P.S.; Ponomaryeva, T.S.; Bakal, A.A.; Mishra, P.K.; Beloglazova, N.V.; Goryacheva, I.Y. Water-Dispersed Luminescent Quantum Dots for MiRNA Detection. *TrAC—Trends Anal. Chem.* **2019**, *111*, 197–205. [CrossRef]
29. Song, W.; Zhang, F.; Song, P.; Zhang, Z.; He, P.; Li, Y.; Zhang, X. Untrasensitive Photoelectrochemical Sensor for MicroRNA Detection with DNA Walker Amplification and Cation Exchange Reaction. *Sens. Actuators B Chem.* **2021**, *327*, 128900. [CrossRef]
30. Asadian, E.; Ghalkhani, M.; Shahrokhian, S. Electrochemical Sensing Based on Carbon Nanoparticles: A Review. *Sens. Actuators B Chem.* **2019**, *293*, 183–209. [CrossRef]
31. Li, H.; Li, Y.; Li, W.; Cui, L.; Huang, G.; Huang, J. A Carbon Nanoparticle and DNase I-Assisted Amplified Fluorescent Biosensor for MiRNA Analysis. *Talanta* **2020**, *213*, 120816. [CrossRef] [PubMed]
32. Liu, Q.; Bai, W.; Guo, Z.; Zheng, X. Enhanced Electrochemiluminescence of Ru(Bpy)32+-Doped Silica Nanoparticles by Chitosan/Nafion Shell@carbon Nanotube Core-Modified Electrode. *Luminescence* **2021**, *36*, 642–650. [CrossRef] [PubMed]
33. Sahtani, K.; Aykut, Y.; Tanik, N.A. Lawsone Assisted Preparation of Carbon Nanofibers for the Selective Detection of MiRNA Molecules. *J. Chem. Technol. Biotechnol.* **2022**, *97*, 254–269. [CrossRef]
34. Gao, Y.; Yu, H.; Tian, J.; Xiao, B. Nonenzymatic DNA-Based Fluorescence Biosensor Combining Carbon Dots and Graphene Oxide with Target-Induced DNA Strand Displacement for MicroRNA Detection. *Nanomaterials* **2021**, *11*, 2608. [CrossRef]
35. Zhou, L.; Wang, T.; Bai, Y.; Li, Y.; Qiu, J.; Yu, W.; Zhang, S. Dual-Amplified Strategy for Ultrasensitive Electrochemical Biosensor Based on Click Chemistry-Mediated Enzyme-Assisted Target Recycling and Functionalized Fullerene Nanoparticles in the Detection of MicroRNA-141. *Biosens. Bioelectron.* **2020**, *150*, 111964. [CrossRef]
36. Wang, Y.; Li, M.; Zhang, Y. Electrochemical Detection of MicroRNA-21 Based on a Au Nanoparticle Functionalized g-C3N4 Nanosheet Nanohybrid as a Sensing Platform and a Hybridization Chain Reaction Amplification Strategy. *Analyst* **2021**, *146*, 2886–2893. [CrossRef] [PubMed]
37. Islam, M.N.; Gorgannezhad, L.; Masud, M.K.; Tanaka, S.; Hossain, M.S.A.; Yamauchi, Y.; Nguyen, N.T.; Shiddiky, M.J.A. Graphene-Oxide-Loaded Superparamagnetic Iron Oxide Nanoparticles for Ultrasensitive Electrocatalytic Detection of MicroRNA. *ChemElectroChem* **2018**, *5*, 2488–2495. [CrossRef]
38. Liu, L.; Wei, Y.; Jiao, S.; Zhu, S.; Liu, X. A Novel Label-Free Strategy for the Ultrasensitive MiRNA-182 Detection Based on MoS_2/Ti_3C_2 Nanohybrids. *Biosens. Bioelectron.* **2019**, *137*, 45–51. [CrossRef]
39. Wang, M.; Chen, W.; Tang, L.; Yan, R.; Miao, P. Duplex-Specific Nuclease Assisted MiRNA Assay Based on Gold and Silver Nanoparticles Co-Decorated on Electrode Interface. *Anal. Chim. Acta* **2020**, *1107*, 23–29. [CrossRef]
40. Yammouri, G.; Mohammadi, H.; Amine, A. A Highly Sensitive Electrochemical Biosensor Based on Carbon Black and Gold Nanoparticles Modified Pencil Graphite Electrode for MicroRNA-21 Detection. *Chem. Afr.* **2019**, *2*, 291–300. [CrossRef]
41. Zhu, R.; Feng, H.; Li, Q.; Su, L.; Fu, Q.; Li, J.; Song, J.; Yang, H. Asymmetric Core–Shell Gold Nanoparticles and Controllable Assemblies for SERS Ratiometric Detection of MicroRNA. *Angew. Chem.* **2021**, *133*, 12668–12676. [CrossRef]
42. Yao, Y.; Zhang, H.; Tian, T.; Liu, Y.; Zhu, R.; Ji, J.; Liu, B. Iodide-Modified Ag Nanoparticles Coupled with DSN-Assisted Cycling Amplification for Label-Free and Ultrasensitive SERS Detection of MicroRNA-21. *Talanta* **2021**, *235*, 122728. [CrossRef]

43. Mehdipour, M.; Gloag, L.; Bennett, D.T.; Hoque, S.; Pardehkhorram, R.; Bakthavathsalam, P.; Gonçales, V.R.; Tilley, R.D.; Gooding, J.J. Synthesis of Gold-Coated Magnetic Conglomerate Nanoparticles with a Fast Magnetic Response for Bio-Sensing. *J. Mater. Chem. C* **2021**, *9*, 1034–1043. [CrossRef]
44. Wang, H.; Tang, H.; Yang, C.; Li, Y. Selective Single Molecule Nanopore Sensing of MicroRNA Using PNA Functionalized Magnetic Core-Shell Fe_3O_4-Au Nanoparticles. *Anal. Chem.* **2019**, *91*, 7965–7970. [CrossRef] [PubMed]
45. Borghei, Y.S.; Hosseini, M.; Ganjali, M.R. A Label-Free Luminescent Light Switching System for MiRNA Detection Based on Two Color Quantum Dots. *J. Photochem. Photobiol. A Chem.* **2020**, *391*, 112351. [CrossRef]
46. Niu, X.; Lu, C.; Su, D.; Wang, F.; Tan, W.; Qu, F. Construction of a Polarity-Switchable Photoelectrochemical Biosensor for Ultrasensitive Detection of MiRNA-141. *Anal. Chem.* **2021**, *93*, 13727–13733. [CrossRef]
47. Pothipor, C.; Jakmunee, J.; Bamrungsap, S.; Ounnunkad, K. An Electrochemical Biosensor for Simultaneous Detection of Breast Cancer Clinically Related MicroRNAs Based on a Gold Nanoparticles/Graphene Quantum Dots/Graphene Oxide Film. *Analyst* **2021**, *146*, 4000–4009. [CrossRef]
48. Wang, W. Label-Free Electrochemical Sensor for MicroRNA Detection Based on a Gold Nanoparticles@Poly(Methylene Blue)-Modified Electrode and a Target Cyclic Amplification Strategy. *Int. J. Electrochem. Sci.* **2020**, *15*, 4631–4639. [CrossRef]
49. Hakimian, F.; Ghourchian, H.; Hashemi, A.S.; Arastoo, M.R.; Behnam Rad, M. Ultrasensitive Optical Biosensor for Detection of MiRNA-155 Using Positively Charged Au Nanoparticles. *Sci. Rep.* **2018**, *8*, 2943. [CrossRef]
50. Vilímová, I.; Chourpa, I.; David, S.; Soucé, M.; Hervé-Aubert, K. Two-Step Formulation of Magnetic Nanoprobes for MicroRNA Capture. *RSC Adv.* **2022**, *12*, 7179–7188. [CrossRef]
51. Afzalinia, A.; Mirzaee, M. Ultrasensitive Fluorescent MiRNA Biosensor Based on a "Sandwich" Oligonucleotide Hybridization and Fluorescence Resonance Energy Transfer Process Using an Ln(III)-MOF and Ag Nanoparticles for Early Cancer Diagnosis: Application of Central Composite Design. *ACS Appl. Mater. Interfaces* **2020**, *12*, 16076–16087. [CrossRef]
52. Bao, J.; Hou, C.; Zhao, Y.; Geng, X.; Samalo, M.; Yang, H.; Bian, M.; Huo, D. An Enzyme-Free Sensitive Electrochemical MicroRNA-16 Biosensor by Applying a Multiple Signal Amplification Strategy Based on Au/PPy–RGO Nanocomposite as a Substrate. *Talanta* **2019**, *196*, 329–336. [CrossRef] [PubMed]
53. Xu, W.; Zhao, A.; Zuo, F.; Khan, R.; Hussain, H.M.J.; Chang, J. Au@Ag Core-Shell Nanoparticles for MicroRNA-21 Determination Based on Duplex-Specific Nuclease Signal Amplification and Surface-Enhanced Raman Scattering. *Microchim. Acta* **2020**, *187*, 384. [CrossRef] [PubMed]
54. Yazdanparast, S.; Benvidi, A.; Azimzadeh, M.; Tezerjani, M.D.; Ghaani, M.R. Experimental and Theoretical Study for MiR-155 Detection through Resveratrol Interaction with Nucleic Acids Using Magnetic Core-Shell Nanoparticles. *Microchim. Acta* **2020**, *187*, 479. [CrossRef]
55. Gessner, I.; Yu, X.; Jüngst, C.; Klimpel, A.; Wang, L.; Fischer, T.; Neundorf, I.; Schauss, A.C.; Odenthal, M.; Mathur, S. Selective Capture and Purification of MicroRNAs and Intracellular Proteins through Antisense-Vectorized Magnetic Nanobeads. *Sci. Rep.* **2019**, *9*, 2069. [CrossRef]
56. Borghei, Y.S.; Hosseini, M. A New Eye Dual-Readout Method for MiRNA Detection Based on Dissolution of Gold Nanoparticles via LSPR by CdTe QDs Photoinduction. *Sci. Rep.* **2019**, *9*, 5453. [CrossRef] [PubMed]
57. Hermanson, G.T. *Bioconjugate Techniques*, 3rd ed.; Audet, J., Preap, M., Eds.; Elsevier: London, UK, 2013; ISBN 9780123822390.
58. Amaral, G.; Bushee, J.; Cordani, U.G.; Kawashita, K.; Reynolds, J.H.; Almeida, F.F.M.D.E.; de Almeida, F.F.M.; Hasui, Y.; de Brito Neves, B.B.; Fuck, R.A.; et al. *Applications of Nanocomposite Materials in Drug Delivery*; Woodhead Publishing: Cambridge, UK, 2013; Volume 369, ISBN 9789896540821.
59. Sunasee, R.; Narain, R. *Covalent and Noncovalent Bioconjugation Strategies*, 1st ed.; Narain, R., Ed.; Wiley: Hoboken, NJ, USA, 2014; ISBN 9781118359143.
60. Xu, Z.-H.; Wang, H.; Wang, J.; Zhao, W.; Xu, J.-J.; Chen, H.-Y. Bidirectional Electrochemiluminescent Sensing: An Application in Detecting MiRNA-141. *Anal. Chem.* **2019**, *91*, 12000–12005. [CrossRef]
61. Chen, W.Y.; Wang, C.H.; Wang, K.H.; Chen, Y.L.; Chau, L.K.; Wang, S.C. Development of Microfluidic Concentrator Using Ion Concentration Polarization Mechanism to Assist Trapping Magnetic Nanoparticle-Bound MiRNA to Detect with Raman Tags. *Biomicrofluidics* **2020**, *14*, 014102. [CrossRef]
62. Gu, T.; Li, Z.; Ren, Z.; Li, X.; Han, G. Rare-Earth-Doped Upconversion Nanocrystals Embedded Mesoporous Silica Nanoparticles for Multiple MicroRNA Detection. *Chem. Eng. J.* **2019**, *374*, 863–869. [CrossRef]
63. Mahani, M.; Mousapour, Z.; Divsar, F.; Nomani, A.; Ju, H. A Carbon Dot and Molecular Beacon Based Fluorometric Sensor for the Cancer Marker MicroRNA-21. *Microchim. Acta* **2019**, *186*, 132. [CrossRef]
64. Salimi, A.; Kavosi, B.; Navaee, A. Amine-Functionalized Graphene as an Effective Electrochemical Platform toward Easily MiRNA Hybridization Detection. *Meas. J. Int. Meas. Confed.* **2019**, *143*, 191–198. [CrossRef]
65. Horny, M.C.; Gamby, J.; Dupuis, V.; Siaugue, J.M. Magnetic Hyperthermia on γ-Fe_2O_3@SiO_2 Core-Shell Nanoparticles for Mi-RNA 122 Detection. *Nanomaterials* **2021**, *11*, 149. [CrossRef] [PubMed]
66. Lillo, A.M.; Lopez, C.L.; Rajale, T.; Yen, H.J.; Magurudeniya, H.D.; Phipps, M.L.; Balog, E.R.M.; Sanchez, T.C.; Iyer, S.; Wang, H.L.; et al. Conjugation of Amphiphilic Proteins to Hydrophobic Ligands in Organic Solvent. *Bioconjug. Chem.* **2018**, *29*, 2654–2664. [CrossRef]
67. Xue, Y.; Li, X.; Li, H.; Zhang, W. Quantifying Thiol-Gold Interactions towards the Efficient Strength Control. *Nat. Commun.* **2014**, *5*, 4348. [CrossRef] [PubMed]

68. Al Mubarak, Z.H.; Premaratne, G.; Dharmaratne, A.; Mohammadparast, F.; Andiappan, M.; Krishnan, S. Plasmonic Nucleotide Hybridization Chip for Attomolar Detection: Localized Gold and Tagged Core/Shell Nanomaterials. *Lab Chip* **2020**, *20*, 717–721. [CrossRef] [PubMed]
69. Zhu, Q.; Li, H.; Xu, D. Sensitive and Enzyme-Free Fluorescence Polarization Detection for MiRNA-21 Based on Decahedral Sliver Nanoparticles and Strand Displacement Reaction. *RSC Adv.* **2020**, *10*, 17037–17044. [CrossRef]
70. Ma, X.; Ma, Y.; Ejeromedoghene, O.; Kandawa-schulz, M.; Song, W.; Wang, Y. Dual-Mode Corroborative Detection of MiRNA-21 Based on Catalytic Hairpin Assembly Reaction and Oxygen Reduction Reaction Combined Strategy for the Signal Amplification. *Sens. Actuators B. Chem.* **2022**, *364*, 131924. [CrossRef]
71. Zhao, Y.; Lu, C.; Zhao, X.; Kong, W.; Zhu, S.; Qu, F. A T-Rich Nucleic Acid-Enhanced Electrochemical Platform Based on Electroactive Silver Nanoclusters for MiRNA Detection. *Biosens. Bioelectron.* **2022**, *208*, 114215. [CrossRef]
72. Sun, Y.; Li, T. Composition-Tunable Hollow Au/Ag SERS Nanoprobes Coupled with Target-Catalyzed Hairpin Assembly for Triple-Amplification Detection of MiRNA. *Anal. Chem.* **2018**, *90*, 11614–11621. [CrossRef]
73. Astakhova, K.; Ray, R.; Taskova, M.; Uhd, J.; Carstens, A.; Morris, K. "clicking" Gene Therapeutics: A Successful Union of Chemistry and Biomedicine for New Solutions. *Mol. Pharm.* **2018**, *15*, 2892–2899. [CrossRef]
74. Lu, X.; Fan, W.; Feng, Q.; Qi, Y.; Liu, C.; Li, Z. A Versatile Dynamic Light Scattering Strategy for the Sensitive Detection of Plant MicroRNAs Based on Click-Chemistry-Amplified Aggregation of Gold Nanoparticles. *Chem.—Eur. J.* **2019**, *25*, 1701–1705. [CrossRef] [PubMed]
75. Wang, Y.; Howes, P.D.; Kim, E.; Spicer, C.D.; Thomas, M.R.; Lin, Y.; Crowder, S.W.; Pence, I.J.; Stevens, M.M. Duplex-Specific Nuclease-Amplified Detection of MicroRNA Using Compact Quantum Dot-DNA Conjugates. *ACS Appl. Mater. Interfaces* **2018**, *10*, 28290–28300. [CrossRef] [PubMed]
76. Ajgaonkar, R.; Lee, B.; Valimukhametova, A.; Nguyen, S.; Gonzalez-rodriguez, R.; Coffer, J.; Akkaraju, G.R.; Naumov, A. V Detection of Pancreatic Cancer MiRNA with Biocompatible Nitrogen-Doped Graphene Quantum Dots. *Materials* **2022**, *15*, 5760. [CrossRef] [PubMed]
77. Su, X.; Wu, Y.J.; Robelek, R.; Knoll, W. Surface Plasmon Resonance Spectroscopy and Quartz Crystal Microbalance Study of Streptavidin Film Structure Effects on Biotinylated DNA Assembly and Target DNA Hybridization. *Langmuir* **2005**, *21*, 348–353. [CrossRef] [PubMed]
78. Tian, B.; Han, Y.; Wetterskog, E.; Donolato, M.; Hansen, M.F.; Svedlindh, P.; Strömberg, M. MicroRNA Detection through DNAzyme-Mediated Disintegration of Magnetic Nanoparticle Assemblies. *ACS Sens.* **2018**, *3*, 1884–1891. [CrossRef]
79. Djebbi, K.; Shi, B.; Weng, T.; Bahri, M.; Elaguech, M.A.; Liu, J.; Tlili, C.; Wang, D. Highly Sensitive Fluorescence Assay for MiRNA Detection: Investigation of the DNA Spacer E Ff Ect on the DSN Enzyme Activity toward Magnetic-Bead-Tethered Probes. *ASC Omega* **2022**, *1*, 2224–2233. [CrossRef]
80. Chan, H.N.; Ho, S.L.; He, D.; Li, H.W. Direct and Sensitive Detection of Circulating MiRNA in Human Serum by Ligase-Mediated Amplification. *Talanta* **2020**, *206*, 120217. [CrossRef]
81. Cheng, W.; Ma, J.; Cao, P.; Zhang, Y.; Xu, C.; Yi, Y.; Li, J. Enzyme-Free Electrochemical Biosensor Based on Double Signal Amplification Strategy for the Ultra-Sensitive Detection of Exosomal MicroRNAs in Biological Samples. *Talanta* **2020**, *219*, 121242. [CrossRef]
82. Segal, M.; Biscans, A.; Gilles, M.E.; Anastasiadou, E.; De Luca, R.; Lim, J.; Khvorova, A.; Slack, F.J. Hydrophobically Modified Let-7b MiRNA Enhances Biodistribution to NSCLC and Downregulates HMGA2 In Vivo. *Mol. Ther.—Nucleic Acids* **2020**, *19*, 267–277. [CrossRef]

Publication 2:

Two-step formulation of magnetic nanoprobes for microRNA capture

Accepted in “RSC Advances”, March 2022

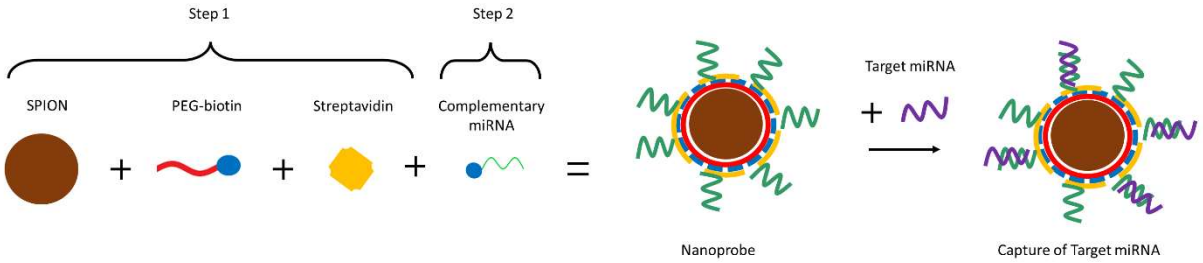

Préambule de la Publication 2

Les microARN (miR) appartiennent à une famille d'ARN endogènes courts non codants. Leur surexpression est corrélée à diverses pathologies : par exemple, le miARN-155 (miR-155) est surexprimé lors du développement des cancers du sein. Cependant, la détection des miRs comme biomarqueurs de la maladie souffre d'une sensibilité insuffisante. Dans la présente étude, nous proposons un protocole pour générer de façon rapide et efficace des nanosondes magnétiques capables d'isoler des miR-155, dans le but d'augmenter leur concentration. En tant que précurseur de nanosonde, nous avons d'abord synthétisé des nanoparticules d'oxyde de fer superparamagnétiques (SPION) recouvertes de polyéthylène glycol, lié de façon covalente, portant des groupements biotines à leur extrémité (PEG-bi). En utilisant des interactions streptavidine-biotine, les nanosondes ont été formulées, en fonctionnalisant la surface des nanoparticules avec la séquence d'ARN complémentaire (CmiR) de la cible miR-155 (TmiR). La formulation en deux étapes a été optimisée et validée à l'aide de plusieurs techniques analytiques, en particulier avec la chromatographie liquide à haute performance par exclusion de taille (SE-HPLC). Enfin, la preuve de l'affinité des nanosondes pour les TmiRs a été démontrée par l'isolation des TmiRs cibles dans des solutions modèles, avec un ratio estimé de 18 : 22 TmiR : CmiR par nanosonde. La stabilité des nanosondes a été confirmée après incubation dans du sérum.

RSC Advances

PAPER

View Article Online
View Journal | View Issue

Check for updates

Cite this: *RSC Adv.*, 2022, **12**, 7179

Two-step formulation of magnetic nanoprobes for microRNA capture

Iveta Vilímová, Igor Chourpa, Stéphanie David, Martin Soucé and Katel Hervé-Aubert *

MicroRNAs (miRs) belong to a family of short non-coding endogenous RNAs. Their over-expression correlates with various pathologies: for instance, miRNA-155 (miR-155) is over-expressed upon the development of breast cancers. However, the detection of miRs as disease biomarkers suffers from insufficient sensitivity. In the present study, we propose a protocol for a rapid and efficient generation of magnetic nanoprobes able to capture miR-155, with the aim of increasing its concentration. As a nanoprobe precursor, we first synthesized superparamagnetic iron oxide nanoparticles (SPIONs) coated with covalently attached polyethylene glycol carrying a free biotin terminus (PEG-bi). Using streptavidin–biotin interactions, the nanoprobes were formulated by functionalizing the surface of the nanoparticles with the miR sequence (CmiR) complementary to the target miR-155 (TmiR). The two-step formulation was optimized and validated using several analytical techniques, in particular with Size-Exclusion High Performance Liquid Chromatography (SE-HPLC). Finally, the proof of the nanoprobe affinity to TmiR was made by demonstrating the TmiR capture on model solutions, with the estimated ratio of 18 : 22 TmiR : CmiR per nanoprobe. The nanoprobes were confirmed to be stable after incubation in serum.

Received 13th December 2021
Accepted 8th February 2022

DOI: 10.1039/d1ra09016j

rsc.li/rsc-advances

Open Access Article. Published on 02 March 2022. Downloaded on 1/8/2023 3:48:03 PM.
This article is licensed under a Creative Commons Attribution-NonCommercial 3.0 Unported Licence.

1. Introduction

MicroRNAs (miR) are small non-coding RNAs with lengths ranging from 19 to 23 nucleotides. MiRs act as regulators in post-transcriptional gene expression by targeting specific messenger RNAs. They play a major part in various biological processes, which are influenced by dysregulation in miR expression levels.[1,2]

As such, miRs are considered as novel biomarkers for diagnostics and therapeutics of various diseases (*e.g.*, numerous types of cancer, neurological and muscle degenerative diseases, cardiovascular disorders, *etc.*). A large part of the scientific research is focused on the atypical expression of miRs present in different types of cancer. Depending on their altered expression, miRs can be oncogenic (increased expression leading to inhibition of tumor suppressor genes and subsequent malignancy), or tumor-suppressing (obstructing the expression of oncogenes).[3] The disruption of the balance between these two types impacts cellular development, leading to cancer development. As the expression levels of multiple miRs either increase or decrease compared to the healthy tissue, the focus is put on developing new methods with better sensitivity and detection limits.[4,5]

One of the popular analytical methods widely used for purity determination and batch-to-batch comparison of compounds (miRs included) in pharmaceutical use is Size Exclusion High Performance Liquid Chromatography (SE-HPLC). It is built on separating the mixture in a solution into smaller components. A liquid mobile phase passes through the column filled with particles of a certain size, *i.e.*, stationary phase. As the solution is pumped through the column, the components of the solution interact differently with the surface of the particles of the stationary phase and are separated in the process, coming out of the column at different and specific retention times. Commercially available miRs are purified by HPLC, in order to eliminate shorter lengths species originating from the possible degradation. Precise determination of separation, isolation, and purification of nucleotides from biological samples still requires a lot of effort, and there are limits for qualitative analysis abilities by the means of quantification and identification.[6–8]

Beyond generally used methods for miR detection (qRT-PCR,[9,10] Northern blotting,[11] next-generation sequencing,[12,13] microarrays,[14,15] *etc.*), other approaches based on nanomaterials are becoming progressively more popular, either in combination with a well-known method or by developing altogether new ones.[16]

Methods and approaches of miR detection based on nanotechnologies offer an alternative path to a faster and less complicated detection process. Nanomaterials used can be in

EA6295 Nanomédicaments et Nanosondes, Université de Tours, Tours, France. E-mail: katel.herve@univ-tours.fr

© 2022 The Author(s). Published by the Royal Society of Chemistry

Open Access Article. Published on 02 March 2022. Downloaded on 1/8/2023 3:48:03 PM.
This article is licensed under a Creative Commons Attribution-NonCommercial 3.0 Unported Licence.

a form of nanoparticles, colloids, substrates, *etc.* They provide unique optical, electrical, and magnetic properties,[17] and most importantly, high surface area, leaving room for a plethora of surface-active chemical groups, which can be utilized in the subsequent immobilization of target biomolecules. The sensing application and efficiency of nanomaterials have been demonstrated.[18,19] Specific challenges include reproducibility, standardization, normalization, and data processing. Surprisingly, a significant part of the reported studies did not deal with natural bodily fluids (serum, blood, saliva, *etc.*) in the presence of possibly interfering biomolecules.[20]

One possible way of using nanoprobes is to capture on their surface the target miR (TmiR) present in the biological fluid. The TmiR capture efficiency and specificity can be enhanced by using the nanoprobe surface decorated with a complementary miR sequence[21] (hereafter called CmiR), double/single-stranded DNA,[22] or sequence of oligonucleotides.[23] Thus, successful design, production, and use of the TmiR-specific nanoprobes depend on several important considerations such as (i) synthesis of the nanomaterial (core), (ii) surface modification (platform), and (iii) surface functionalization (specific activation).

Hybrid nanoprobes (inorganic core–organic shell) are of high interest since their utilization allows to take benefit from unique physical properties of the inorganic core while controlling the stability due to the organic shell.[24]

The core–shell nanoprobes chosen for this study are based on the hybrid nanoparticles developed by our group and made of superparamagnetic iron oxide nanoparticles (SPIONs) coated with polyethylene glycol (PEG).[25]

Our working hypothesis was that the TmiR present in biological samples can be efficiently captured on the surface of the nanoprobes functionalized with specific CmiR and then the TmiR can be reconcentrated by magnetic sorting (Fig. 1A), thus favoring their more sensitive detection. PEGylation of SPIONs is used for enhancement of their biocompatibility and colloidal stability in aqueous media while preserving relative surface neutrality. We have selected a PEG chain modified with *N*-succinimidyl ester (NHS) on one end, and with biotin on the other (here-after called PEG-bi), for further conjugation *via* streptavidin–biotin affinity interactions.[26] Streptavidin- and biotin-modified materials are widely commercially available, for either the nanomaterial matrix or the biomolecule shell. Streptavidin-coated magnetic nanoparticles,[27] microparticles, or beads are very popular: for instance, they were exploited for detection of miR-144 (ref. 28) (*via* fluorescence signal amplification), or miR-21 (ref. 29) (*via* liquid chromatography-electrospray ionization tandem mass spectrometry). In our study, we formulated the nanoprobes starting from the PEGylated SPIONs and using streptavidin as a linker between the biotinylated nanoparticle surface and biotinylated CmiR (Fig. 1B). The idea is that the PEGylated SPIONs play a role of a versatile nanoplatform that can be used to easily formulate nanoprobes decorated with various CmiRs and therefore adaptable to various TmiRs.

After synthesis and characterization of SPION–PEG-bi nanoplatforms, we formulated and characterized several batches of the nanoprobes decorated with a model CmiR, specific to TmiR-155 upregulated in breast cancer cells and one of the most commonly reported miRs in body fluids.[1,30]

Several physicochemical characteristics of the nanosystems were established by means of a spectrum of analytical techniques: nanoparticle size (hydrodynamic diameter – D_H by DLS-dynamic light scattering) and chemical composition (iron concentration by AAS – atomic absorption spectrophotometry, organic shell identification by IR spectrophotometry, miR concentrations by SE-HPLC). The results confirmed the successful synthesis of the SPION–PEG-bi nanoplatforms and allowed us to optimize the nanoprobes formulation in terms of their surface saturation with streptavidin (formulation step 1) and of their functionalization with CmiR (formulation step 2). The function of synthesized nanoprobes was confirmed by trying out their ability to capture TmiR-155, and their stability was tested by an incubation in serum.

2 Experimental

2.1 Materials

Deionized water (18 MΩ) was used in all experiments. α-Biotinyl-ω-NHS PEG, M_w 5000 Da, (NHS–PEG_{5000}–biotin, PEG-bi) was purchased from Rapp Polymere (Tübingen, Germany). Streptavidin in lyophilized form, CmiR-155 modified with biotin ([Btn]-5′-ACCCCUAUCACGAUUAGCAUUAA-3′, 7674 g mol^{-1}) and TmiR-155 (5′-UUAAUGCUAAUCGUGAUAGGGGU-3′, 7391 g mol^{-1}) were purchased from Sigma-Aldrich (Saint Quentin-Fallavier, France). Standard miR solutions at required concentrations were prepared by adding RNAse-free deionized water.

2.2 Synthesis of the nanoprobe precursors – SPIONs coated with PEG-bi (NP)

The synthesis of PEG-biotin-coated SPIONs was divided into 3 steps: (i) the coprecipitation of initial SPIONs, (ii) the silanization of SPION's surface, and (iii) the covering of silanized SPIONs with the PEG-bi layer.

The synthesis of initial SPIONs by improved Massart's method and the silanization of SPIONs *via* surface amination with 3-aminopropyl-trimethoxysilane (APS) were performed according to the protocol published by our group.[25] Afterwards, the surface of the particles was PEGylated by the following procedure.

A mixture of 1.6 mL of silanized SPIONs (0.14 mmol of iron) and 10 mL of DMSO was prepared, and the solution was dehydrated in a vacuum for 5 h with a rotary evaporator. Lyophilized NHS–PEG_{5000}–biotin (220 mg, 0.04 mmol) was dissolved in 5 mL of dehydrated DMSO and added to the SPIONs mixture. The suspension was stirred for 24 h at the room temperature and afterward purified by dialysis (MWCO 1000 kDa) against water at the room temperature for 48 h.

2.3 Formulation of the nanoprobes

The formulation was made in two steps: (i) modification of the NP surface with streptavidin to result in NP–STR; and (ii)

© 2022 The Author(s). Published by the Royal Society of Chemistry

Open Access Article. Published on 02 March 2022. Downloaded on 1/8/2023 3:48:03 PM.
This article is licensed under a Creative Commons Attribution-NonCommercial 3.0 Unported Licence.

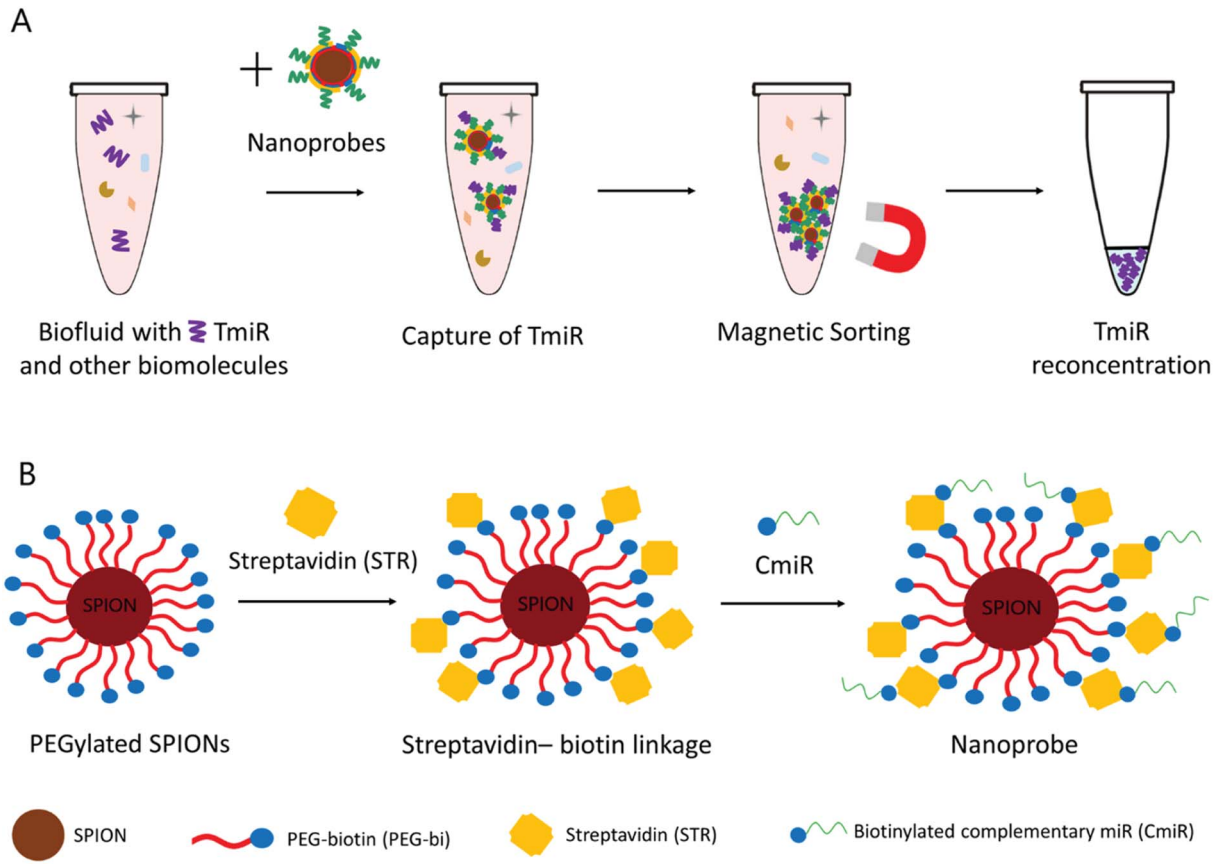

Fig. 1 (A) TmiR capture and reconcentration in a biofluid. (B) Schematic representation of the nanoprobe formulation from the PEGylated SPIONs.

functionalization of the NP–STR with CmiR to result in NP-STR-CmiR.

2.3.1 Streptavidin-modified nanoparticles (NP–STR). For modification of PEGylated SPIONs with STR, we used the interaction between STR and the biotin functional groups already present on the PEG-bi shell of the NP. To optimize the STR coating, we studied three batches of NP–STR with Fe/STR molar ratios of 280 (NP–STR1), 1400 (NP–STR2), and 2100 (NP–STR3).

NP-STR1 (Fe/STR = 280 molar ratio) was generated by mixing 400 μL of NP suspension at an iron concentration of 350 mg L^{-1} with 500 μL of 1 mg mL^{-1} STR and 100 μL of PBS 10X. The other two batches, NP-STR2 (Fe/STR = 1400) and NP–STR3 (Fe/STR = 2100) were generated accordingly.

All the samples were shaken overnight at room temperature. The resulting NP–STR were purified by magnetic separation (protocol described in Section 2.6) in order to eliminate an excess of streptavidin.

2.3.2 NP–STR functionalized with C-miR (NP–STR–CmiR). The batch NP–STR1 was selected as optimally modified with STR and was further functionalized by incubating it for 2 hours with 1, 5, or 10 μM aqueous solution of biotinylated complementary CmiR sequence. According to the CmiR concentration used, the resulting batches were named respectively: NP–STR–CmiR1 (1 μM CmiR); NP–STR–CmiR5 (5 μM CmiR); NP–STR–CmiR10 (10 μM CmiR). The final molar ratio Fe/CmiR in those batches was respectively 1.9, 4.75, and 9.5. The resulting NP–STR–CmiR were purified by magnetic separation (protocol in Section 2.6) in order to eliminate an excess of CmiR.

The number of CmiR molecules per nanoparticle (N) was determined with the following formula:

$$N = C \times \frac{\pi D^3}{6} \times d \times 6.10^{23}$$

with C: the amount of CmiR in mol per g of iron; D: diameter of SPION core (m, as defined by TEM); d: mass density of magnetite $= 5.2 \times 10^6$ g m^{-3}; Avogadro's number $= 6 \times 10^{23}$ mol^{-1}.

2.4. TmiR capture by nanoprobes

The batch of nanoprobes NP–STR–CmiR5 (5 μM CmiR) was combined with the solution of TmiR to reach a 5 μM final concentration of TmiR and incubated for 2 hours. The resulting sample NP–STR–CmiR–TmiR was purified by magnetic separation (protocol in Section 2.6) in order to eliminate any free TmiR.

2.5 Stability of nanoprobes

The batch of nanoprobes NP-STR-CmiR5 (5 μM CmiR) was combined with the solution of fetal bovine serum (FBS)

© 2022 The Author(s). Published by the Royal Society of Chemistry

Open Access Article. Published on 02 March 2022. Downloaded on 1/8/2023 3:48:03 PM.
This article is licensed under a Creative Commons Attribution-NonCommercial 3.0 Unported Licence.

(Eurobio, Les Ulis, France) in the ratio 1 : 1, and incubated at room temperature for 4 and 12 hours. The resulting samples (S4)-NP–STR–CmiR5 and (S12)-NP–STR–CmiR5 were purified by magnetic separation (protocol in the Section 2.6).

2.6 Magnetic separation

Magnetic separation (MS) was performed with MS columns (MACS® Column Technology, Miltenyi Biotec GmbH, Germany). The volume of the SPIONs suspension (up to 500 μL, depending on the initial volume of the sample) was applied into a MS column held in a magnetic MACS separator, and the separated liquid was collected. The column was then washed three times with the buffer (PBS 1X). The column was removed from the magnetic separator and flushed with the buffer (75% of the initial volume) resulting in a sample, utilized in the following synthetic procedures. MS was used for purification of the batches after each step of the synthesis, *i.e.*, after saturation with STR, after functionalization with CmiR, and after TmiR capture.

2.7 Analytical methods

2.7.1 Size and zeta potential measurements. A Nanosizer instrument (Zetasizer®, Malvern Instrument, UK) was used for the determination of the hydrodynamic diameter (D_H), the polydispersity index (PDI), and the zeta potential (ZP) of suspension nanoparticles. All the measurements were performed in triplicate and the mean value ± standard deviation is presented. The measurements were performed in H_2O and PBS 1×, for the batches adjusted at the iron concentration of 50 mg L^{-1}. For ZP measurements, the ionic strength was fixed by adding NaCl to a final concentration of 10 mM.

2.7.2. IR spectroscopy characterization. FT-IR measurements were carried out in ATR mode on a Bruker Vector 22 FT-IR spectrometer (Bruker, Germany) equipped with a Golden Gate single reflection diamond (Specac). The spectral window from 4000 to 500 cm^{-1} was typically recorded as an average of 32 scans.

2.7.3 Iron concentration determination. Iron concentrations of suspensions were measured by Atomic Absorption Spectrophotometry (AAS) (iCE 3000 spectrometer, Thermo Instruments, France). The synthesized samples were mineralized for a minimum of 2 hours with concentrated hydrochloric acid (6 M), then diluted with hydrochloric acid (1%). The concentration of the samples was determined by using a calibration curve (iron absorption at 248.3 nm, standard iron solutions at 0.25; 0.5; 1.0; 2.0 and 5.0 mg L^{-1}).

2.7.4 Analysis by size exclusion HPLC (SE-HPLC). SE-HPLC measurements were performed with the Shimadzu system (Kyoto, Japan), using LC Column AdvanceBio SEC 300A, 2.7 μM, 7.8 × 300 mm, 1.0 mL min^{-1} flow rate. Software LC Solution was used for data acquisition and analysis.

All SE-HPLC measurements were performed in phosphate buffer mobile phase (0.15 mol L^{-1}; the combination of KH_2PO_4 at 0.075 mol L^{-1} and $Na_2HPO_4 \cdot 2H_2O$ at 0.075 mol L^{-1}), with the flow rate 1.0 mL min^{-1}, injection volume 10 μL, temperature 30 °C, duration 15 min and UV detection at 260 nm and 280 nm.

All samples for SE-HPLC measurements containing PEGylated SPIONs were magnetically separated, and the liquid from the sample was measured, in order to not inject a large concentration of magnetic nanoparticles into the column.

3 Results and discussion

3.1 Synthesis and characterization of the nanoprobe precursors

Coating nanosystems with neutral hydrophilic molecules such as PEG is important for biomedical applications, since it provides colloidal stability in aqueous media, independently from the pH (due to a sterical hindrance). In our study, the PEG chains were covalently attached to the silanized SPION surface, and the process involved three synthetic stages (Fig. 2), as described in the Experimental section. After the synthesis of initial SPIONs by coprecipitation of iron salts, the nanoparticles were silanized, *i.e.* coated with 3-aminopropyltrimethoxysilane (APS) molecules. The latter is bound to the hydroxyl groups abundant on the surface of SPIONs. The primary amines of APS remain available to form amide bonds with the activated esters of α-biotinyl-ω-NHS PEG. The resulting amide bond is well-known for its strength and stability.[25] The PEGylated SPIONs were then extensively purified from the residual free PEG molecules by dialysis against water for 48 hours and stored in aqueous suspensions.

The nanoparticles were characterized by a spectrum of analytical techniques: IR spectrometry to confirm the molecular composition and DLS to measure the NP D_H and ZP. The iron concentration was determined by means of AAS and used for calculating the molar ratio in the next steps of the nanoprobe formulation.

Successful PEGylation of SPIONs was firstly confirmed by IR bands (Fig. 3A) characteristic of the PEG molecules: the strong bands at 3444 cm^{-1} (O–H stretching), 2921 cm^{-1} (C–H stretching of in CH_2 and methylene groups), and 2853 cm^{-1} (C–H stretching). The amide bonds formed between PEG and silane were seen due to the C=O stretching band at 1651 cm^{-1}. More importantly, strong bands at 1099 cm^{-1} (O–H and C–O–H stretching, siloxane Si–O–SI stretching) characteristic for PEG molecules were observed and assigned to polycondensation of silanes.

Likewise, the successful formation of the polymeric shell was confirmed by the DLS results with the D_H increase, from 36.9 ± 1.4 nm for initial SPIONs to 43.5 ± 3.4 nm after their silanization and 63.0 ± 4.0 nm after their PEGylation.

Similarly, ZP also changed after PEGylation: being positively charged for silanized SPIONs (18 ± 2.5 mV, pH 7) it became nearly neutral (−3.47 ± 0.97 mV, pH 7). The curves of ZP as a function of pH changed after the nanoparticle modification (Fig. 3B). The ZP of the initial SPIONs at lower pH is positive due to the presence of OH_2^+ on the surface of nanoparticles. The ZP decreases to nearly zero at pH 7 (isoelectric point), due to deprotonation of OH_2^+ to OH. At higher pH, the surface of SPIONs is covered with O^- and the ZP is negative. For silanized SPIONs, the isoelectric point shifted closer to pH 9. As expected, the ZP of the PEGylated SPIONs was less sensitive to pH change

© 2022 The Author(s). Published by the Royal Society of Chemistry

Open Access Article. Published on 02 March 2022. Downloaded on 1/8/2023 3:48:03 PM.
This article is licensed under a Creative Commons Attribution-NonCommercial 3.0 Unported Licence.

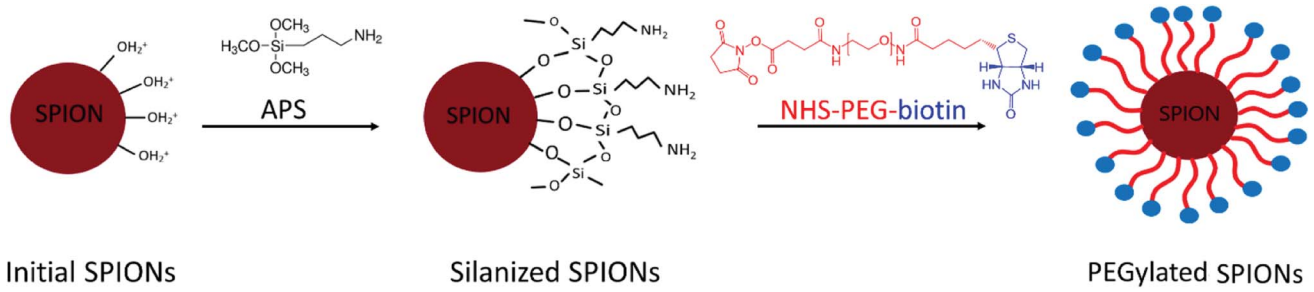

Fig. 2 Schematic representation of the PEGylated SPIONs synthesis in 3 steps: (i) synthesis of the initial SPIONs; (ii) silanization of the SPIONs surface; (iii) PEGylation of the silanized SPIONs.

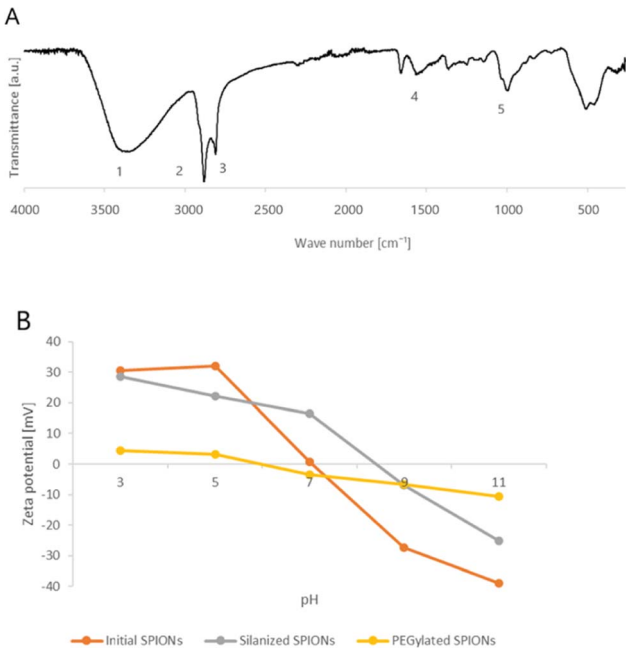

Fig. 3 Physicochemical properties of SPIONs. (A) IR spectra of PEGylated SPIONs, with the major bands labelled as follows: (1) 3444 cm^{-1}; (2) 2921 cm^{-1}; (3) 2853 cm^{-1}; (4) 1651 cm^{-1}; (5) 1099 cm^{-1}. (B) Evolution of zeta potential (ZP) of initial SPIONs (red line), silanized SPIONs (grey line), and PEGylated SPIONs (yellow line) as a function of pH.

and remained nearly zero. It can be concluded that the PEGylated SPIONs remained colloidally stable at neutral pH due to sterical hindrance.

3.2 Nanoprobe formulation and characterization

In our study, we have chosen a method of conjugation of miR to the PEGylated SPIONs *via* biotin (Bi)–streptavidin (STR) interaction, since the protocol is simple and cost-effective, requiring no additional reagents. Biotin-modified polymers and miRs are widely commercially available, and biotin insertion into the biomolecules is not intended to affect their properties or activity. Interaction between streptavidin and biotin is irreversible under physiologic conditions since the resulting bond is approaching in strength the covalent one and is unaffected by variation of temperature, pH, organic solvents, and denaturing agents. Furthermore, STR has four available binding sites, one in each of the four subunits of this protein, that allows each STR molecule to complex several molecules of biotin and thus of biotinylated molecules like PEG or miRs. Void of carbohydrate residues, STR has a low capability of forming non-specific bonds with other molecules. Once bound to the PEG-bi shell of the nanoparticles, STR should still have sites available for binding of biotinylated CmiR and thus enable the formation of nanoprobe described in Fig. 1.[22,27]

3.2.1 SE-HPLC method for analysis of the formulation ingredients. We used SE-HPLC which appears appropriate for confirmation of the successful formulation of the nanoprobes. SE-HPLC is known as a routine analytical method compared to XPS or element analysis. SE-HPLC enables the confirmation that each separate component present in the synthesis is able to bind with its intended match.

First of all, the SE chromatograms were obtained for the ingredients taken separately (nanoparticles, STR, CmiR) then we analyzed their binary complexes (STR–CmiR), and finally the samples from nanoprobe synthesis steps. Fig. 4 presents chromatograms of PEGylated SPIONs, STR, CmiR, and of complex STR–CmiR. While all the chromatograms were also recorded with UV detection at 280 nm, CmiR has stronger absorbance at 260 nm, ergo herein mentioned results are obtained at this wavelength.

PEGylated SPIONs had a relatively strong chromatographic peak at *ca.* 4.4 min (Fig. 4A). The peak of 1 g L^{-1} solution of streptavidin was observed at *ca.* 8.2 min (Fig. 4B). The strong peak of CmiR at concentration 5 μM was detected at *ca.* 8.8 min (Fig. 4C). The fact that the NP are eluted earlier than molecules is concomitant with their much bigger size. On the other hand, the close retention time about 8.2 and 8.8 min observed respectively for STR (M_w of *ca.* 55 kDa) and biotinylated CmiR (M_w of *ca.* 7.6 kDa) is much less expectable.

The formation of the complex STR–CmiR at molar ratio 3.78 : 1 was visible as the new peak rose at *ca.* 6.8 min (Fig. 4D) since the complex was larger than separate molecules. The uniform peak of the complex is in favor that all possible binding places on STR are probably occupied by the biotinylated CmiRs. In the mixed sample, the peak of free CmiR (*ca.* 8.8 min) decreased in intensity almost by a half (37.1 *vs.* 76.5 AU) compared to the free CmiR taken at the same concentration.

© 2022 The Author(s). Published by the Royal Society of Chemistry

Open Access Article. Published on 02 March 2022. Downloaded on 1/8/2023 3:48:03 PM.
This article is licensed under a Creative Commons Attribution-NonCommercial 3.0 Unported Licence.

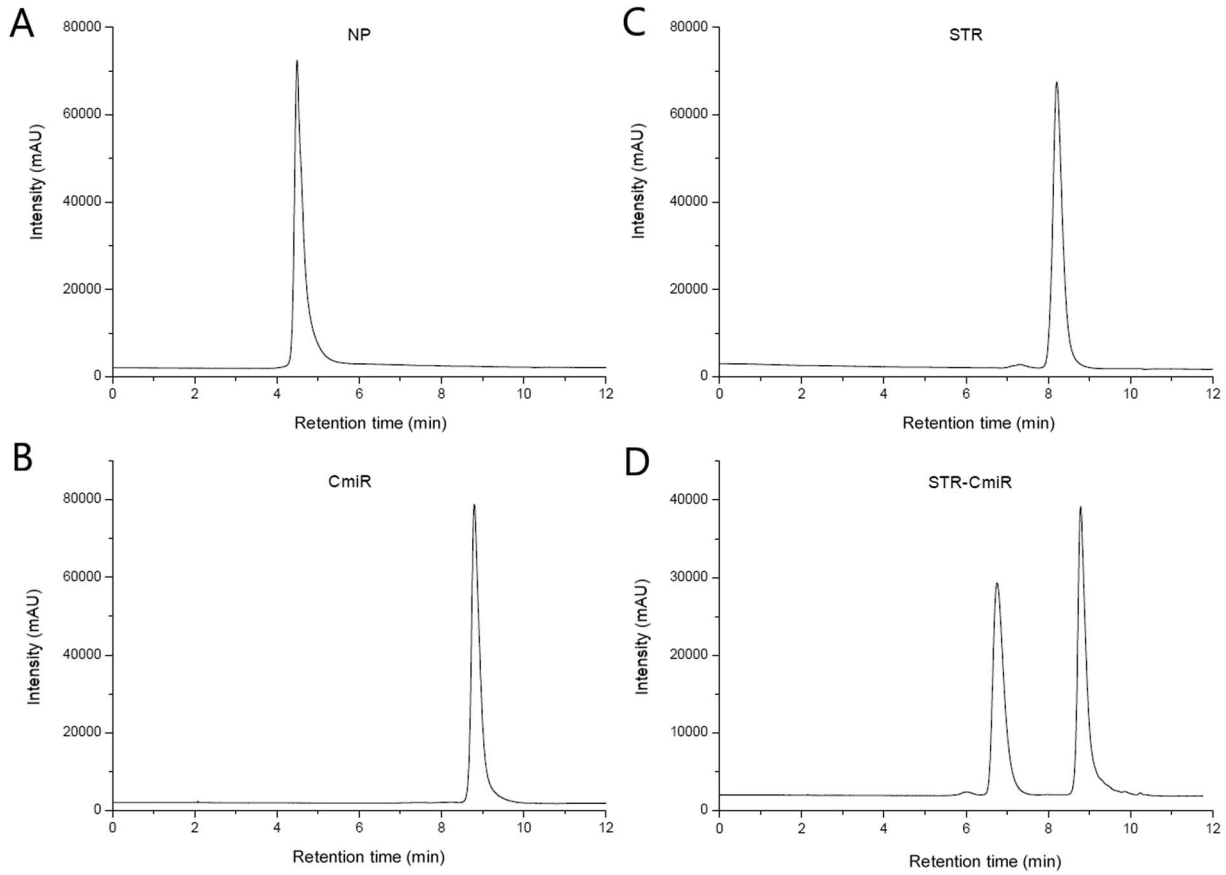

Fig. 4 SE-HPLC chromatograms. (A) PEGylated SPIONs (NP), t_R: 4.4 min, (B) STR, t_R: 8.2 min, (C) biotinylated CmiR, t_R: 8.8 min, (D) STR–CmiR complex, t_R: 6.8 and 8.8 min.

The absence of the free STR peak (around 8.2 min) allows to suppose that, at the conditions used, all the STR molecules were bound to CmiR.

3.2.2 Validation of the nanoprobe formulation steps. As explained above, the nanoprobe synthesis included 2 steps: (1) modification of the PEGylated SPIONs with STR to obtain the NP–STR; and (2) functionalization of the NP–STR with CmiR to produce the NP–STR–CmiR batches.

Formulation step 1 – modification of PEGylated SPIONs with STR. Aiming for a maximal coverage with STR at the biotin sites on the surface of the NP to achieve the best efficiency, we made the attempts with three Fe/STR molar ratios: 2100, 1400, and 280. At the lower Fe/STR molar ratio of 280 (sample NP–STR1), a weak peak of free STR was still present in the chromatograms (t_R 8.2 min), while at higher Fe/STR molar ratio of 1400 and 2100 (the samples NP–STR2 and NP–STR3), no free STR peak was detected (Fig. 5). Thus, one could suppose that at the highest concentration (sample NP–STR1), the STR was able to saturate the available biotin sites.

The weak peaks at 6.3, 6.5 and 6.9 min observed in those samples were possibly due to the presence of PEG-bi chains which were detached from the NP into solution after their complexation with the high molecular weight STR. Indeed, one can reasonably suppose that despite the purification *via* dialysis which was used to remove the excess of the free PEG-bi, it was still possible to desorb from the nanoparticles some minor fraction of the PEG-bi bound to STR. In agreement with this hypothesis, the peak of the molecular complex STR–PEG (Fig. 5B) had a close retention time of *ca.* 6.7 min. The 3 peaks at 6.3, 6.5 and 6.9 min might correspond to complex fractions with different STR binding sites. This result demonstrates the importance of the purification between the two formulation steps.

The presence of the free STR and the STR–PEG complexes in the NP–STR samples was undesirable since they might compete with STR-modified NP for the binding to the CmiR upon the next step of the nanoprobes formulation. Thus, we applied magnetic separation to purify the NP-STR and successfully eliminate the free STR and the PEG-bi–STR complexes.

Ideally, all the biotin sites on the PEGylated SPIONs surface would be occupied with STR. However, the steric hindrance of the large STR molecules can possibly prevent achieving the saturation of all the biotin sites since some of them are not accessible.

Since the sample NP–STR1 was the best covered with STR, the corresponding batches were purified from unbound species and used for the second formulation step.

Formulation step 2 – functionalization of the NP–STR with CmiR. Here again, our aim was to functionalize the NP–STR with as many CmiR as possible since it is supposed to favor the

© 2022 The Author(s). Published by the Royal Society of Chemistry

Open Access Article. Published on 02 March 2022. Downloaded on 1/8/2023 3:48:03 PM.
This article is licensed under a Creative Commons Attribution-NonCommercial 3.0 Unported Licence.

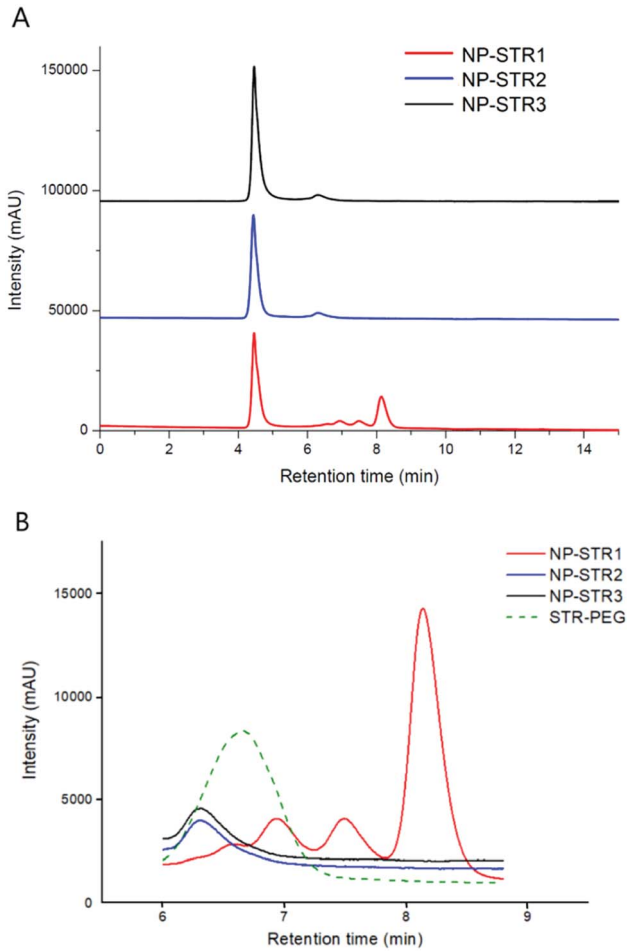

Fig. 5 SE-HPLC analysis of the NP–STR (A): the full chromatograms of the samples: NP–STR1 (molar ratio Fe/STR = 280, red line, t_R: 4.5, 6.9, 7.5 and 8.2 min), NP–STR2 (molar ratio Fe/STR = 1400, blue line, t_R: 4.4, 6.3 min), NP–STR3 (molar ratio Fe/STR = 2100, black line, t_R: 4.5 min and 6.3 min). (B) Zoom on the interval from 6 to 8.8 min with the overlayed peaks of the samples NP–STR1, NP–STR2, NP–STR3, and that of the STR–PEG-bi molecular complex (green dashed line).

efficiency of the final nanoprobes. We started with the CmiR concentration of 5 μM and generated the samples NP–STR–CmiR5. As the formation of STR–CmiR complex was proved to be relatively fast, the 2 hours of incubation of the NP–STR with CmiR (under stirring, at the room temperature) was supposed long enough. The conjugation of both STR and CmiR did not markedly change the physicochemical properties of the respective batches (Table 1).

The batches of PEGylated SPIONs showed a comparable D_H in both deionized water and in PBS 1X (Table 1): 61.6 ± 2.0 nm *vs.* 63.0 ± 4.0 nm. After the modification with STR, the D_H in PBS 1X slightly increased to 67.0 ± 0.5 nm (Table 1), presumably due to the presence of STR molecules on the surface of the nanoparticles. Functionalization with CmiR led only to a minor increase of D_H till 71.2 ± 0.4 nm. Zeta potential remained largely unchanged (Table 1), with values close to neutral. Interestingly, the PDI values diminished in going to the formulated nanoprobes compared to the PEGylated SPIONs.

Table 1 Physicochemical properties of the batches NP (PEGylated SPIONs), NP–STR1 and NP–STR–CmiR5

	D_H [nm]	PDI	Zeta potential [mV]
NP (PEGylated SPIONs)	61.6 ± 2.0	0.20 ± 0.00	2.7 ± 0.1
NP–STR1	67.0 ± 0.5	0.13 ± 0.01	3.1 ± 0.2
NP–STR–CmiR5	71.2 ± 0.4	0.11 ± 0.01	2.5 ± 0.4

The PDI value of 0.11 is typically considered as characteristic of a monodisperse nanoparticle population. To summarize, the formulation steps did not decrease the colloidal stability of the nanoprobes.

The amount of CmiR bound to the nanoprobes was determined by means of the SE-HPLC analysis. The NP–STR–CmiR5 sample (Fig. 6) revealed 2 peaks: that of nanoparticles at *ca.* 4.4 min and that of the free CmiR at *ca.* 8.7 min. The latter decreased in the intensity down to 73.9% compared to the chromatogram of the pure CmiR. Thus, after incubation with 5 μM CmiR solution, about 26% of CmiR were bound to the nanoprobes (the concentration of the bound CmiR was 1.3 μM).

Subsequently, we also prepared samples by incubating NP–STR with the lower and higher concentrations of CmiR: 1 μM (NP–STR–CmiR1) and 10 μM (NP–STR–CmiR10). According to the SE-HPLC data, at 1 μM and 10 μM of incubated CmiR, the nanoprobe-bound CmiR fraction was respectively 66% and 12% and corresponded to concentrations of 0.66 and 1.2 μM (Table 2). To summarize, using a 5 μM concentration of CmiR would be more advisable than 1 μM. In contrast, larger excess of 10 μM does not allow to increase the bound CmiR concentration and leads to use-less loss of the nucleic acid.

The estimated number of CmiR molecules grafted per nanoprobe was 11, 22 and 20 for the samples NP–STR–CmiR1, NP–STR–CmiR5, and NP–STR–CmiR10 respectively. To the best of our knowledge, very few publications reported the quantity of grafted CmiR[31,32] or other oligonucleotides[27] per nanoprobe or

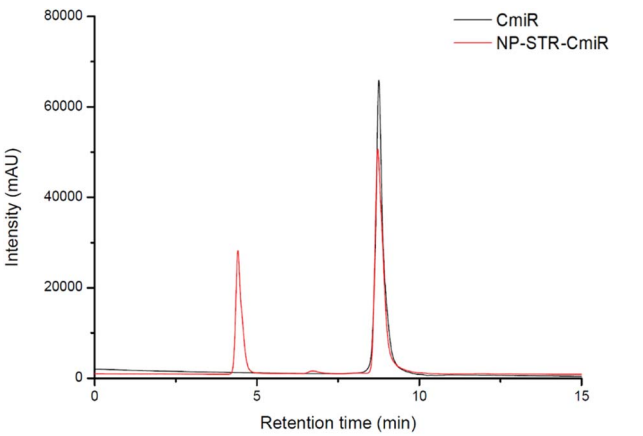

Fig. 6 SE-HPLC results for the second (final) step of the nanoprobes formulation. Typical chromatograms of NP–STR–CmiR5 (red curve, peaks at 4.4 and 8.7 min) compared to those of the pure CmiR at the same concentration of 5 μM (black curve, peak at *ca.* 8.8 min).

Open Access Article. Published on 02 March 2022. Downloaded on 1/8/2023 3:48:03 PM.
This article is licensed under a Creative Commons Attribution-NonCommercial 3.0 Unported Licence.

Table 2 Comparative results of functionalization of NP–STR–CmiR batches

Sample	Fraction of bound CmiR	Fraction of bound CmiR (concentration)	Number of bound CmiRs per NP
NP–STR–CmiR1	66%	0.66 μM	11
NP–STR–CmiR5	26%	1.3 μM	22
NP–STR–CmiR10	12%	1.2 μM	20

even the concentration of grafted CmiR.[33,34] Although less explored in the literature, these values are important since they allow to evaluate both the conjugation method used and the expected efficiency of TmiR capture.[35] It has been reported that only one CmiR per nanoprobe may be sufficient for TmiR detection.[32]

3.3 Proof of the nanoprobes affinity to TmiR-155

To determine the ability of nanoprobes to capture the target miR, the purified NP–STR–CmiR5 samples were incubated with the 5 μM solution of the TmiR-155, then were magnetically sorted. The chromatography data indicate that after the sorting, 21% (≈1 μM) of TmiR were bound to the nanoprobes, which corresponds to approximately 18 TmiRs per nanoprobe. This result is promising since it confirms that the nanoprobes were able to adsorb TmiR and they allowed to remove a significant fraction of it. The 18 : 22 molar ratio for TmiR : CmiR is also promising, while has not been considered as definitive, since it depends on the application protocols.

3.4 Proof of the stability of the nanoprobes in serum

To confirm the stability of the nanoprobes NP–STR–CmiR5 (5 μM CmiR), a new batch was prepared and combined with the solution of fetal bovine serum to be incubated for 4 and 12 hours, resulting in the samples (S4)-NP–STR–CmiR5 and (S12)-NP–STR–CmiR5 respectively. The sample (S4)-NP–STR–CmiR5 was visually monitored for signs of aggregation after 1, 2 and 3 hours, with no apparent change to the solution visible by the eye. We measured the physicochemical properties of the nanoprobes prior to the mixing with serum, and after the incubation and purification *via* magnetic separation (Table 3). The batch NP–STR–CmiR5 showed similar D_H to the one after the incubation in the serum for both 4 h and 12 h, the size increased only slightly, 72.8 ± 3.3 nm *vs.* 78.2 ± 6.1 nm *vs.* 78.2 ± 1.7 nm, with a bigger standard deviation in the case of the sample (S4)-NP–STR–CmiR5. The polydispersity remained stable for all three batches. The zeta potential of the new batch NP–STR–CmiR5 shifted to the negative value of −7.1 ± 2.0 mV, and after the incubation showed no significant variation. The small changes in physicochemical properties could be explained by a small-scale absorption of proteins present in the serum to the surface of the nanoprobes. The nanoprobes however remain colloidally stable, with their properties not influenced even by a long incubation in the serum.

Table 3 Physicochemical properties of the batches NP–STR–CmiR5, (S4)-NP–STR–CmiR5 and (S12)-NP–STR–CmiR5

	D_H [nm]	PDI	Zeta potential [mV]
NP–STR–CmiR5	72.8 ± 3.3	0.18 ± 0.01	−7.1 ± 2.0
(S4)-NP–STR–CmiR5	78.2 ± 6.1	0.19 ± 0.02	−6.6 ± 1.0
(S12)-NP–STR–CmiR5	78.2 ± 1.7	0.18 ± 0.01	−4.7 ± 1.3

4. Conclusion

In this study, CmiR-functionalized magnetic nanoprobes were designed for TmiR-155 capture. As precursors of the nanoprobes, we synthesized SPIONs coated with covalently bound PEG biotinylated on its external terminus. Then, the precursors were used to formulate nanoprobes in two steps: (i) modification of the biotinylated external shell with streptavidin and (ii) functionalization of the STR-modified shell with biotinylated CmiR. Saturation of the surface of NP with streptavidin was achieved with molar ratio Fe/STR = 280. The corresponding batches of the NP–STR were then incubated with biotinylated CmiR (5 μM), and 26% of the latter were bound. The nanoprobes coated with 22 CmiR per nanoprobe were able to capture 18 TmiR per nanoprobe from the 5 μM TmiR solution. The nanoprobes were proved to be stable after an incubation in the serum. This result is promising, while in real samples the nanoprobes concentration has to be certainly used in excess compared to that of TmiR. The capture protocols optimization is a subject of an independent study we are starting.

In close future, the developed nanoprobes will be also studied concerning their ability to capture the target miR (miR-155) in serum from patients and thus to monitor their concentration before and after an anti-cancer treatment.

Conflicts of interest

There are no conflicts to declare.

Acknowledgements

We are grateful to the ''Ligue Nationale contre le Cancer" for their financial support (project NANOmiR) and especially to the local comities 53 and 56.

References

1 H.-Y. Loh, B. P. Norman, K.-S. Lai, N. M. A. N. A. Rahman, N. B. M. Alitheen and M. A. Osman, The Regulatory Role of MicroRNAs in Breast Cancer, *Int. J. Mol. Sci.*, 2019, **20**(19), 4940, DOI: 10.3390/ijms20194940.

© 2022 The Author(s). Published by the Royal Society of Chemistry

Open Access Article. Published on 02 March 2022. Downloaded on 1/8/2023 3:48:03 PM. This article is licensed under a Creative Commons Attribution-NonCommercial 3.0 Unported Licence.

2 P. Krishnan and S. Damaraju, The Challenges and Opportunities in the Clinical Application of Noncoding RNAs: The Road Map for MiRNAs and PiRNAs in Cancer Diagnostics and Prognostics, *Int. J. Genomics*, 2018, **2018**(12), 1–18, DOI: 10.1155/2018/5848046.

3 A. A. Svoronos, D. M. Engelman and F. J. Slack, OncomiR or Tumor Suppressor? The Duplicity of MicroRNAs in Cancer, *Cancer Res.*, 2016, **76**(13), 3666–3670, DOI: 10.1158/0008-5472.CAN-16-0359.

4 R. D'Agata and G. Spoto, Advanced Methods for MicroRNA Biosensing: A Problem-Solving Perspective, *Anal. Bioanal. Chem.*, 2019, **411**(19), 4425–4444, DOI: 10.1007/s00216-019-01621-8.

5 T. Ouyang, Z. Liu, Z. Han and Q. Ge, MicroRNA Detection Specificity: Recent Advances and Future Perspective, *Anal. Chem.*, 2019, **91**(5), 3179–3186, DOI: 10.1021/acs.analchem.8b05909.

6 A. Kanavarioti, HPLC Methods for Purity Evaluation of Man-Made Single-Stranded RNAs, *Sci. Rep.*, 2019, **9**(1), 1–13, DOI: 10.1038/s41598-018-37642-z.

7 M. Kullolli, E. Knouf, M. Arampatzidou, M. Tewari and S. Pitteri, *J. Am. Soc. Mass Spectrom.*, 2011, **72**(2), 181–204, DOI: 10.1007/s13361-013-0759-x.Intact.

8 E. Boros, O. R. Pinkhasov and P. Caravan, Metabolite Profiling with HPLC-ICP-MS as a Tool for *in vivo* Characterization of Imaging Probes, *EJNMMI Radiopharm. Chem.*, 2018, **3**(1), DOI: 10.1186/s41181-017-0037-5.

9 E. M. Kroh, R. K. Parkin, P. S. Mitchell and M. Tewari, Analysis of Circulating MicroRNA Biomarkers in Plasma and Serum Using Quantitative Reverse Transcription-PCR (QRT-PCR), *Methods*, 2010, **50**(4), 298–301, DOI: 10.1016/j.ymeth.2010.01.032.

10 M. Y. Pratama, L. Cavalletto, C. Tiribelli, L. Chemello and D. Pascut, Selection and Validation of MiR-1280 as a Suitable Endogenous Normalizer for QRT-PCR Analysis of Serum MicroRNA Expression in Hepatocellular Carcinoma, *Sci. Rep.*, 2020, **10**(1), 3128, DOI: 10.1038/s41598-020-59682-0.

11 É. Várallyay, J. Burgyán and Z. Havelda, MicroRNA Detection by Northern Blotting Using Locked Nucleic Acid Probes, *Nat. Protoc.*, 2008, **3**(2), 190–196, DOI: 10.1038/nprot.2007.528.

12 L. W. Lee, S. Zhang, A. Etheridge, L. Ma, D. Martin, D. Galas and K. Wang, Complexity of the MicroRNA Repertoire Revealed by Next-Generation Sequencing, *Rna*, 2010, **16**(11), 2170–2180, DOI: 10.1261/rna.2225110.

13 A. D. Martinez-Gutierrez, O. M. Catalan, R. Vázquez-Romo, F. I. P. Reyes, A. Alvarado-Miranda, F. L. Medina, J. E. Bargallo-Rocha, L. T. O. Moreno, D. C. de León, L. A. Herrera, C. López-Camarillo, C. Pérez-Plasencia and A. D. Campos-Parra, MiRNA Profile Obtained by Next-generation Sequencing in Metastatic Breast Cancer Patients Is Able to Predict the Response to Systemic Treatments, *Int. J. Mol. Med.*, 2019, **44**(4), 1267–1280, DOI: 10.3892/ijmm.2019.4292.

14 M. Rusek, M. Michalska-Jakubus, M. Kowal, J. Bełtowski and D. Krasowska, A Novel MiRNA-4484 Is up-Regulated on Microarray and Associated with Increased MMP-21 Expression in Serum of Systemic Sclerosis Patients, *Sci. Rep.*, 2019, **9**(1), 1–13, DOI: 10.1038/s41598-019-50695-y.

15 J. E. Ideozu, X. Zhang, V. Rangaraj, S. McColley and H. Levy, Microarray Profiling Identifies Extracellular Circulating MiRNAs Dysregulated in Cystic Fibrosis, *Sci. Rep.*, 2019, **9**(1), 1–11, DOI: 10.1038/s41598-019-51890-7.

16 M. K. Masud, M. Umer, M. S. A. Hossain, Y. Yamauchi, N. T. Nguyen and M. J. A. Shiddiky, Nanoarchitecture Frameworks for Electrochemical MiRNA Detection, *Trends Biochem. Sci.*, 2019, **44**(5), 433–452, DOI: 10.1016/j.tibs.2018.11.012.

17 P. Christian, F. Von Der Kammer, M. Baalousha and T. Hofmann, Nanoparticles: Structure, Properties, Preparation and Behaviour in Environmental Media, *Ecotoxicology*, 2008, **17**(5), 326–343, DOI: 10.1007/s10646-008-0213-1.

18 G. Barbillon, Latest Novelties on Plasmonic and Non-Plasmonic Nanomaterials for SERS Sensing, *Nanomaterials*, 2020, **10**(6), 1–17, DOI: 10.3390/nano10061200.

19 L. Gloag, M. Mehdipour, D. Chen, R. D. Tilley and J. J. Gooding, Advances in the Application of Magnetic Nanoparticles for Sensing, *Adv. Mater.*, 2019, **31**(48), 1–26, DOI: 10.1002/adma.201904385.

20 I. Gessner, J. W. U. Fries, V. Brune and S. Mathur, Magnetic Nanoparticle-Based Amplification of MicroRNA Detection in Body Fluids for Early Disease Diagnosis, *J. Mater. Chem. B*, 2021, **9**(1), 9–22, DOI: 10.1039/d0tb02165b.

21 I. Gessner, X. Yu, C. Jüngst, A. Klimpel, L. Wang, T. Fischer, I. Neundorf, A. C. Schauss, M. Odenthal and S. Mathur, Selective Capture and Purification of MicroRNAs and Intracellular Proteins through Antisense-Vectorized Magnetic Nanobeads, *Sci. Rep.*, 2019, **9**(1), 1–10, DOI: 10.1038/s41598-019-39575-7.

22 B. Tian, Y. Han, E. Wetterskog, M. Donolato, M. F. Hansen, P. Svedlindh and M. Strömberg, MicroRNA Detection through DNAzyme-Mediated Disintegration of Magnetic Nanoparticle Assemblies, *ACS Sens.*, 2018, **3**(9), 1884–1891, DOI: 10.1021/acssensors.8b00850.

23 S. Grijalvo, A. Alagia, A. F. Jorge and R. Eritja, Covalent Strategies for Targeting Messenger and Non-Coding RNAs: An Updated Review on SiRNA, MiRNA and AntimiR Conjugates, *Genes*, 2018, **9**(2), 74–111, DOI: 10.3390/genes9020074.

24 N. Knežević, I. Gadjanski and J. O. Durand, Magnetic Nanoarchitectures for Cancer Sensing, Imaging and Therapy, *J. Mater. Chem. B*, 2019, **7**(1), 9–23, DOI: 10.1039/c8tb02741b.

25 K. Hervé, L. Douziech-Eyrolles, E. Munnier, S. Cohen-Jonathan, M. Soucé, H. Marchais, P. Limelette, F. Warmont, M. L. Saboungi, P. Dubois and I. Chourpa, The Development of Stable Aqueous Suspensions of PEGylated SPIONs for Biomedical Applications, *Nanotechnology*, 2008, **19**(46), 465608–465614, DOI: 10.1088/0957-4484/19/46/465608.

26 Y. Du and P. W. T. Pong, Multi-Binding Biotinylated Iron Oxide Nanoparticles as a Promising Versatile Material for

Open Access Article. Published on 02 March 2022. Downloaded on 1/8/2023 3:48:03 PM.
This article is licensed under a Creative Commons Attribution-NonCommercial 3.0 Unported Licence.

Magnetic Biomedical Applications, *Micro Nano Lett.*, 2018, **13**(4), 415–420, DOI: 10.1049/mnl.2017.0348.

27 Y. Wang, P. D. Howes, E. Kim, C. D. Spicer, M. R. Thomas, Y. Lin, S. W. Crowder, I. J. Pence and M. M. Stevens, Duplex-Specific Nuclease-Amplified Detection of MicroRNA Using Compact Quantum Dot-DNA Conjugates, *ACS Appl. Mater. Interfaces*, 2018, **10**(34), 28290–28300, DOI: 10.1021/acsami.8b07250.

28 M. Oishi, Comparative Study of DNA Circuit System-Based Proportional and Exponential Amplification Strategies for Enzyme-Free and Rapid Detection of MiRNA at Room Temperature, *ACS Omega*, 2018, **3**(3), 3321–3329, DOI: 10.1021/acsomega.7b01866.

29 X. Li, J. Zhao, R. Xu, L. Pan and Y. M. Liu, Mass Spectrometric Quantification of MicroRNAs in Biological Samples Based on Multistage Signal Amplification, *Analyst*, 2020, **145**(5), 1783–1788, DOI: 10.1039/c9an02064k.

30 P. K. Lo, B. Wolfson, X. Zhou, N. Duru, R. Gernapudi and Q. Zhou, Noncoding RNAs in Breast Cancer, *Briefings Funct. Genomics*, 2016, **15**(3), 200–221, DOI: 10.1093/bfgp/elv055.

31 G. Yammouri, H. Mohammadi and A. Amine, A Highly Sensitive Electrochemical Biosensor Based on Carbon Black and Gold Nanoparticles Modified Pencil Graphite Electrode for MicroRNA-21 Detection, *Chem. Africa*, 2019, **2**(2), 291–300, DOI: 10.1007/s42250-019-00058-x.

32 M. Wang, W. Chen, L. Tang, R. Yan and P. Miao, Duplex-Specific Nuclease Assisted MiRNA Assay Based on Gold and Silver Nanoparticles Co-Decorated on Electrode Interface, *Anal. Chim. Acta*, 2020, **1107**, 23–29, DOI: 10.1016/j.aca.2020.01.041.

33 H. N. Chan, S. L. Ho, D. He and H. W. Li, Direct and Sensitive Detection of Circulating MiRNA in Human Serum by Ligase-Mediated Amplification, *Talanta*, 2020, **206**, 120217, DOI: 10.1016/j.talanta.2019.120217.

34 W. K. Wong, S. H. D. Wong and L. Bian, Long-Term Detection of Oncogenic MicroRNA in Living Human Cancer Cells by Gold@Polydopamine-Shell Nanoprobe, *ACS Biomater. Sci. Eng.*, 2020, **6**(7), 3778–3783, DOI: 10.1021/acsbiomaterials.0c00633.

35 H. Wang, H. Tang, C. Yang and Y. Li, Selective Single Molecule Nanopore Sensing of MicroRNA Using PNA Functionalized Magnetic Core–Shell Fe_3O_4-Au Nanoparticles, *Anal. Chem.*, 2019, **91**(12), 7965–7970, DOI: 10.1021/acs.analchem.9b02025.

© 2022 The Author(s). Published by the Royal Society of Chemistry

Part II

Development of protocols for nanoprobe-mediated TmiR isolation from biological samples

Publication 3:

Magnetic nanoprobes for miRNA-484 capture in human serum

In revision, to be submitted in "Langmuir"

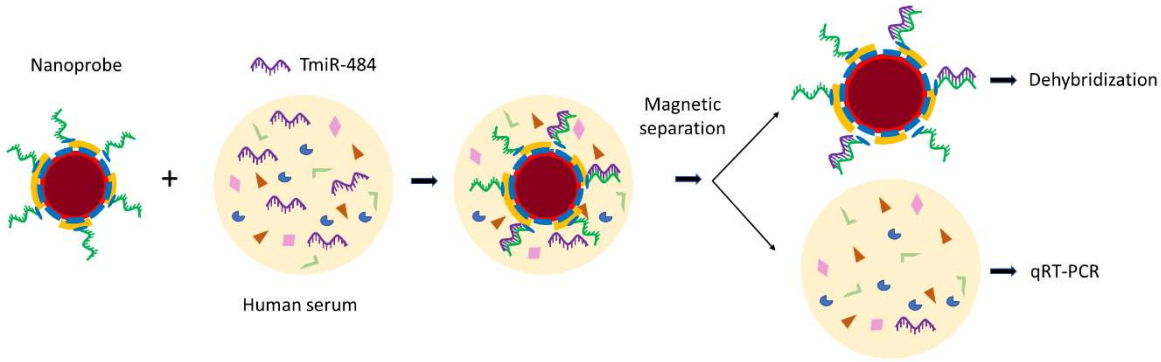

Préambule de la Publication 3

Les miARN (miR) sont de courtes séquences d'ARN non codantes présentes dans les fluides biologiques tels que le sang, le plasma et le sérum. La perturbation de leurs niveaux d'expression peut être corrélée avec les différents stades de diverses maladies, ce qui les rend d'excellents candidats comme biomarqueurs. Dans cette étude, nous présentons des nanosondes magnétiques conçues pour capturer des miRs d'intérêts dans des fluides biologiques. Les nanosondes ont été synthétisées à partir de SPIONs PEGylées, qui ont été fonctionnalisées via des interactions streptavidine-biotine avec une séquence d'ADN complémentaire (ADNc-484) au miR cible (TmiR-484). La formulation en deux étapes a été contrôlée par SE-HPLC, en suivant le protocole précédemment établi. La stabilité et la capacité des nanosondes à capturer le TmiR choisi ont d'abord été déterminées dans des solutions modèles, suivies d'expériences dans du sérum humain. La stabilité et la fonctionnalité des nanosondes ont été confirmées à l'aide de qRT-PCR - il a été possible d'analyser à la fois la capacité de capture des nanosondes dans le sérum humain et sa déshybridation ultérieure à partir de nanosondes dans des solutions modèles.

Magnetic nanoprobes for miRNA-484 capture in human serum

Iveta Vilímová[1], Stéphanie David[1], William Raoul[2], Laetita Babin[3], Yoann Misericordia[1], Igor Chourpa[1], Katel Hervé-Aubert[1]*

1. EA6295 Nanomédicaments et Nanosondes, Université de Tours, Tours, France

2. Inserm UMR 1069 Nutrition, Croissance et Cancer, Université de Tours, Tours, France

3. EMR CNRS 7001 LNOx, Université de Tours, Tours, France

Abstract

miRNAs (miRs) are short, non-coding RNA sequences that are present in biofluids such as blood, plasma, and serum. Their disrupted levels of expression correlate with different stages of various diseases, marking them suitable as potential biomarkers. In this study, we present magnetic nanoprobes designed to capture miRs of interest in biofluids. The nanoprobes were synthesized from PEGylated SPIONs, which were functionalized via streptavidin-biotin interactions with complementary DNA sequence (cDNA-484) to the target miR (TmiR-484). The two-step formulation was monitored by SE-HPLC, following the previously established protocol. The ability of nanoprobes to capture the chosen TmiR were first determined in model solutions, determining the increasing efficiency of TmiR capture at lower concentrations. In human serum, the nanoprobes remained colloidally stable, and their functionality was confirmed using qRT-PCR – it was possible to analyze both the capture ability of nanoprobes in human serum and its following dehybridization from nanoprobes in model solutions.

Keywords

SPIONs, nanoprobes, miRNA, cDNA, miR-484, qRT-PCR, serum

1. Introduction

The capture of miRNAs (miRs), followed by their detection and quantification, presents an interesting challenge for the current research in this field. Since miRs are short, small, non-coding strands of RNA with lengths ranging from 19 to 23 nucleotides, there are several obstacles to overcome before using them as readily available biomarkers [1]. Due to their small size, slight differences between respective miRs or between precursor and mature miRs, and overall minuscule amounts present in body fluids, the expression of miRs differs and makes their capture and detection a complex task [2].

Generally, miRs can be found in tissue samples, cultured cells [3], and biofluids (e.g., blood [4], respectively in serum [5] and plasma [6]). Since miRs function as regulators of multiple cellular processes, their screening could help in the assessment of various disease prognostics and progress monitoring [7]. In cancer-related problematic, miRs are presented as either tumour suppressor genes, oncogenes, or a mix of both depending on their levels of expression [8]. For example, miR-484 is closely connected to colorectal cancer, the third most common cancer in the world [9], and miR-484 levels of expression in cancer tissues and plasma are correlated to the stage of the disease [10]. In the early stage, expression levels of miR-484 in serum were significantly lower compared to the control samples, while abnormal elevation occurred in the advanced stage [11]. Thus, monitoring miR levels in serum could lead to early diagnosis.

One of the most advanced methods for miR detection is qRT-PCR (quantitative Reverse Transcription Polymerase Chain Reaction, also called quantitative real-time PCR) [12]. In RT, a DNA strand complementary to miR is formed, functioning as a template to form a second DNA strand. The second strand also serves as a template, eliciting the amplification, and repeating the process according to the required number of cycles [13]. For the detection of miRs with qRT-PCR, fluorescence is generally used to determine the amplification of initial strands present in the sample. However, obtaining sufficient precision and sensitivity for the analysis of circulating miRs from human plasma or serum calls for RNA extraction methods from the starting material. There are factors influencing miRs extraction efficiency, e.g. the variability of samples of the same type of biofluid, along with overall small amounts of miR present, and subsequent technical issues with the PCR method, such as the susceptibility to contaminations and subsequent error amplification [14,15].

For that, nanomaterials are already well-established as detection platforms for target biomolecules, and particularly nanoprobes present a novel path, offering both unique physical properties and surface modifications [16,17]. Nanoprobes are suited for biomolecular detection, transport, and release, and are already being used for miR detection and quantification in multiple variations [18–20]. Magnetic nanoparticles display the advantage of magnetic separation and efficient extraction from analyzed media. Often, magnetic properties are combined with other materials, such as core-shell Fe3O4-Au nanoparticles for miR-155 detection [21], modified magnetic beads combined with Au nanoparticles for detection of miR-141 [22,23], silica-coated γ-Fe2O3 nanoparticles for the detection of a target sequence mimicking miR-122 [24], and silica-coated conglomerates of SPIONs covered with Au shell for miR-21 detection [25].

Nanoprobes presented in this work are based on the concept of magnetic nanoprobes functionalized with a complementary oligonucleotide sequence, which can be inserted in biological samples, and using magnetic separation, the nanoprobes can be reclaimed with captured target miR (TmiR). Re-concentration of nanoprobes via magnetic separation would enable the capture of sufficient concentrations of TmiRs for their detection. The nanoprobes have cores of superparamagnetic iron oxide nanoparticles (SPIONs), which are modified and functionalized for the capture of TmiR-484. Continuing from the groundwork of our previous publication [26] where we tested nanoprobes functionalized with complementary miR sequence (CmiR), here the PEGylated SPIONs were functionalized via streptavidin-biotin interaction with complementary DNA (cDNA-484). The synthesized nanoprobes were tested for their stability and ability to capture the TmiR-484 in model solutions, with the levels of TmiR being monitored by SE-HPLC and the physico-chemical properties determined by the dynamic light scattering (DLS) measurement. Following the promising results of increasing the efficiency of TmiR capture at lower concentrations, we moved on to experiments with human serum samples from healthy adult volunteers. Proving the stability of nanoprobes in serum samples, we analyzed TmiR capture in samples from human serum: (i) sample without any additional TmiR, (ii) spiked with additional TmiR-484, (iii) with nanoprobes added, and (iv) spiked with TmiR and nanoprobes added, with the results being determined by qRT-PCR.

2. Experimental

2.1 Materials

In all experiments was used deionized water (18 MΩ). α-Biotinyl-ω-NHS PEG, M_w 5000 Da, (NHS-PEG_{5000}-biotin, PEG-b) was purchased from Rapp Polymere (Tübingen, Germany). Streptavidin in lyophilized form was purchased from Alfa Aesar (Kandel, Germany).

cDNA-484 modified with biotin (Btn]-5'-ATCGGGAGGGGACTGAGCCTGA-3', 7303 $gmol^{-1}$), and TmiR-484 (5'-UCAGGCUCAGUCCCCUCCCGAU-3', 6890 $gmol^{-1}$) were purchased from Sigma-Aldrich (Saint Quentin-Fallavier, France).

PCR Primer Mix hsa-miR-484 and UniSp6, from miRCURY LNA™ miRNA PCR Assay, MiRCURY LNA™ RT Kit, and miRCURY LNA™ SYBR Green PCR Kit (600) were purchased from QIAGEN Sciences (Maryland USA). Extraction kit NucleoSpin® miRNA Plasma was purchased from MACHERY-NAGEL (Düren, Germany). Serum samples from healthy adult volunteers were collected in accordance with Institutional Research Protection Agreement No. CA-REC-2019-188) at the French Blood Establishment, Center Val de Loire, France. Standard miR solutions at required concentrations were prepared by adding RNAse-free deionized water.

2.2 Formulation of the nanoprobes

A detailed description of the full protocol of the synthesis was described in our previous study [26]. The formulation of nanoprobes is divided into two steps; surface modification of nanoprobes precursors with streptavidin, and subsequent functionalization with cDNA. Precursors of the nanoprobes, PEG-b-coated SPIONs, were synthesized in three steps, starting with the synthesis of initial SPIONs, followed by the silanization of their surface, which was then covered with the PEG-b layer using lyophilized NHS–PEG_{5000}–biotin (in accordance with the protocol previously developed by our group [27]).

2.2.1 Surface modification with streptavidin

Using streptavidin-biotin interactions, the surface of PEGylated SPIONs (NP) was modified with STR, as presented in our previous study [26]. In short, the batch NP-STR was generated by combining 400 μL of NP at an iron concentration of 600 mg L^{-1} with 100 μL

of PBS 10X and adding 500 µL of 1 mg mL^{-1} STR to this suspension. The sample was shaken overnight at room temperature.

2.2.2 Functionalization with cDNA

The batch NP-STR was purified by magnetic separation and 380 µL was shaken overnight at room temperature with 20 µL of the stock solution of cDNA-484 (prepared with RNAse-free H_2O) with a concentration of 100 µM, so the final concentration of cDNA was 5 µM, resulting in the batch NP-STR-cDNA. Again, magnetic separation protocol was applied to eliminate the excess of cDNA.

2.3 TmiR capture in model solutions

Nanoprobes in the batch NP-STR-cDNA were stirred overnight at room temperature with the stock solution of TmiR-484 (prepared with RNAse-free H_2O) with the concentration of 100 µM in four different final concentrations of TmiR: 5 µM, 2.5 µM, 1 µM, and 0.5 µM. The magnetic separation protocol was applied to eliminate any remaining free TmiR, which was then quantified by SE-HPLC.

2.4 Estimation of the number of grafted cDNA and TmiR molecules

The number of cDNA and TmiR molecules per nanoparticle (N) was determined with the following formula:

$$N = C \times \frac{\pi D^3}{6} \times d \times 6.10^{23}$$

with C: the amount of cDNA or TmiR in mol per g of iron; D: diameter of SPION core (m, as defined by TEM); d: mass density of magnetite = 5.2×10^6 g/m^3; Avogadro's number = 6×10^{23} mol^{-1}.

2.5 Magnetic separation - Purification method

MS Columns (MACS® Column Technology, Miltenyi Biotec GmbH, Germany) were used for magnetic separation (MS), as a purification method during all experiments with nanoprobes. MS column was held in a magnetic MACS separator and the chosen volume of the SPIONs suspension (up to 500 µL, depending on the initial volume of the sample) was inserted. Nanoparticles remained captured in the column and the separated liquid was collected (MS 1). After washing the column two or three times (MS 2) with the buffer (PBS 1X), the column was removed from the magnetic separator and flushed with the

buffer at chosen volume, resulting in an MS 3 sample. Both MS 1 and MS 3 were utilized in the following synthetic procedures.

2.5.1 Reconcentration of nanoprobes

To determine if magnetic separation allows the reconcentration of synthesized nanoprobes in the steps of functionalization of NP-STR with cDNA, iron concentrations of the solutions were measured (section 2.8.3). Thus, the iron concentration was determined for the batch NP-STR-cDNA before magnetic separation. Afterward, 260 μL of this batch was inserted into the magnetic column, washed, and after releasing the column from the magnetic holder, the column was flushed out with the volume of 100 μL. The initial concentration of the nanoprobes in a larger volume and the final concentration of nanoprobes flushed out of the column were measured.

2.6 Nanoprobe stability in human serum

The stability of nanoprobes was determined for three different samples of human serum, using the following protocol: reconcentrated nanoprobes NP-STR-cDNA of approximated iron concentration of 500 mg/L, were inserted into 300 μL of human serum. The sample was left shaking overnight at room temperature, purified with magnetic separation, and the redispersed nanoprobes in PBS 1X were characterized by DLS measurement.

2.7 TmiR capture in human serum

The protocol applied for TmiR capture in human serum (HS) was similar to section 2.6, with the aim to obtain four samples; (i) sample without any additional TmiR: HS-H_2O-PBS, (ii) spiked with additional TmiR-484: HS-TmiR-PBS, (iii) with nanoprobes added: HS-H_2O-NPR, and (iv) spiked with TmiR and nanoprobes added: HS-TmiR-NPR. Into a 300 μL of human serum was inserted either 10 μL of H_2O or TmiR stock solution (at the concentration of 20 μM so the final sample had the concentration of 0.5 μM), and after mixing, 90 μL of either concentrated nanoprobes or PBS1X were added, according to Table 2. The samples were stirred overnight, and on the next day, magnetic separation was performed on all four samples. The serum purified from nanoprobes was then used for miR extraction and qRT-PCR (section 2.8.4).

2.8 Analytical methods

2.8.1 Size and Zeta potential

The physico-chemical properties of nanoprobes were determined by a Nanosizer instrument (Zetasizer®, Malvern Instrument, UK), for the measurements of the hydrodynamic diameter (D_H), the polydispersity index (PDI), and the zeta potential (ZP). The measurements were performed in PBS 1X at the iron concentration of 50 mg L^{-1} and were performed in triplicate with the mean value ± standard deviation presented. For ZP measurements, the ionic strength was fixed by adding NaCl to a final concentration of 10 mM.

2.8.2 Size exclusion HPLC analysis

SE HPLC measurements were performed with the Shimadzu system (Kyoto, Japan), using LC Column AdvanceBio SEC 300A, 2.7 µM, 7.8 x 300 mm, 1.0 mL/min flow rate. The Software LC Solution was used for data acquisition and analysis.

All samples containing nanoprobes were purified by magnetic separation before SE HPLC measurements, with the liquid MS 1 measured. For the measurements was used phosphate buffer mobile phase (0.15 mol/L; the combination of KH_2PO_4 at 0,075 mol/L and Na_2HPO_4,2 H_2O at 0,075 mol/L), which was used for all SE HPLC measurements, with the flow rate 1.0 mL/min, injection volume 10 µL, temperature 30°C, duration 15 min and UV detection at 260 nm and 280 nm.

2.8.3 Iron concentrations measurements

Iron concentrations were determined by Atomic Absorption Spectrophotometry (AAS) (iCE 3000 spectrometer, Thermo Instruments, France). The samples were mineralized for a minimum of 2 hours with concentrated hydrochloric acid (6 M), then diluted with H_2O. The concentration of the samples was determined by using a calibration curve (with iron absorption at 248.3 nm, and standard iron solutions at 0.25; 0.5; 1.0; 2.0; 5.0 mg/L).

2.8.4 qRT-PCR experiments

Extraction of miRs from the samples of human serum was performed with the Extraction kit NucleoSpin® miRNA (Macherey-Nagel). qRT-PCR was performed in

triplicates using miR-484 and UniSp6 primer mix, with kits MiRCURY LNA™ RT Kit, and miRCURY LNA™ SYBR Green PCR Kit (600) according to the instruction of the manufacturer (Qiagen) and as previously described [28], using T100™ Thermal Cycler and CFX96™ Real-Time System from BIO-RAD Laboratories. A 35 Ct-threshold was considered the value above which there is no physiological relevancy.

3. Results and Discussion

3.1 Formulation of nanoprobes

To generate the nanoprobes, we followed our previously established protocol [26], briefly outlined in the experimental section. As the precursors we used PEGylated SPIONs (NP), modified with α-Biotinyl-ω-NHS PEG, to enable further conjugation via streptavidin-biotin interactions. The streptavidin surface modification allowed approximate saturation and coverage of the surface, with available biotin-binding spots for biotinylated complementary DNA sequence (cDNA) as shown in Figure 1.

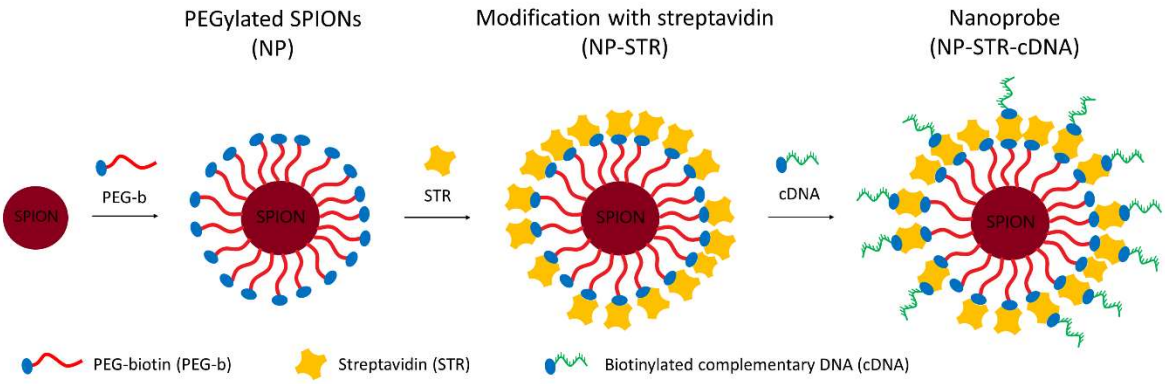

Figure 1 – Schematic representation of the nanoprobe formulation

To confirm the formulation of the nanoprobes, we used SE-HPLC to closely monitor both the precursor (NP) surface modification with streptavidin (NP-STR) and its functionalization with cDNA (NP-STR-cDNA). For the NP surface modification, we used the optimal Fe/STR molar ratio of 280, which was previously determined optimal for the

saturation of the available biotin sites at the surface of the NP. The amount of cDNA at the surface of NP after purification was about 40%, as deduced by comparing the cDNA peak areas in chromatograms: the excess cDNA not grafted on NPs vs cDNA solution at initial concentration.

The molar concentration of cDNA-484 was 5 μM, and the estimated number of cDNA molecules grafted per nanoprobe was 17. This result is in accordance with our previous publication, where we used the complementary miR (CmiR) at the concentration of 5 μM, and in our estimations, we grafted 22 CmiR molecules per nanoprobe. Notably, the iron concentration of both the starting NP batch and the NP-STR batch was higher during the functionalization with cDNA (600 mg/L) than with CmiR (350 mg/L). This result also confirmed that a more concentrated NP-STR-cDNA batch can be generated with nearly the same efficiency.

The batches NP, NP-STR, and NP-STR-cDNA had shown comparable physico-chemical properties, as displayed in Table 1. Across the batches, the hydrodynamic diameter (D_H) showed a slightly increasing tendency, 61.6 ± 2.0 nm *vs.* 67.0 ± 0.5 nm *vs.* 72.8 ± 2.6 nm, although the difference was not prominent enough to consider as proof of the successful conjugation on its own. The polydispersity around 0.2 was within the acceptable range, while the zeta potential (ZP), although still close to the neutral values, dipped down in the case of the NP-STR-cDNA batch to -7.5 ± 1.7 mV, possibly due to the negative charge of cDNA. Overall, the surface modification and the functionalization of nanoprobes did not decrease their colloidal stability.

Table 1 - Physico-chemical properties of batches NP, NP-STR, and NP-STR-cDNA in each step of the synthesis

Sample	D_H [nm]	PDI	ZP [mV]
NP (PEGylated SPIONs)	61.6 ± 2.0	0.20 ± 0.01	2.7 ± 0.1
NP-STR	67.0 ± 0.5	0.13 ± 0.01	3.1 ± 0.2
NP-STR-cDNA	72.8 ± 2.6	0.19 ± 0.03	-7.5 ± 1.7

3.2 TmiR capture in model solutions

The next step was confirmation that the nanoprobes functionalized with cDNA-484 are able to capture TmiR-484 (Figure 2A).

After the incubation of the NP-STR-cDNA sample with the sample of TmiR at the concentration of 5 µM, the data indicated that approximately 20% of TmiR was bound to nanoprobes, which matched with the result of our previous study. With respect to the increased concentration of NP-STR-cDNA nanoprobes, it corresponded with 9 TmiR molecules being bound per nanoprobe. As such, it is clear that following this protocol, the nanoprobes can be functionalized with either CmiR or cDNA of whichever sequence, without influencing their ability to capture chosen TmiR.

Additionally, we incubated the NP-STR-cDNA sample with decreasing concentrations of TmiR: 2.5 µM, 1 µM, and 0.5 µM, and compared the disappearance of TmiR. As seen in Figure 2B, the efficiency of TmiR capture rapidly increases at lower TmiR concentrations, reaching 91% at the TmiR concentration of 0.5 µM, which was the limit for obtaining a distinct and strong peak in chromatogram with SE-HPLC. This result was encouraging for the transfer of the study to biofluids, where the TmiRs are notably sparse.

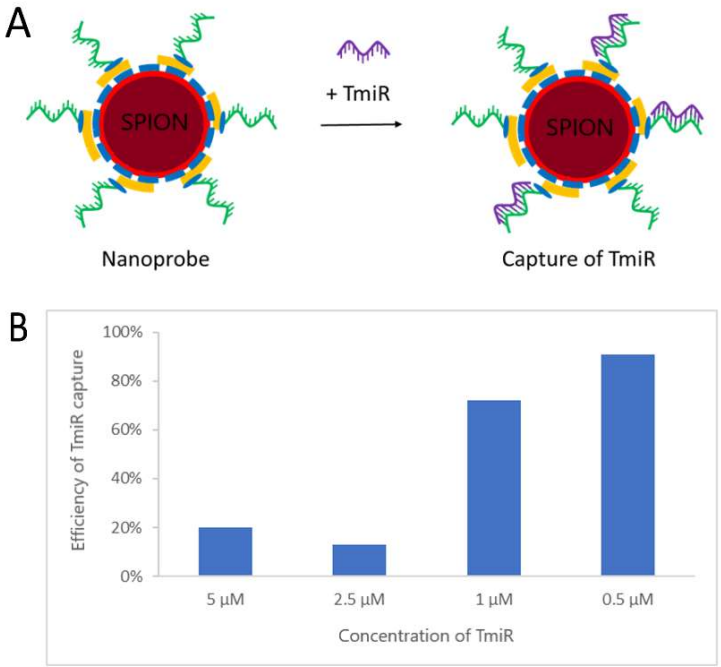

Figure 2 - A) Schematic representation of the TmiR capture process B) Histogram of the percentual efficiency of TmiR capture in model solutions at concentrations of 5 µM, 2.5 µM, 1 µM, and 0.5 µM.

3.3 Stability of nanoprobes in human serum

The stability of nanoprobes NP-STR-cDNA was tested in three different samples (a, b, and c) of human serum, as shown in Figure 3. The initial value of D_H, 72.8 ± 2.6 nm, changed after the incubation to 89.7 ± 4.7 nm (serum a), 98.2 ± 5.1 nm (serum b), or 106.8 ± 1.8 nm (serum c). The change in the measured size can be attributed to the adsorption of a variety of proteins naturally present in human serum to the surface of nanoprobes. The increase is not significant enough to suggest aggregation and disruption of stability, and the rising tendency could be simply due to differences in the samples of human serum. Although the polydispersity increased in serum samples (a) and (b) after the incubation, the values of all three samples did not differ greatly with respect to the standard deviations. The zeta potential remained practically unchanged in lower negative values. Therefore, despite the occurring adsorption of proteins on the surface, the colloidal stability of nanoprobes was not affected. Thus, the nanoprobes were eligible for experiments in human serum, with their properties remaining impervious to incubation in this body fluid.

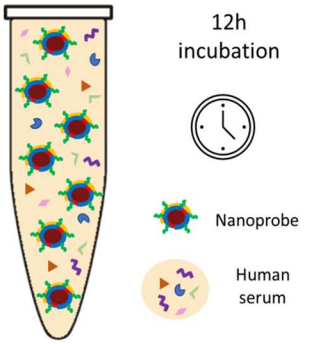

\+ Magnetic Separation ⟶ Measurement of physicochemical properties

Sample	Size [nm]	PDI	ZP [mV]
NP-STR-cDNA	72.8 ± 2.6	0.193 ± 0.028	-7.5 ± 1.7
NP-STR-cDNA in Serum(a)	89.7 ± 4.7	0.314 ± 0.015	-6.3 ± 1.3
NP-STR-cDNA in Serum(b)	98.2 ± 5.1	0.265 ± 0.037	-8.5 ± 0.5
NP-STR-cDNA in Serum(c)	106.8 ± 1.8	0.168 ± 0.007	-9.4 ± 0.9

Figure 3 – Colloidal stability of nanoprobes in human serum

3.4 TmiR capture in human serum

The nanoprobes NP-STR-cDNA (hereafter called NPR) were tested for their ability to capture TmiR in human serum (a supernatant of centrifugated blood samples that was allowed to spontaneously clot). Four samples were prepared, as described in the Experimental section. Briefly, human serum (HS) was mixed with either H_2O or TmiR, and then with either NPR or PBS 1X (according to Table 2); obtaining (i) sample without any additional TmiR: HS-H_2O-PBS, (ii) spiked with additional TmiR-484: HS-TmiR-PBS,

(iii) with nanoprobes added: HS-H_2O-NPR, and (iv) spiked with TmiR and nanoprobes added: HS-TmiR-NPR. After stirring overnight, the samples were purified with magnetic separation, regardless of whether they contained NPR or not, to ensure equal conditions.

Table 2 – Samples prepared for TmiR capture

Sample	300 uL	10 uL		90 uL	
	Serum	H_2O	TmiR	PBS 1X	NPR
HS-H_2O-PBS	●	●		●	
HS-TmiR-PBS	●		●	●	
HS-H_2O-NPR	●	●			●
HS-TmiR-NPR	●		●		●

Afterward, the miR extraction protocol was performed on the purified serums, followed by reverse transcription (RT) and quantitative Polymerase Chain Reaction (PCR). In our protocol, we have used SYBR green, a fluorophore that emits a strong fluorescence signal directly proportional to the amount of double-stranded DNA present in the sample [29].

The cycle threshold (Ct) is indicated by the thermocycler, showing the number of cycles needed for the fluorescence to cross the threshold value [13] (red line in Figures 4 and 5B). The higher concentration of TmiR-484 present in the sample corresponds with lower Ct, and we used the comparison of Ct values to determine differences between the samples. In figure 4 are amplification curves and Ct values of Serum (a) and samples HS-H_2O-PBS, HS-TmiR-PBS, HS-H_2O-NPR, and HS-TmiR-NPR obtained from the same serum.

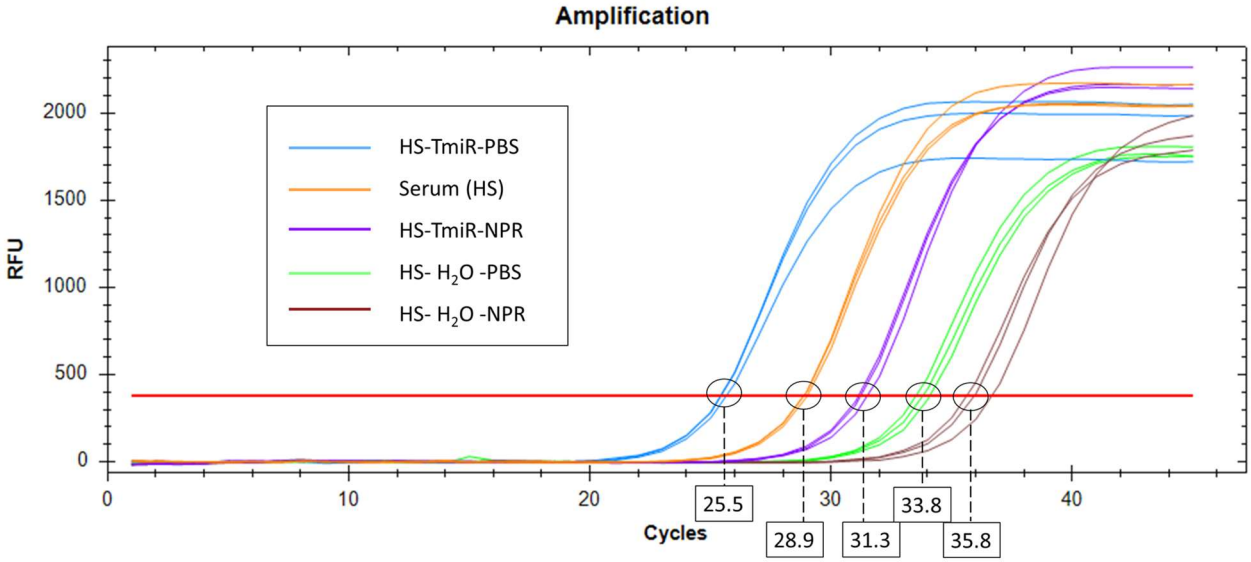

Figure 4 – The amplification curves of samples HS-H2O-PBS (green), HS-TmiR-PBS (blue), HS-H2O-NPR (brown), and HS-TmiR-NPR (purple) from Serum (a) (orange).

For miR-484 naturally present in the serum of healthy adult volunteers, the Ct values were in the interval 28-29, as was shown with the Ct value of 28.9 of untreated serum (orange line in Figure 4). Interestingly, the sample HS-H2O-PBS (green line in Figure 4) which is technically diluted serum, had higher Ct 33.8, showing the influence of the dilution on the miR extraction efficiency from the serum.

The sample HS-TmiR-PBS (blue line in Figure 4) was spiked with TmiR to obtain the final TmiR concentration at 0.5 µM. The stronger concentration was intended to circumvent the possible degradation of miR in the serum. However, the obtained Ct values were overall lower than expected. For the sample from serum (a), the Ct value was 25.5, corresponding to higher TmiR concentration than in the case of both the undiluted serum and the sample HS-H2O-PBS.

The sample HS-H2O-NPR (brown line in Figure 4) served to determine whether serum purified from NPR can be used for the qRT-PCR method. With the Ct value of 35.8, it can be concluded that nanoprobes do not cause any contamination to the serum samples. Indeed, the Ct values >35 can be considered null, with the amount of miR being too low to be detected. The difference between Ct values of the samples HS-H2O-PBS (33.8) and HS-

H2O-NPR (>35) is in all likelihood too small to safely determine whether the nanoprobes were able to capture the low amount of TmiR naturally present since the serums were without overexpressed TmiR levels.

Finally, the sample HS-TmiR-NPR (purple line in Figure 4) was spiked with the same concentration of TmiR 0.5 μM as the sample HS-TmiR-PBS, and afterward, NPR were inserted. Comparing the Ct values of the samples HS-TmiR-PBS and HS-TmiR-NPR, 25.5 vs. 31.3 respectively, it is clear that the nanoprobes captured a significant amount of TmiR present in the serum.

3.3.1 Sample-to-sample serum variability in TmiR capture

To examine the possible variations across different serum samples, we repeated the experiment of TmiR capture with samples HS-H_2O-PBS, HS-TmiR-PBS, HS-H_2O-NPR, HS-TmiR-NPR prepared from another sample of human serum (b). The comparison of Ct values across samples from both serums is presented in Table 3.

The Ct values of undiluted serum, and samples HS-H_2O-PBS and HS-H_2O-NPR proved similar for both serums. For serum (b), the sample HS-TmiR-PBS had a Ct value of 29.3, closer to the value of 28.3 of undiluted serum (b). This result means a strong degradation of synthetic TmiR sequences in serum. That could be due to the fact that circulating miRs naturally present in biofluids are associated with RNA-binding proteins, lending stability and protecting them from RNAse degradation [30], while synthetically produced TmiR is simply a bare sequence of nucleotides. The sample-to-sample difference in spiking can be attributed to serum (a) and (b) being obtained from different donors. The serum has a high concentration of proteins, and there is a significant difference across the samples regarding the protein and lipid content of each sample [12].

Table 3 – Comparison of Ct values of samples made from serum (a) and serum (b)

Sample	Ct	
	Serum (a)	Serum (b)
Serum (HS)	28.9	28.3
HS-H_2O-PBS	33.8	34.1
HS-TmiR-PBS	25.5	29.3
HS-H_2O-NPR	35.8	35.3
HS-TmiR-NPR	31.3	33.9

The difference between the samples HS-TmiR-PBS and HS-TmiR-NPR from serum (b), 29.3 vs. 33.9 respectively, was not as pronounced, however still notable enough to conclude the same capture ability in a different serum sample. Also, the samples HS-H2O-PBS and HS-TmiR-NPR in serum (b) gave very close values of 34.1 vs. 33.9, Thus indicating that NPR were able to capture all spiked TmiR present in the sample.

Overall, the nanoprobes demonstrated the ability to capture TmiR in the human serum. A sufficient amount of TmiR was found in all samples of HS-H2O-PBS, HS-TmiR-PBS, and HS-TmiR-NPR to provide conclusive results. On the other hand, additional spiking of the serum with TmiR proved to be unreliable. In the future, it would be interesting to use samples of human serums with natural overexpression of chosen TmiR and investigate their capture with suitably functionalized nanoprobes.

3.5 Dehybridization of TmiR

The last step of the successful TmiR capture with nanoprobes is the dehybridization of captured TmiRs. There are several approaches for disruption of the bond between the TmiR and the oligonucleotide sequence used for their capture [16,31,32]. In this study, we chose the dehybridization with heating, due to the simplicity of application and the ability to produce straightforward results without the interference of other molecules.

Following the scheme illustrated in Figure 5A, we repeated the experiment of TmiR capture as described in section 3.2, using PBS 1X as a model solution. The concentration of TmiR-484 in the model solution was 2 fmol/μL and after magnetic separation, we obtained a solution with remaining uncaptured TmiR, and nanoprobes with captured TmiR. We have attempted to dehybridize TmiR from nanoprobes by incubating the magnetically separated nanoprobes for 15 minutes at 60°C. Afterward, we performed a second magnetic separation, obtaining the dehybridized TmiR from nanoprobes.

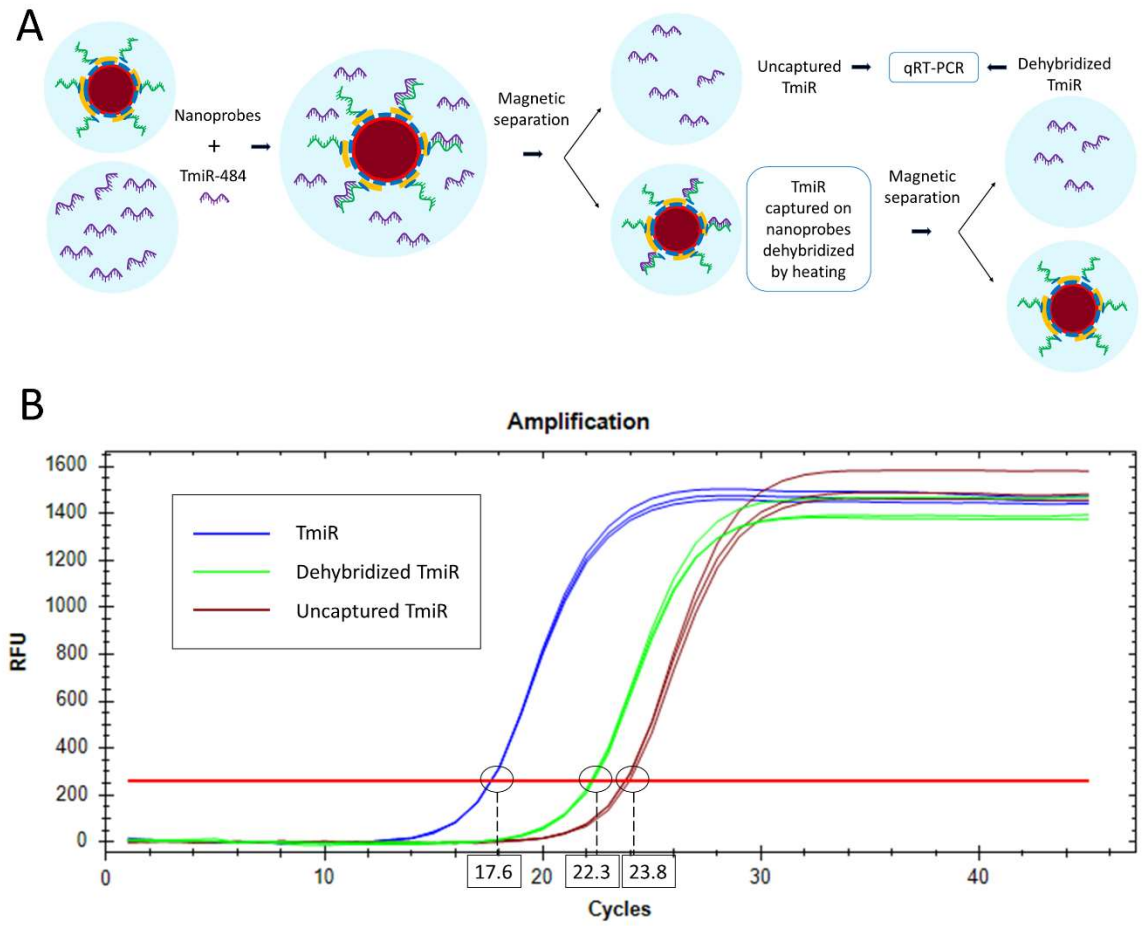

Figure 5 – A) Schematic representation of the experimental protocol of the dehybridization, B) The amplification curves of samples TmiR at the concentration of 2 fmol/µL (blue), dehybridized TmiR (green), and uncaptured TmiR (brown), with the Ct values.

We performed qRT-PCR on both the uncaptured TmiR and dehybridized TmiR, with a control solution of TmiR at the concentration of 2 fmol/µL. The amplification curves and Ct values are shown in Figure 5B: the pure TmiR solution had a strong Ct value of 17.6, and after the insertion of nanoprobes, the value shifted to 23.8 for the sample of uncaptured TmiR. After the heating, the Ct value for the sample of dehybridized TmiR was 22.3. This was a relatively high value of Ct, higher than of uncaptured TmiR, suggesting that a strong concentration of captured TmiR was dehybridized from the nanoprobes, and was possible to be recovered from the solution. The next steps would be to determine the optimal dehybridization method for TmiR captured in human serum, which would be at a much lower concentration than in our model solutions. It would be interesting to look for

a dehybridization process that keeps the functionality of nanoprobes intact for repeated use, however, it is not mandatory due to the relatively simple method of their synthesis.

4. Conclusions

In this study, we presented magnetic nanoprobes functionalized with cDNA-484 for the capture of TmiR-484. Nanoprobes were synthesized according to our previously established protocol and tested for their stability and functionality in the model solution of PBS 1X. The relatively unchanged values of physico-chemical properties of nanoprobes after their functionalization with cDNA-484 showed that their colloidal stability was preserved. The capture of TmiR-484 proved their increasing efficiency in lower concentrations, leading to experiments in human serum. In samples of human serum, the colloidal stability of nanoprobes was satisfactory while their hydrodynamic diameter increased a little due to the adsorption of various serum proteins. We tested the capture ability of nanoprobes in human serum, with the aid of the qRT-PCR method. Four samples were prepared from the human serum: (i) sample without any additional TmiR, (ii) spiked with additional TmiR-484, (iii) with nanoprobes added, and (iv) spiked with TmiR and nanoprobes added. Spiked TmiR proved to be unstable in serum samples, nevertheless, a clear distinction between TmiR levels was shown in spiked samples with and without nanoprobes. As such, nanoprobes were able to capture the TmiR in a complex medium that is the human serum. Finally, the heating-induced dehybridization of the majority of captured TmiR from nanoprobes was validated in model solutions. The above-described results are promising for using the nanoprobes to capture and to reconcentrate any TmiR of interest with low expression in biofluids. The next step would be to apply the nanoprobes in serum with naturally elevated TmiR levels.

Conflicts of interest

There are no conflicts to declare

Acknowledgments

We are grateful to the ‘‘Ligue Nationale Contre le Cancer” for their financial support (project NANOmiR) and especially to the local comities 53 and 56. This project was also supported

by grants on behalf of the following french department committees of Ligue Contre le Cancer Grand Ouest: 16 (Charente), 37 (Indre-et-Loire), 49 (Maine-et-Loire) and 72 (Sarthe). The authors would like to thank Juliette Lamamy and Valérie Gouilleux-Gruart (EA 7501 GICC) for the human serum samples.

5. References

1. Chandrasekaran, A.R.; Punnoose, J.A.; Zhou, L.; Dey, P.; Dey, B.K.; Halvorsen, K. DNA Nanotechnology Approaches for MicroRNA Detection and Diagnosis. *Nucleic Acids Res.* **2019**, 1–17, doi:10.1093/nar/gkz580.

2. Lo, P.K.; Wolfson, B.; Zhou, X.; Duru, N.; Gernapudi, R.; Zhou, Q. Noncoding RNAs in Breast Cancer. *Brief. Funct. Genomics* **2016**, *15*, 200–221, doi:10.1093/bfgp/elv055.

3. Li, M.; Li, J.; Zhang, X.; Yao, M.; Li, P.; Xu, W. Simultaneous Detection of Tumor-Related MRNA and MiRNA in Cancer Cells with Magnetic SERS Nanotags. *Talanta* **2021**, *232*, 122432, doi:10.1016/j.talanta.2021.122432.

4. Fauth, M.; Saul, M.J. Validation of Extracellular MiRNA Quantification in Blood Samples Using RT - QPCR. **2019**, 481–492, doi:10.1096/fba.2019-00018.

5. Shen, Z.; He, L.; Wang, W.; Tan, L.; Gan, N. Highly Sensitive and Simultaneous Detection of MicroRNAs in Serum Using Stir-Bar Assisted Magnetic DNA Nanospheres-Encoded Probes. *Biosens. Bioelectron.* **2020**, *148*, 111831, doi:10.1016/j.bios.2019.111831.

6. Ban, E.; Song, E.J. Considerations and Suggestions for the Reliable Analysis of MiRNA in Plasma Using QRT-PCR. **2022**.

7. Loh, H.-Y.; Norman, B.P.; Lai, K.-S.; Rahman, N.M.A.N.A.; Alitheen, N.B.M.; Osman, M.A. The Regulatory Role of MicroRNAs in Breast Cancer. *Int. J. Mol. Sci.* **2019**, *20*, 4940, doi:10.3390/ijms20194940.

8. Svoronos, A.A.; Engelman, D.M.; Slack, F.J. OncomiR or Tumor Suppressor? The Duplicity of MicroRNAs in Cancer. *Cancer Res.* **2016**, *76*, 3666–3670, doi:10.1158/0008-5472.CAN-16-0359.

9. Jia, Y.Z.; Liu, J.; Wang, G.Q.; Song, Z.F. MiR-484: A Potential Biomarker in Health and Disease. *Front. Oncol.* **2022**, *12*, 1–22, doi:10.3389/fonc.2022.830420.

10. Chai, J.; Wang, S.; Han, D.; Dong, W.; Xie, C.; Guo, H. MicroRNA-455 Inhibits Proliferation and Invasion of Colorectal Cancer by Targeting RAF Proto-Oncogene Serine/Threonine-Protein Kinase. *Tumor Biol.* **2015**, *36*, 1313–1321, doi:10.1007/s13277-014-2766-3.

11. Lu, X.; Lu, J. The Significance of Detection of Serum MiR-423-5p and MiR-484 for Diagnosis of Colorectal Cancer. *Clin. Lab.* **2015**, *61*, 187–190.

12. Kroh, E.M.; Parkin, R.K.; Mitchell, P.S.; Tewari, M. Analysis of Circulating MicroRNA Biomarkers in Plasma and Serum Using Quantitative Reverse Transcription-PCR (QRT-PCR). *Methods* **2010**, *50*, 298–301, doi:10.1016/j.ymeth.2010.01.032.

13. Moukengue, B.; Amiaud, J.; Jacques, C.; Charrier, C.; Ory, B.; Lamoureux, F. Analysis of MRNA, MiRNA, and DNA in Bone Cells by RT-QPCR and in Situ Hybridization. *Methods Mol. Biol.* **2019**, *1914*, 169–196, doi:10.1007/978-1-4939-8997-3_9.

14. Chan, H.N.; Ho, S.L.; He, D.; Li, H.W. Direct and Sensitive Detection of Circulating MiRNA in Human Serum by Ligase-Mediated Amplification. *Talanta* **2020**, *206*, 120217, doi:10.1016/j.talanta.2019.120217.

15. Pratama, M.Y.; Cavalletto, L.; Tiribelli, C.; Chemello, L.; Pascut, D. Selection and Validation of MiR-1280 as a Suitable Endogenous Normalizer for QRT-PCR Analysis of Serum MicroRNA Expression in Hepatocellular Carcinoma. *Sci. Rep.* **2020**, *10*, 3128, doi:10.1038/s41598-020-59682-0.

16. Coutinho, C.; Somoza, Á. MicroRNA Sensors Based on Gold Nanoparticles. *Anal. Bioanal. Chem.* **2019**, *411*, 1807–1824, doi:10.1007/s00216-018-1450-7.

17. Goryacheva, O.A.; Vostrikova, A.M.; Kokorina, A.A.; Mordovina, E.A.; Tsyupka, D. V.; Bakal, A.A.; Markin, A. V.; Shandilya, R.; Mishra, P.K.; Beloglazova, N. V.; et al. Luminescent Carbon Nanostructures for MicroRNA Detection. *TrAC - Trends Anal. Chem.* **2019**, *119*, 115613, doi:10.1016/j.trac.2019.07.024.

18. Gessner, I.; Yu, X.; Jüngst, C.; Klimpel, A.; Wang, L.; Fischer, T.; Neundorf, I.; Schauss, A.C.; Odenthal, M.; Mathur, S. Selective Capture and Purification of MicroRNAs and Intracellular Proteins through Antisense-Vectorized Magnetic Nanobeads. *Sci. Rep.* **2019**, *9*, 1–10, doi:10.1038/s41598-019-39575-7.

19. Pang, Y.; Wang, C.; Wang, J.; Sun, Z.; Xiao, R.; Wang, S. Fe3O4@Ag Magnetic Nanoparticles for MicroRNA Capture and Duplex-Specific Nuclease Signal Amplification Based SERS Detection in Cancer Cells. *Biosens. Bioelectron.* **2016**, *79*, 574–580, doi:10.1016/j.bios.2015.12.052.

20. Wong, W.K.; Wong, S.H.D.; Bian, L. Long-Term Detection of Oncogenic MicroRNA in Living Human Cancer Cells by Gold@ Polydopamine-Shell Nanoprobe. *ACS Biomater. Sci. Eng.* **2020**, *6*, 3778–3783, doi:10.1021/acsbiomaterials.0c00633.

21. Al Mubarak, Z.H.; Premaratne, G.; Dharmaratne, A.; Mohammadparast, F.; Andiappan, M.; Krishnan, S. Plasmonic Nucleotide Hybridization Chip for Attomolar Detection: Localized Gold and Tagged Core/Shell Nanomaterials. *Lab Chip* **2020**, *20*, 717–721, doi:10.1039/c9lc01150a.

22. Xu, Z.-H.; Wang, H.; Wang, J.; Zhao, W.; Xu, J.-J.; Chen, H.-Y. Bidirectional Electrochemiluminescent Sensing: An Application in Detecting MiRNA-141. *Anal. Chem.* **2019**, *91*, 12000–12005, doi:10.1021/acs.analchem.9b02914.

23. Song, W.; Zhang, F.; Song, P.; Zhang, Z.; He, P.; Li, Y.; Zhang, X. Untrasensitive Photoelectrochemical Sensor for MicroRNA Detection with DNA Walker Amplification and Cation Exchange Reaction. *Sensors Actuators, B Chem.* **2021**, *327*, 128900, doi:10.1016/j.snb.2020.128900.

24. Horny, M.C.; Gamby, J.; Dupuis, V.; Siaugue, J.M. Magnetic Hyperthermia on γ-Fe2O3@SiO2 Core-Shell Nanoparticles for Mi-RNA 122 Detection. *Nanomaterials* **2021**, *11*, 1–15, doi:10.3390/nano11010149.

25. Mehdipour, M.; Gloag, L.; Bennett, D.T.; Hoque, S.; Pardehkhorram, R.; Bakthavathsalam, P.; Gonçales, V.R.; Tilley, R.D.; Gooding, J.J. Synthesis of Gold-Coated Magnetic Conglomerate Nanoparticles with a Fast Magnetic Response for Bio-Sensing. *J. Mater. Chem. C* **2021**, *9*, 1034–1043, doi:10.1039/d0tc04702c.

26. Vilímová, I.; Chourpa, I.; David, S.; Soucé, M.; Hervé-Aubert, K. Two-Step Formulation of Magnetic Nanoprobes for MicroRNA Capture. *RSC Adv.* **2022**, *12*, 7179–7188, doi:10.1039/d1ra09016j.

27. Hervé, K.; Douziech-Eyrolles, L.; Munnier, E.; Cohen-Jonathan, S.; Soucé, M.; Marchais, H.; Limelette, P.; Warmont, F.; Saboungi, M.L.; Dubois, P.; et al. The Development of Stable Aqueous Suspensions of PEGylated SPIONs for Biomedical Applications. *Nanotechnology* **2008**, *19*, doi:10.1088/0957-4484/19/46/465608.

28. Chautard, R.; Corset, L.; Ibrahim, S.; Desvignes, C.; Paintaud, G.; Baroukh, N.; Guéguinou, M.; Lecomte, T.; Raoul, W. Panitumumab and Cetuximab Affect Differently MiRNA Expression in Colorectal Cancer Cells. *Biomark. Med.* **2021**, *15*, 685–696, doi:10.2217/bmm-2020-0520.

29. Tajadini, M.; Panjehpour, M.; Javanmard, S. Comparison of SYBR Green and TaqMan Methods in Quantitative Real-Time Polymerase Chain Reaction Analysis of Four Adenosine Receptor Subtypes. *Adv. Biomed. Res.* **2014**, *3*, 85, doi:10.4103/2277-9175.127998.

30. Junqueira-Neto, S.; Batista, I.A.; Costa, J.L.; Melo, S.A. Liquid Biopsy beyond Circulating Tumor Cells and Cell-Free DNA. *Acta Cytol.* **2019**, *63*, 479–488, doi:10.1159/000493969.

31. Wang, M.; Chen, W.; Tang, L.; Yan, R.; Miao, P. Duplex-Specific Nuclease Assisted MiRNA Assay Based on Gold and Silver Nanoparticles Co-Decorated on Electrode Interface. *Anal. Chim. Acta* **2020**, *1107*, 23–29, doi:10.1016/j.aca.2020.01.041.

32. Qi, T.; Song, C.; He, J.; Shen, W.; Kong, D.; Shi, H.; Tan, L.; Pan, R.; Tang, S.; Lee, H.K. Highly Sensitive Detection of Multiple MicroRNAs by High-Performance Liquid Chromatography Coupled with Long and Short Probe-Based Recycling

Amplification. *Anal. Chem.* **2020**, *92*, 5033–5040, doi:10.1021/acs.analchem.9b05301.

GENERAL DISCUSSION

The research field of miR detection based on nanomaterials is indisputably wide and varied, due to the diverse possibilities presented by nanotechnology. The detection of TmiRs in biofluid promises a potential for diagnostic enhancement of various life-threatening disorders. Magnetic nanomaterials present an interesting option of magnetic extraction and reconcentration, with the prospect of bypassing the traditional extraction methods. Current challenges lie in the detection in biofluids, with the overall low amount of TmiRs and the presence of other interfering biomolecules in the complex media [1].

On previous pages, we have reported our progress regarding the successful development of magnetic nanoprobes for miR capture. The nanoprobes were based on Superparamagnetic Iron Oxide Nanoparticles - SPIONs, coated with a polyethylene glycol (PEG) chain structured to have NHS group on one end and biotin on the other. Using PEGylated SPIONs as a precursor, the nanoprobes were formulated in two steps: i) surface modification of the PEGylated SPIONs with streptavidin, and ii) functionalization with complementary sequence (CmiR-155, cDNA-484) to the target miR (TmiR-155 and TmiR-484). The main analytical method for monitoring the synthesis was Size Exclusion High-Performance Liquid Chromatography (SE HPLC), while the physico-chemical properties of the nanoprobes were determined by DLS measurement, atomic absorption spectrophotometry, and IR spectrophotometry. With SPIONs in the core, it was possible to use magnetic sorting as a purification method and to separate the nanoprobes from their media. The nanoprobes were tested for their capture efficiency of both TmiRs in model solution at different concentrations, and TmiR-484 was also captured from samples of human serum. The amount of TmiR-484 present in the serum was monitored with qRT-PCR, confirming the ability and function of the nanoprobes, and the captured TmiR was dehybridized by heating.

Nevertheless, there were several adjustments and difficulties to overcome on the road to obtaining functional nanoprobes.

For the core of the nanoprobes, we have chosen SPIONs, which are already a well-established platform for targeted nanomedicine [2] and are useful as contrast agents for magnetic resonance imaging [3]. Our team had instituted a protocol for their synthesis and

surface modification [4], through the steps of (i) synthesis of initial SPIONs by coprecipitation of iron salts, (ii) the silanization of SPIONs (coating with APS, 3-aminopropyltrimethoxysilane molecules), and (iii) their PEGylation (coating with PEG) [5]. PEG is non-toxic and non-immunogenic, hydrophilic, and highly labile [6], and a wide variety of PEG modifications is commercially available. The PEGylation is arguably the most important step since it provides to SPIONs the colloidal stability in aqueous media, due to the steric hindrance not being dependent on pH. The PEG layer can be optimized in terms of its density, and the PEG structure can be modified with certain terminal groups useful for further functionalization.

Initially, we had intended to attach CmiR covalently to the surface of PEGylated SPIONs, using carbodiimide chemistry of the amine group with N-hydroxysuccinimidyl (NHS)-activated carboxylic compound [7,8]. As was summarized in our first publication, such covalent conjugation would provide a strong bond with high stability, and it is a quite popular approach for miR functionalization. Indeed, amine-modified or carboxyl-modified CmiR can be simply produced and purchased, and carboxyl or amine groups are easy to generate on the surface of SPIONs by well-known chemical modifications [9–11].

In our case, we coated silanized SPIONs with the amino-reactive PEG derivative carrying NHS groups on both ends (NHS-PEG-NHS), which led to the PEG shell decorated with NHS groups. The latter were then activated with 1-ethyl-3-(3-dimethylaminopropyl)carbodiimide (EDC) and NHS, resulting in the presence of a carboxyl group that was able to bind an NH_2-modified CmiR-155. However, in this particular combination, the generally sure-fire carbodiimide chemistry proved to be unsuitable, or at least it was not possible to confirm the successful functionalization. Either because no CmiR was bound or because of an unsuitable analytical technique. Regarding the first option, it was possible that the long chains of the PEG might have become tangled or wrapped around the surface of SPION in such a way that the NHS groups were not accessible for activation and/or for binding to CmiR molecules. In the literature, long linkers are usually not used to obtain carboxyl groups on the surface of the nanomaterial [9,12–14].

As for the second option, we realized the difficulty to determine the NPs functionalization with CmiR, since regular and widely available analytical methods were not very efficient in this regard. MiR molecules are too small to confirm their binding to the NPs by measuring their hydrodynamic diameter [15]. Similarly, the attachment of negatively

charged CmiRs to NPs usually does not change significantly their zeta potential, although in some cases a significant shift has been reported [16]. In principle, measuring the absorbance of miRs at 260 nm [17] is useful for that purpose, however, it requires high concentrations of miR. In the alternative, for some nanomaterial substrates (for example Au NPs, QDs), the approach based on the binding-induced absorbance changes (band shift) can be used [18,19]. As such, UV-vis measurement proved to be ineffective especially for characterizing the surface of PEGylated SPIONs, due to their own inherent absorbance, along with the signal of potential CmiR added on their surface being too weak for detection. Additionally, the measurement of the sample purified via magnetic separation of SPIONs had shown that the EDC/NHS compounds, particularly NHS ester, also presented strong absorbance around 260 nm [6], overwhelming the signal from CmiR.

Gel electrophoresis is another analytical method used to determine the attachment of the nanomaterial and the ligand [20] or between two ligands [21] (CmiR-TmiR), from the difference between the gel migration of the free or bound compounds, depending on their size and the molecular weight [22]. Again, the electrophoresis proved to be ill-suited to our combination of PEGylated SPION – CmiR. First of all, miR itself leaves a very weak trace through the gel (weaker than for example siRNA), circling back to the necessity of using stronger concentration. At the same time, PEGylated SPIONs did not migrate through the gel, leaving it impossible to determine whether any CmiR was attached to their surface or not. Similarly, the trace of residual unattached CmiR that was present in the solution with SPIONs did not have either the brightness or consistency of free CmiR alone taken at the same concentration. From the result of functionalization via streptavidin-biotin interactions, it was determined that the amount of CmiR attached to the surface of SPIONs corresponded approximately to the concentration of 1 μM, which was already a too-weak concentration of miR for agarose gel electrophoresis.

Spectroscopic techniques likewise showed no real benefit in the control of our nanoprobe formulation. While we used infrared (IR) spectroscopy [23] for the confirmation of silanization and PEGylation of SPIONs, it was not able to determine the conjugation of CmiR due to its too-weak signal. Similarly, we did not have structural and elemental techniques available in our laboratory, such as X-ray photoelectron spectroscopy, which would enable us to determine the changed elemental ratio if the conjugation was successful [24,25]. Additionally, although fluorescence spectroscopy and imaging are very popular for monitoring the conjugation of the complementary sequence and even the hybridization of

the target miRNA (based on the increase of the signal or its quenching during the binding event) [23,26,27], we aimed to avoid using fluorescent compounds in the formulation.

As such, we concluded two things: it was necessary to find an analytical technique that would allow us to monitor each step of the formulation, and also to construct the formulation in such a way that would eliminate avoidable shortcomings presented in our earlier attempt. Thus, we chose Size-Exclusion High-Performance Liquid Chromatography (SE HPLC), which allows the separation and monitoring of each component in the formulation. In the literature, HPLC is mostly used for the analysis and purification of commercially available nucleotide sequences [28], or for fluorescence-based signal detection of miRs [29,30], but not for monitoring the process of nanoprobe formulation.

For the formulation, the solution arose in finding an intermediary for binding the CmiR to the PEGylated SPIONs, and so going forward we decided upon using streptavidin-biotin interactions. Streptavidin-modified nanomaterials [31,32] and biotin-modified oligonucleotide sequences [33,34] are commercially produced and widely used, with streptavidin-biotin interactions providing specific and stable bonds [35,36]. The PEGylation process using the PEG chain with biotin on its end proved to be working with the same efficiency. With the biotin working as an ending group on the surface of PEGylated SPIONs, the attachment of streptavidin allowed the formation of a layer that again had many available binding sites for biotinylated CmiR. The interval between our presented optimal ratio for the saturation of the surface with streptavidin (280 Fe/STR) and the next tested ratio (1400 Fe/STR) was wide, and it is possible in the future to optimize the ratio more precisely. We investigated more in-depth the CmiR concentration necessary for the functionalization, and our to-go concentration of CmiR at 5 uM was confirmed as having a good balance between the efficiency of the conjugation and the unnecessary excess of an expensive compound. We applied the previously tested estimation of conjugated antibody fragments to the surface of SPIONs [37] to calculate the number of the CmiR molecules bound to the surface of nanoprobes. With the ratio of 22:18 for CmiR:TmiR per nanoprobe, the majority of bound CmiR was available to capture the TmiR, confirming the functionality of nanoprobes.

Following this thread, there were imperative questions to answer regarding the versatility of the nanoprobes (functionalization and capture with different sequence/TmiR),

their stability in biofluid (human serum, which contains circulating free miRs [32,38]), and the ability to capture TmiR as well as its dehybridization from the surface of the nanoprobes.

Based on the results from our third publication, the formulation and capture worked correspondingly with cDNA and TmiR-484, and the protocols could be adapted depending on whether CmiR-TmiR or cDNA-TmiR pair is desired. Similarly, the colloidal stability of the nanoprobes was preserved in human serum, despite the adsorption of serum proteins on their surface.

For the capture of TmiR-484 from the serum, there were several points to consider: first, the choice of analytical method came up again, as it is not possible to introduce human serum in the SE column. Additionally, we aimed for the capture of lower concentrations of TmiR, below the detection limit of the SE HPLC. For the detection and quantification of miR, qRT-PCR is considered the most reliable method, and it was a good fit for our concept of future improvement of miR detection with any analytical technique. Second, the design of the experiment, in the sense of fine-tuning the ratio of nanoprobes versus the human serum, to achieve good concentration for both steps, i.e., the capture and the following magnetic sorting.

As for magnetic sorting, it also raised its own challenges. We have decided to use it as a purification method, which would allow us to separate the nanoprobes from the biological fluid and to reconcentrate them in a new solution. We determined that the efficiency is not one hundred percent, presumably due to the fact that some particles are permanently adsorbed to the surface of magnetic beads in the column. Since the effectiveness of the magnetic separation directly influences the yield of TmiR and the following quantification [39], further research is necessary to confirm the adequacy of the amount of TmiR obtained with this method. Regarding the TmiR reconcentration, it was possible to obtain between a twofold and fivefold concentration increase, depending on the starting volume of the nanoprobes solution (200 – 500 μL). While this result is encouraging for the redispersion of concentrated nanoprobes into a larger volume of fluid, there is still a need for further studies, since the intended reconcentration of captured TmiR is so far arguably negligible.

For the qRT-PCR experiments, it was necessary to again separate the nanoprobes with captured TmiR from the human serum, so the miR can be extracted and analyzed. The extraction of miR from body fluids brings its own specific challenges, with the efficiency

influenced by many factors, such as the type of the extraction kit and sample-to-sample variations which are uniquely dependent on the donor [40,41]. We have discovered that combining the serum with the nanoprobes also directly influences the miR extraction, resulting in weaker signal amplification in qRT-PCR. Additionally, miR concentrations in serum can be very low, (10^{-12} to 10^{-16} M, or even lower [42]), as we confirmed by comparing the TmiR amplification from untreated serum from healthy adult volunteers vs. the TmiR in the model solution where the concentration of 2 fmol/μL was notably stronger.

The last conundrum to overcome was dehybridization. In the literature can be often found the dehybridization with duplex-specific nuclease (DSN) [13,43], an enzyme capable of disrupting DNA-DNA and DNA-RNA duplexes [44]. That was the initial reason why we chose cDNA-484 as opposed to possible CmiR-484. However, the available amount of DSN was insufficient to dissociate the cDNA-TmiR complex. Further optimization would be required for obtaining the necessary activity of the enzyme in the sample with the nanoprobes. Additionally, when performing agarose gel electrophoresis, the cDNA, TmiR, and cDNA-TmiR complex moved identically through the gel, with the only difference in the intensity of the trace. Thus, the recommended control for monitoring the enzyme activity was impractical in this case – our complementary sequences to the TmiR have the same length (23 nucleotides for CmiR-155 and TmiR-155, 22 nucleotides for cDNA-484 and TmiR-484), and it is not possible to distinguish between the sequences of the same molecular weight. As such, monitoring DSN activity with agarose gel electrophoresis can be applied to other structures, such as hairpin DNA. Similarly, performing SE-HPLC analysis had shown no difference in the peak of the cDNA-TmiR complex, except for an uneven baseline and additional peak coming from the DSN storage buffer.

The other options of dehybridization were in the form of denaturation of DNA through chemical approaches, such as a change of pH by adding either acid or NaOH [45]. However, this option was unappealing due to the fact that with SE-HPLC as the main analytical method we were constrained by the necessity of using a buffer with neutral pH for the SE column. Also, the pH change would disrupt the colloidal stability of nanoprobes, and the resulting destruction of the nanoprobes could lead to the release of the compound into the solution, which would hinder the TmiR detection even more. Although the same could be said for dehybridization through physical means, like sonication and heating [10], the streptavidin-biotin bonds are presented to be stable at least up to 70°C, similarly to the PEGylated SPIONs, and as such we were confident in the stability of the nanoprobes

remaining unchanged at least up to 65°C [6]. With SE-HPLC, we detected an appearance of a tiny peak of single oligonucleotide sequences in the solution of the cDNA-Tmir complex after the sonication and/or the heating treatment. With this confirmation, we did not explore if a significant prolongation of the heating would deal adequately with the strong concentration required for SE-HPLC, and instead switched to the qRT-PCR analysis that allowed us to move into lower concentrations. Indeed, the results presented in the third publication had shown that the dehybridization is easier to monitor in lower concentrations, and that similarly the relatively short amount of the heating time (15 min) is more appropriate for the amount of cDNA-TmiR complexes formed on the nanoprobes than it was for a strong concentration of only cDNA-TmiR complex.

Overall, each segment of our presented concept leaves ample space for further optimization, however, the most interesting is probably the exploration of TmiR capture efficiency and enhancement of the detections of the dysregulated miR levels with qRT-PCR.

CONCLUSIONS AND PERSPECTIVES

miRs are a short non-coding endogenous RNA family with a length from 19 to 23 nucleotides. They play an important role in various cellular processes and have been identified as authentic oncogenes or tumour suppressor genes. Dysregulation of their levels of expression has been associated with numerous pathologies, such as cancer. They are shaping to be new diagnostic and prognostic markers in the future, as indicators of therapeutic response. Development of nanoprobes that would facilitate target miR (TmiR) capture and isolation is a possible step to enhance miR detection with already established methods.

The objectives of the thesis were the following: i) development and characterization of the nanoprobes, and ii) development of protocols for nanoprobe-mediated TmiR isolation from biological samples.

The study was accordingly divided into two parts – in the first part, we examined the conjugation approaches leading to the functionalization of the nanomaterial (Publication 1), and the subsequent formulation of nanoprobes (Publication 2). In the second part, we examined the application of the nanoprobes for TmiR capture in human serum (Publication 3).

For any experimental setup with the goal of TmiR capture and detection, the design of the chosen form of nanoprobes remains the starting point. Keeping in mind the available materials and analytical techniques, as well as the simplicity of the procedure and the suitable stability of the final product, is the first step leading to a successful synthesis. For the detection methods based on hybrid nanomaterials, it is quite common to conjugate on the surface of the nanomaterial either RNA or DNA oligonucleotides in a complementary sequence to the intended TmiR. As such, the choice of the conjugation approach between the nanomaterial and the complementary sequence is the important cornerstone. Linking of nanomaterials with various targeting biomolecules can be done through a wide array of strategies, and due to the relatively recent emergence of miR-targeting research, not all of them have been yet implemented, leaving ample space for more detailed investigation. Indeed, for miR-related detection, the most frequent approaches are also the most well-known ones, both in covalent and non-covalent linking. In the first publication, we presented some of the unique properties of various nanomaterials, and analytical techniques that are

frequently used for the characterization of functionalized nanomaterials, with the main focus on the popular conjugation approaches, both the covalent and non-covalent with their specific advantages and drawbacks.

Following the acquired knowledge about various conjugation approaches, we advanced toward the formulation of our magnetic nanoprobes.

The functionalization of a nanomaterial can be at times challenging since various concerns need to be taken into the consideration. For the synthesis of nanoprobes for miR capture, the concerns can be the following: available reactive groups on the surface, colloidal stability, reliable characterization method for the functionalization, effectiveness, and reproducibility of the procedure and resulting capture ability of the synthesized product. Herein we presented a two-step formulation of magnetic nanoprobes for TmiR capture. The core of nanoprobes was based on SPIONs, superparamagnetic iron oxide nanoparticles, which are colloidally stable after their surface is coated by PEG chains. Using a PEG chain with suitable modification allows a possible variety of conjugation approaches since its free end can be modified with various functional groups, allowing it to bind the complementary miR sequence (CmiR) and form the nanoprobe. With both biotinylated PEG chain and biotinylated CmiR, using streptavidin-biotin interactions and having streptavidin as a linker allowed the ideal coverage of the surface of PEGylated SPIONs, ensuring that the CmiR had many binding spots available. This resulted in a two step-approach of saturation of the surface of PEGylated SPIONs with streptavidin, and subsequent functionalization with biotinylated CmiR-155 (complementary to TmiR-155) presented in the second publication. Equally important was to find a way to verify that each step of the synthesis was adequately performed. That was realized by choosing size-exclusion HPLC (SE HPLC) as an indirect analytical method. SE HPLC allowed the analysis of the solution after the purification of SPIONs via magnetic separation. That provided a straightforward method to synthesize the nanoprobes while confirming the completion of each step. Similarly, it was possible to ascertain both the concentration of CmiR bound to the nanoprobes and the concentration of captured TmiR, along with the estimation of the number of sequences bound per nanoprobe. The nanoprobes were coated with 22 CmiR per nanoprobe and were able to capture 18 TmiR per nanoprobe from the TmiR solution at the concentration of 5 μM. The colloidal stability was assessed by measuring their hydrodynamic diameter (DH) and zeta potential (ZP) - the resulting nanoprobes had a size of about 70 nm and nearly neutral ZP.

Following the foundation of magnetic nanoprobes functionalized for TmiR-155 capture, the next step was to test the functionalization with a new complementary sequence and the capture of different TmiR. The focus was shifted to the functionalization with complementary DNA sequence (cDNA-484) to TmiR-484 presented in the third publication, repeating the previously described formulation of the nanoprobes and its verification to ensure the effective functionalization was reproduced, along with a confirmation of TmiR capture in model solutions. The efficiency of the capture proved to be increased in lower concentrations, presenting an encouraging outlook for the capture in human serum. Using magnetic separation as the purification method allowed the reconcentration of nanoprobes, supporting the idea of inserting a smaller, concentrated volume of nanoprobes into a larger volume of biofluid. Similarly, nanoprobes proved to be stable in human serum, despite the present absorption of proteins on the surface of nanoprobes. The confirmation of their function was analyzed with quantitative reverse transcription polymerase chain reaction (qRT-PCR) and nanoprobes proved their capture ability in serum spiked with TmiR-484. The final point was to examine a method of dehybridization of captured TmiR from the nanoprobes – after heating, a notable concentration of TmiR was again present in the purified solution.

Altogether, the nanoprobes demonstrated their ability to capture target miRs in biological samples, with the potential to enhance the sensing of dysregulated levels of miR expression in future use.

Due to the novelty of the topic in our team, there are many questions left to answer regarding various steps of our presented protocols. While the formulation of nanoprobes is composed of two relatively simple steps, the second step of the functionalization opens door to a wide array of possibilities, since we demonstrated either CmiR or cDNA can be used. It would be interesting to investigate the functionalization with different sequences, with changed modifications and structures. Similarly, the ratio of miR-per-nanoprobe and the concentration of prepared nanoprobe suspension should be adaptable if necessary. Correspondingly, the monitoring of the formulation via SE HPLC could be fine-tuned for lower concentrations if necessary, and there are other analytical techniques (such as X-ray photoelectron spectroscopy) to consider as viable options, depending on available time and equipment.

The most interesting would be the following study of the efficiency of TmiR capture in biological samples, such as human serum, and its subsequent reconcentration. Our reported results are mostly the preliminary confirmations of nanoprobe stability and function in the serum, and the corroboration of a basic working protocol for nanoprobe-mediated TmiR detection in combination with qRT-PCR. The protocol itself is composed of several steps which require further consideration. The insertion of concentrated nanoprobes into the serum was shown to be influencing the yield of extracted miR, and similarly, additionally spiked TmiR proved to be unstable in the serum. Adjustments to both the sample preparation and the extraction protocol should be considered, to achieve consistent results. Additionally, the reported experiments were performed in serum with no remarkable dysregulations in the expression levels of targeted TmiR and it is necessary to investigate the function of nanoprobes in biofluid with over-regulated levels of chosen TmiR.

The captured TmiR needs to be properly quantified, as well as the TmiR released from the nanoprobes in the dehybridization process. The dehybridization itself should be considered in unison with TmiR reconcentration, and the dehybridization protocols need in-depth investigation regarding their efficiency in relation to formulated nanoprobes.

Overall, this study shows a basis for the concept of functional magnetic nanoprobes that can be inserted into a biofluid containing TmiR and other molecules, and that can effectively capture the chosen TmiR, allowing its reconcentration and more sensitive detection with an established analytical method. Since functionalized nanomaterials have lately become a viable option for the enhancement of analytical techniques and detection methods for targeting miR, future research in this field is full of possibilities and questions left to be answered.

CONCLUSIONS ET PERSPECTIVES

Les miRs sont une famille d'ARN endogènes courts non codants d'une longueur de 19 à 23 nucléotides. Ils jouent un rôle important dans divers processus cellulaires et ont été identifiés comme d'authentiques oncogènes ou gènes suppresseurs de tumeurs. La dérégulation de leurs niveaux d'expression a été associée à de nombreuses pathologies, comme le cancer. Ils s'annoncent comme de nouveaux marqueurs diagnostiques et pronostiques à l'avenir, en tant qu'indicateurs de la réponse thérapeutique. Le développement de nanosondes facilitant la capture et l'isolement du miR cible (TmiR) est une étape possible pour améliorer la détection des miRs avec des méthodes déjà établies.

Les objectifs de la thèse étaient les suivants : i) développement et caractérisation des nanosondes, et ii) développement de protocoles pour l'isolement de TmiR à l'aide de nanosondes à partir d'échantillons biologiques.

L'étude a donc été divisée en deux parties – dans la première partie, nous avons examiné les approches de conjugaison conduisant à la fonctionnalisation des nanomatériaux (Publication 1), et la formulation ultérieure des nanosondes (Publication 2). Dans la deuxième partie, nous avons étudié l'application des nanosondes pour la capture de TmiR dans le sérum humain (Publication 3).

Dans l‘objectif de la capture et la détection de TmiR, le design des nanosondes choisies reste le point de départ. Le choix du type de matériaux et des techniques analytiques disponibles, ainsi que la simplicité de la procédure et la stabilité appropriée du produit final, constituent la première étape menant à une synthèse réussie. Pour les méthodes de détection basées sur des nanomatériaux hybrides, il est assez courant de conjuguer à la surface des nanomatériaux soit des oligonucléotides d'ARN soit d'ADN dans une séquence complémentaire au TmiR ciblé. A ce titre, le choix de l'approche de conjugaison entre les nanomatériaux et la séquence complémentaire est essentiel. La liaison des nanomatériaux avec diverses biomolécules de ciblage peut se faire grâce à un large éventail de stratégies, et en raison de l'émergence relativement récente de la recherche sur le ciblage des miRs, elles n'ont pas encore toutes été mises en œuvre, laissant amplement d'espace pour des recherches approfondies. En effet, pour la détection des miRs, les approches de bioocnjugaison les plus fréquentes sont aussi les plus connues, à la fois en liaison covalente et en non covalente.

Dans la première publication, nous avons présenté les propriétés uniques des nanomatériaux les plus utilisés pour la détection des miRs. Les principales techniques analytiques fréquemment utilisées pour la caractérisation des nanomatériaux fonctionnalisés ont été développées, en mettant l'accent sur les approches de bioconjugaison, à la fois covalentes et non covalentes avec leurs avantages et inconvénients spécifiques.

Suite aux connaissances acquises sur les différentes approches de conjugaison, nous avons avancé vers la formulation de nos nanosondes magnétiques.

La fonctionnalisation des nanomatériaux peut parfois être difficile car divers facteurs doivent être pris en considération. Pour la synthèse de nanosondes pour la capture de miRs, les facteurs peuvent être les suivants: groupements réactifs disponibles sur la surface, stabilité colloïdale, méthode de caractérisation fiable pour la fonctionnalisation, efficacité et reproductibilité de la procédure et capacité de capture résultante du produit synthétisé. Ici, nous avons présenté une formulation en deux étapes de nanosondes magnétiques pour la capture de TmiR. Le cœur des nanosondes était basé sur des SPIONs, des nanoparticules d'oxyde de fer superparamagnétiques, qui sont colloïdalement stables après que leur surface soit recouverte de chaînes PEG. L'utilisation d'une chaîne PEG avec une modification appropriée permet une variété possible d'approches de conjugaison puisque son extrémité libre peut être modifiée avec divers groupes fonctionnels, lui permettant de se lier à la séquence complémentaire des miRs (CmiR) et de former la nanosonde. Avec à la fois la chaîne PEG biotinylée et le CmiR biotinylé, l'utilisation d'interactions streptavidine-biotine et la présence de streptavidine comme linker ont permis un habillage idéal de la surface des SPIONs PEGylées, garantissant de nombreux points d’attache pour les CmiRs. Il en est résulté une approche en deux étapes: la saturation de la surface des SPIONs PEGylées avec de la streptavidine, puis une fonctionnalisation ultérieure avec du CmiR-155 biotinylé (complémentaire du TmiR-155). Ce travail est présenté dans la deuxième publication. Il était tout aussi important de trouver un moyen de vérifier que chaque étape de la synthèse a été effectuée de manière adéquate. Cela a été réalisé en choisissant la chromatographie liquide à haute performance par exclusion de taille (SE HPLC) comme méthode d'analyse indirecte. La SE HPLC a permis l'analyse de la solution après la purification des SPIONs par séparation magnétique. Cela a fourni une méthode simple pour contrôler la synthèse des nanosondes en confirmant chaque étape. De même, il a été possible de déterminer à la fois la concentration de CmiR lié aux nanosondes et la concentration de TmiR capturé, ainsi que l'estimation du nombre de séquences liées par nanosonde. Une nanosonde a été recouverte en moyenne de

22 CmiR et a pu capturer 18 TmiR à partir d‘une solution de TmiR à la concentration de 5 µM. La stabilité colloïdale a été évaluée en mesurant leur diamètre hydrodynamique (DH) et leur potentiel zêta (ZP) - les nanosondes résultantes avaient une taille d'environ 70 nm et une ZP presque neutre.

Suite à la formulation de nanosondes magnétiques fonctionnalisées pour la capture de TmiR-155, l'étape suivante consistait à tester la fonctionnalisation avec une nouvelle séquence complémentaire et la capture de différents TmiR. L'objectif consistait à fonctionnaliser la surface des nanosondes avec une séquence d'ADN complémentaire (ADNc-484) du TmiR-484. Cette étude est présentée dans la troisième publication, où la formulation précédemment décrite pour les nanosondes avec des CmiR-155 a été utilisée. Puis la confirmation de capture des TmiR dans des solutions modèles a été étudiée. L'efficacité de la capture s'est avérée augmentée à des concentrations plus faibles, présentant des perspectives encourageantes pour la capture des miRs dans du sérum humain. L'utilisation de la séparation magnétique comme méthode de purification a permis la reconcentration des nanosondes, soutenant l'idée d'insérer un volume plus petit et concentré de nanosondes dans un plus grand volume de fluides biologiques. De même, les nanosondes se sont avérées stables dans le sérum humain, malgré l’absorption des protéines sériques à la surface des nanosondes. La confirmation des capacités de capture des nanosondes a été analysée par réaction quantitative en chaîne de la polymérase de transcription inverse (qRT-PCR). Les nanosondes ont prouvé leur capacité de capture dans le sérum dopé avec des TmiR-484. Le dernier point était d'examiner une méthode de déshybridation des TmiR captés à la surface des nanosondes. Après chauffage, une concentration notable de TmiR était à nouveau présente dans la solution purifiée.

Dans l'ensemble, les nanosondes ont démontré leur capacité à capturer les miR cibles dans des échantillons biologiques, avec le potentiel d'améliorer la détection de miRs dont les niveaux d'expression peuvent être dérégulés.

En raison de la nouveauté du sujet dans notre équipe, il reste de nombreuses questions à répondre concernant les différentes étapes des protocoles présentés. Alors que la formulation de nanosondes est composée de deux étapes relativement simples, et que la deuxième étape de la fonctionnalisation ouvre la porte à un large éventail de possibilités, puisque nous avons démontré que le CmiR ou l'ADNc peuvent être utilisés. Il serait intéressant d'étudier la fonctionnalisation avec différentes séquences, avec des modifications

et des structures modifiées. De même, le nombre de miRs en surface des nanosondes et la concentration de la suspension de nanosondes doivent être adaptées si nécessaire. En conséquence, le contrôle de la formulation via SE HPLC pourrait être affinée pour des concentrations plus faibles si nécessaire. De plus, d'autres techniques analytiques (telles que la spectrométrie photoélectronique à rayons X) peuvent être à considérer comme des options intéressantes, en fonction du temps et de l'équipement disponibles.

Le plus intéressant serait l'optimisation de l'efficacité de la capture de TmiR dans des échantillons biologiques, tels que le sérum humain, et sa reconcentration ultérieure. Nos résultats rapportés sont principalement des expériences préliminaires sur la stabilité et les capacité de capture des nanosondes dans le sérum via la qRT-PCR. Le protocole utilisé est composé de plusieurs étapes qui nécessitent un examen plus approfondi. L'insertion de nanosondes concentrées dans le sérum s'est avérée influer sur le rendement du miR extrait, et de même, le TmiR enrichi s'est avéré instable dans le sérum. Des ajustements à la fois sur la préparation de l'échantillon et sur le protocole d'extraction doivent être envisagés pour obtenir des résultats cohérents. De plus, les expériences rapportées ont été réalisées dans du sérum de patients sains dont les niveaux d'expression du TmiR ciblé n'étaient pas dérégulés. Il serait donc intéressant d'étudier les capacités des nanospndes développées dans des échantillons sériques de patients atteints de cancer.

De plus, les TmiRs captés doivent être correctement quantifiés, ainsi que les TmiR libérés par les nanosondes dans le processus de déshybridation. La déshybridation elle-même doit être considérée en parallèle de la reconcentration des TmiR, et les protocoles de déshybridation nécessitent une enquête approfondie concernant leur efficacité par rapport aux nanosondes formulées. Dans l'ensemble, cette étude représente une base pour le concept de nanosondes magnétiques fonctionnelles qui peuvent être insérées dans des fluides biologiques pour capter spécifiquement les TmiR choisis et permettre leur reconcentration pour une détection plus sensible. Étant donné que les nanomatériaux fonctionnalisés sont récemment devenus des outils de choix pour l'amélioration des techniques analytiques et des méthodes de détection pour cibler les miRs, les recherches futures dans ce domaine regorgent de possibilités et de questions auxquelles il reste à répondre.

Literature

1. Gessner, I.; Fries, J.W.U.; Brune, V.; Mathur, S. Magnetic Nanoparticle-Based Amplification of MicroRNA Detection in Body Fluids for Early Disease Diagnosis. *J. Mater. Chem. B* **2021**, *9*, 9–22, doi:10.1039/d0tb02165b.

2. Janko, C.; Ratschker, T.; Nguyen, K.; Zschiesche, L.; Tietze, R.; Lyer, S.; Alexiou, C. Functionalized Superparamagnetic Iron Oxide Nanoparticles (SPIONs) as Platform for the Targeted Multimodal Tumor Therapy. *Front. Oncol.* **2019**, *9*, 1–9, doi:10.3389/fonc.2019.00059.

3. Xiao, Y. Superparamagnetic Nanoparticles for Biomedical Applications. *J. Mater. Chem. B* **2020**, *8*, 354–367, doi:10.1039/c9tb01955c.

4. Hervé, K.; Douziech-Eyrolles, L.; Munnier, E.; Cohen-Jonathan, S.; Soucé, M.; Marchais, H.; Limelette, P.; Warmont, F.; Saboungi, M.L.; Dubois, P.; et al. The Development of Stable Aqueous Suspensions of PEGylated SPIONs for Biomedical Applications. *Nanotechnology* **2008**, *19*, doi:10.1088/0957-4484/19/46/465608.

5. Herve, K.; Allard-vannier, E.; Joubert, N.; Lakhrif, Z.; Alric, C.; Martin, C.; Dimier-poisson, I.; Aubrey, N.; Chourpa, I. Impact of Site-Speci Fi c Conjugation of ScFv to Multifunctional Nanomedicines Using Second Generation Maleimide. **2018**, doi:10.1021/acs.bioconjchem.8b00091.

6. Hermanson, G.T. *Bioconjugate Techniques: Third Edition*; Audet, J., Preap, M., Eds.; Elsevier, 2013; ISBN 9780123822390.

7. Lillo, A.M.; Lopez, C.L.; Rajale, T.; Yen, H.J.; Magurudeniya, H.D.; Phipps, M.L.; Balog, E.R.M.; Sanchez, T.C.; Iyer, S.; Wang, H.L.; et al. Conjugation of Amphiphilic Proteins to Hydrophobic Ligands in Organic Solvent. *Bioconjug. Chem.* **2018**, *29*, 2654–2664, doi:10.1021/acs.bioconjchem.8b00354.

8. Amaral, G.; Bushee, J.; Cordani, U.G.; KAWASHITA, K.; Reynolds, J.H.; ALMEIDA, F.F.M.D.E.; de Almeida, F.F.M.; Hasui, Y.; de Brito Neves, B.B.; Fuck, R.A.; et al. *Applications of Nanocomposite Materials in Drug Delivery*; 2013; Vol. 369; ISBN 9789896540821.

9. Yao, Y.; Zhang, H.; Tian, T.; Liu, Y.; Zhu, R.; Ji, J.; Liu, B. Iodide-Modified Ag Nanoparticles Coupled with DSN-Assisted Cycling Amplification for Label-Free and Ultrasensitive SERS Detection of MicroRNA-21. *Talanta* **2021**, *235*, doi:10.1016/j.talanta.2021.122728.

10. Yazdanparast, S.; Benvidi, A.; Azimzadeh, M.; Tezerjani, M.D.; Ghaani, M.R. Experimental and Theoretical Study for MiR-155 Detection through Resveratrol Interaction with Nucleic Acids Using Magnetic Core-Shell Nanoparticles. *Microchim. Acta* **2020**, *187*, doi:10.1007/s00604-020-04447-9.

11. Horny, M.C.; Gamby, J.; Dupuis, V.; Siaugue, J.M. Magnetic Hyperthermia on γ-Fe2O3@SiO2 Core-Shell Nanoparticles for Mi-RNA 122 Detection. *Nanomaterials* **2021**, *11*, 1–15, doi:10.3390/nano11010149.

12. Salimi, A.; Kavosi, B.; Navaee, A. Amine-Functionalized Graphene as an Effective Electrochemical Platform toward Easily MiRNA Hybridization Detection. *Meas. J. Int. Meas. Confed.* **2019**, *143*, 191–198, doi:10.1016/j.measurement.2019.05.008.

13. Xu, W.; Zhao, A.; Zuo, F.; Khan, R.; Hussain, H.M.J.; Chang, J. Au@Ag Core-Shell Nanoparticles for MicroRNA-21 Determination Based on Duplex-Specific Nuclease Signal Amplification and Surface-Enhanced Raman Scattering. *Microchim. Acta* **2020**, *187*, doi:10.1007/s00604-020-04330-7.

14. Gessner, I.; Yu, X.; Jüngst, C.; Klimpel, A.; Wang, L.; Fischer, T.; Neundorf, I.; Schauss, A.C.; Odenthal, M.; Mathur, S. Selective Capture and Purification of MicroRNAs and Intracellular Proteins through Antisense-Vectorized Magnetic Nanobeads. *Sci. Rep.* **2019**, *9*, 1–10, doi:10.1038/s41598-019-39575-7.

15. Mehdipour, M.; Gloag, L.; Bennett, D.T.; Hoque, S.; Pardehkhorram, R.; Bakthavathsalam, P.; Gonçales, V.R.; Tilley, R.D.; Gooding, J.J. Synthesis of Gold-Coated Magnetic Conglomerate Nanoparticles with a Fast Magnetic Response for Bio-Sensing. *J. Mater. Chem. C* **2021**, *9*, 1034–1043, doi:10.1039/d0tc04702c.

16. Wang, H.; Tang, H.; Yang, C.; Li, Y. Selective Single Molecule Nanopore Sensing of MicroRNA Using PNA Functionalized Magnetic Core-Shell Fe3O4-Au Nanoparticles. *Anal. Chem.* **2019**, *91*, 7965–7970, doi:10.1021/acs.analchem.9b02025.

17. Li, H.; Cai, Q.; Yan, X.; Jie, G.; Jie, G. Ratiometric Electrochemical Biosensor Based on Silver Nanoparticles Coupled with Walker Amplification for Sensitive Detection of MicroRNA. *Sensors Actuators B Chem.* **2022**, *353*, 131115, doi:10.1016/j.snb.2021.131115.

18. Wei, S.; Chen, G.; Jia, X.; Mao, X.; Chen, T.; Mao, D.; Zhang, W.; Xiong, W. Exponential Amplification Reaction and Triplex DNA Mediated Aggregation of Gold Nanoparticles for Sensitive Colorimetric Detection of MicroRNA. *Anal. Chim. Acta* **2020**, *1095*, 179–184, doi:10.1016/j.aca.2019.10.020.

19. Borghei, Y.S.; Hosseini, M.; Ganjali, M.R. A Label-Free Luminescent Light Switching System for MiRNA Detection Based on Two Color Quantum Dots. *J. Photochem. Photobiol. A Chem.* **2020**, *391*, 112351, doi:10.1016/j.jphotochem.2019.112351.

20. Afzalinia, A.; Mirzaee, M. Ultrasensitive Fluorescent MiRNA Biosensor Based on a "Sandwich" Oligonucleotide Hybridization and Fluorescence Resonance Energy Transfer Process Using an Ln(III)-MOF and Ag Nanoparticles for Early Cancer Diagnosis: Application of Central Composite Design. *ACS Appl. Mater. Interfaces* **2020**, *12*, 16076–16087, doi:10.1021/acsami.0c00891.

21. Bao, J.; Hou, C.; Zhao, Y.; Geng, X.; Samalo, M.; Yang, H.; Bian, M.; Huo, D. An Enzyme-Free Sensitive Electrochemical MicroRNA-16 Biosensor by Applying a Multiple Signal Amplification Strategy Based on Au/PPy–RGO Nanocomposite as a Substrate. *Talanta* **2019**, *196*, 329–336, doi:10.1016/j.talanta.2018.12.082.

22. Sun, Y.; Li, T. Composition-Tunable Hollow Au/Ag SERS Nanoprobes Coupled with Target-Catalyzed Hairpin Assembly for Triple-Amplification Detection of MiRNA. *Anal. Chem.* **2018**, *90*, 11614–11621, doi:10.1021/acs.analchem.8b03067.

23. Gao, Y.; Yu, H.; Tian, J.; Xiao, B. Nonenzymatic DNA-Based Fluorescence Biosensor Combining Carbon Dots and Graphene Oxide with Target-Induced DNA Strand Displacement for MicroRNA Detection. *Nanomaterials* **2021**, *11*, doi:10.3390/nano11102608.

24. Zhou, L.; Wang, T.; Bai, Y.; Li, Y.; Qiu, J.; Yu, W.; Zhang, S. Dual-Amplified Strategy for Ultrasensitive Electrochemical Biosensor Based on Click Chemistry-Mediated Enzyme-Assisted Target Recycling and Functionalized Fullerene Nanoparticles in the Detection of MicroRNA-141. *Biosens. Bioelectron.* **2020**, *150*, doi:10.1016/j.bios.2019.111964.

25. Liu, L.; Wei, Y.; Jiao, S.; Zhu, S.; Liu, X. A Novel Label-Free Strategy for the Ultrasensitive MiRNA-182 Detection Based on MoS 2 /Ti 3 C 2 Nanohybrids. *Biosens. Bioelectron.* **2019**, *137*, 45–51, doi:10.1016/j.bios.2019.04.059.

26. Borghei, Y.S.; Hosseini, M. A New Eye Dual-Readout Method for MiRNA Detection Based on Dissolution of Gold Nanoparticles via LSPR by CdTe QDs Photoinduction. *Sci. Rep.* **2019**, *9*, 1–9, doi:10.1038/s41598-019-41898-4.

27. Zhu, Q.; Li, H.; Xu, D. Sensitive and Enzyme-Free Fluorescence Polarization Detection for MiRNA-21 Based on Decahedral Sliver Nanoparticles and Strand Displacement Reaction. *RSC Adv.* **2020**, *10*, 17037–17044, doi:10.1039/d0ra01950j.

28. Studzińska, S.; Buszewski, B. Analysis of MicroRNA and Modified Oligonucleotides with the Use of Ultra High Performance Liquid Chromatography Coupled with Mass Spectrometry. *J. Chromatogr. A* **2018**, *1554*, 71–80, doi:10.1016/j.chroma.2018.04.037.

29. Qi, T.; Song, C.; He, J.; Shen, W.; Kong, D.; Shi, H.; Tan, L.; Pan, R.; Tang, S.; Lee, H.K. Highly Sensitive Detection of Multiple MicroRNAs by High-Performance Liquid Chromatography Coupled with Long and Short Probe-Based Recycling Amplification. *Anal. Chem.* **2020**, *92*, 5033–5040, doi:10.1021/acs.analchem.9b05301.

30. Pan, L.; Zhang, H.; Zhao, J.; Li, X.; Xu, R.; Mo, Y.; Paul, B.; Liu, Y.; St, S. A Highly Sensitive and Selective Signal-on Strategy for MicroRNA Quantification. *Anal Chim Acta* **2021**, 258–266, doi:10.1016/j.aca.2019.12.003.A.

31. Lee, T.; Mohammadniaei, M.; Zhang, H.; Yoon, J.; Choi, H.K.; Guo, S.; Guo, P.; Choi, J.W. Single Functionalized PRNA/Gold Nanoparticle for Ultrasensitive MicroRNA Detection Using Electrochemical Surface-Enhanced Raman Spectroscopy. *Adv. Sci.* **2020**, *7*, doi:10.1002/advs.201902477.

32. Chan, H.N.; Ho, S.L.; He, D.; Li, H.W. Direct and Sensitive Detection of Circulating MiRNA in Human Serum by Ligase-Mediated Amplification. *Talanta* **2020**, *206*, 120217, doi:10.1016/j.talanta.2019.120217.

33. Tian, B.; Han, Y.; Wetterskog, E.; Donolato, M.; Hansen, M.F.; Svedlindh, P.; Strömberg, M. MicroRNA Detection through DNAzyme-Mediated Disintegration of Magnetic Nanoparticle Assemblies. *ACS Sensors* **2018**, *3*, 1884–1891, doi:10.1021/acssensors.8b00850.

34. Cheng, W.; Ma, J.; Cao, P.; Zhang, Y.; Xu, C.; Yi, Y.; Li, J. Enzyme-Free Electrochemical Biosensor Based on Double Signal Amplification Strategy for the Ultra-Sensitive Detection of Exosomal MicroRNAs in Biological Samples. *Talanta* **2020**, *219*, 121242, doi:10.1016/j.talanta.2020.121242.

35. Pereira, G.; Monteiro, C.A.P.; Albuquerque, G.M.; Pereira, M.I.A.; Cabrera, M.P.; Cabral Filho, P.E.; Pereira, G.A.L.; Fontesa, A.; Santos, B.S. (Bio)Conjugation Strategies Applied to Fluorescent Semiconductor Quantum Dots. *J. Braz. Chem. Soc.* **2019**, *30*, 2536–2560, doi:10.21577/0103-5053.20190163.

36. Su, X.; Wu, Y.J.; Robelek, R.; Knoll, W. Surface Plasmon Resonance Spectroscopy and Quartz Crystal Microbalance Study of Streptavidin Film Structure Effects on Biotinylated DNA Assembly and Target DNA Hybridization. *Langmuir* **2005**, *21*, 348–353, doi:10.1021/la047997u.

37. Nguyen, P.V.; Hervé-Aubert, K.; David, S.; Lautram, N.; Passirani, C.; Chourpa, I.; Aubrey, N.; Allard-vannier, E. Targeted Nanomedicine with Anti-EGFR ScFv for SiRNA Delivery into Triple Negative Breast Cancer Cells. **2020**, *157*, 74–84, doi:10.1016/j.ejpb.2020.10.004.

38. Shen, Z.; He, L.; Wang, W.; Tan, L.; Gan, N. Highly Sensitive and Simultaneous Detection of MicroRNAs in Serum Using Stir-Bar Assisted Magnetic DNA Nanospheres-Encoded Probes. *Biosens. Bioelectron.* **2020**, *148*, 111831, doi:10.1016/j.bios.2019.111831.

39. Leong, S.S.; Yeap, S.P.; Lim, J.K. Working Principle and Application of Magnetic Separation for Biomedical Diagnostic at High- and Low-Field Gradients. *Interface Focus* **2016**, *6*, doi:10.1098/rsfs.2016.0048.

40. Kroh, E.M.; Parkin, R.K.; Mitchell, P.S.; Tewari, M. Analysis of Circulating MicroRNA Biomarkers in Plasma and Serum Using Quantitative Reverse Transcription-PCR (QRT-PCR). *Methods* **2010**, *50*, 298–301, doi:10.1016/j.ymeth.2010.01.032.

41. Junqueira-Neto, S.; Batista, I.A.; Costa, J.L.; Melo, S.A. Liquid Biopsy beyond Circulating Tumor Cells and Cell-Free DNA. *Acta Cytol.* **2019**, *63*, 479–488, doi:10.1159/000493969.

42. Gooding, J.J.; Gaus, K. Single-Molecule Sensors : Challenges and Opportunities for Quantitative Analysis Angewandte. **2016**, 11354–11366, doi:10.1002/anie.201600495.

43. Wang, M.; Chen, W.; Tang, L.; Yan, R.; Miao, P. Duplex-Specific Nuclease Assisted MiRNA Assay Based on Gold and Silver Nanoparticles Co-Decorated on Electrode Interface. *Anal. Chim. Acta* **2020**, *1107*, 23–29, doi:10.1016/j.aca.2020.01.041.

44. Shagin, D.A.; Rebrikov, D. V; Kozhemyako, V.B.; Altshuler, I.M.; Shcheglov, A.S.; Zhulidov, P.A.; Bogdanova, E.A.; Staroverov, D.B.; Rasskazov, V.A.; Lukyanov, S. A Novel Method for SNP Detection Using a New Duplex-Specific Nuclease From Crab Hepatopancreas. **2002**, 1935–1942, doi:10.1101/gr.547002.1.

45. Wang, X.; Lim, H.J.; Son, A. Characterization of Denaturation and Renaturation of DNA for DNA Hybridization. *Environ. Health Toxicol.* **2014**, *29*, 1–8, doi:http://dx.doi.org/10.5620/eht.2014.29.e2014007.

CURRICULUM VITAE

Iveta VILÍMOVÁ

Date of birth: 6. 4. 1994

Email address: vilimovai4@gmail.com Vilimova.I@seznam.cz

Educational history

- October 2019 – December 2022
  Université de Tours (Doctoral programme)
- September 2017 – June 2019
  University Palacký Olomouc: Nanotechnology (Master degree programme)
- September 2014 – June 2017
  University Palacký Olomouc: Nanotechnology (Bachelor degree programme)

Employment history

- October 2019 – October 2022
  PhD candidate at Université de Tours, France
- March 2017 – March 2018
  Lab assistant at Joint Laboratory of Optics, Palacký University Olomouc and Institute of Physics of Academy of Sciences of the Czech Republic

Research experience

- PhD thesis: *Development of nanoprobes for detection and quantification of miRNA*
- Supervisor: Katel Hervé-Aubert, Co-Supervisor: Igor Chourpa
  (Published 2022)
- Master thesis: *Properties of the nanoparticles prepared by seeded-growth method and their interaction with a protein*
  Supervisor: Assoc. Prof. RNDr. Karolína Machalová Šišková, Ph.D.
  (Published 2019)
- Bachelor thesis: *Interferometric measurement of the shape of optical surfaces*
  Supervisor: RNDr. Pavel Pavlíček, Ph.D. (Published 2017)

Techniques and skills:

- Synthesis of superparamagnetic nanoparticles,
- synthesis of core-shell Au-Ag nanoparticles,
- characterization of NPs colloidal properties (DLS, ZetaSizer),
- Size-exclusion chromatography, HPLC,
- Electrophoresis on gels,
- analytical methods (UV-vis, FT-IR, AAS),
- DNA and RNA extraction, qRT-PCR.

Teaching experience:

- 2016 – 2018
  Leader of seminars *White-light interferometry* and *Construction of interferometers*
  Joint International Physics Summer School

Publications

- **Distinctly Different Morphologies of Bimetallic Au-Ag Nanostructures and Their Application in Submicromolar SERS-Detection of Free Base Porphyrin**
  Iveta Vilímová and Karolína Šišková
  Nanomaterials, 2021, https://doi.org/10.3390/nano11092185

- **Two-step formulation of magnetic nanoprobes for microRNA capture**
  Iveta Vilímová, Igor Chourpa, Stéphanie David, Martin Soucé and Katel Hervé-Aubert
  RSC Advances, 2022, https://doi.org/10.1039/D1RA09016J

- **Formation of miRNA nanoprobes – conjugation approaches leading to the functionalization**
  Iveta Vilímová, Katel Hervé-Aubert, and Igor Chourpa
  Molecules, 2022, https://doi.org/10.3390/molecules27238428

Communications

- 14èmes journées Cancéropôle Grand Ouest – 26 and 27 October 2020 - Angers
  Poster: **Development of nanoprobes for detection and quantification of miRNA**
  Authors: Iveta Vilímová, Stéphanie David, Igor Chourpa, Katel Hervé-Aubert

- 15èmes journées Cancéropôle Grand Ouest – 1st and 2nd July 2021 - Angers
  Poster: **Development of nanoprobes for miRNA targeting using streptavidin-biotin interactions**
  Authors: Iveta Vilímová, Igor Chourpa, Martin Soucé, Katel Hervé-Aubert

- 4th NANOMED EMJMD's workshop, 7 - 9 July 2021 - Angers
  Poster: **Design and synthesis of nanoprobes for miRNa detection**
  Authors: Iveta Vilímová, Igor Chourpa, Martin Soucé, Katel Hervé-Aubert

- 33e Colloque Biotechnocentre – 7 and 8 October 2021 – Center Parcs Sologne
  Poster: **Design and synthesis of nanoprobes for miRNa targeting using streptavidin-biotin interactions**
  Authors: Iveta Vilímová, Igor Chourpa, Katel Hervé-Aubert

- 2021 SFNano Annual Meeting – 6 to 8 December– Angers
  Poster: **miRNa nanoprobes: easy formulation using streptavidin-biotin interactions**
  Authors: Iveta Vilímová, Igor Chourpa, Katel Hervé-Aubert

- 16èmes Journées du Cancéropôle Grand Ouest - 23 and 24 June 2022 – Angers
  Poster: **Two-step formulation of magnetic nanoprobes for microRNA capture**
  Authors: Iveta Vilímová, Stéphanie David, Igor Chourpa, Martin Soucé, Katel Hervé-Aubert
  2nd Award for the best Poster

Other skills

Languages: Czech (native), English (oral and written fluency, FCE at C1 level), Spanish (A2), French (B1)

Software: Microsoft Office (Word, Excel, PowerPoint...), reference software, various software used for lab work, proficient in internet research

Driving license

References

Prof. Igor Chourpa

EA 6295 Nanomédicaments et Nanosondes

URF des Sciences Pharmaceutiques

31 Avenue Monge, 37 200 Tours, France

Tel: +33 (0)2 47 36 71 62

Mail: igor.chourpa@univ-tours.fr

Dr. Katel Hervé Aubert

EA 6295 Nanomédicaments et Nanosondes

URF des Sciences Pharmaceutiques

31 Avenue Monge, 37 200 Tours, France

Tel: +33 (0)2 47 36 71 57

Mail: katel.herve@univ-tours.fr

Doc. Karolína Šišková

Department of Experimental Physics

Šlechtitelů 27, 783 71 Olomouc, Czech Republic

Tel: +420 58 563 4175

Mail: karolina.machalova@upol.cz

Dr. Pavel Pavlíček

Joint Laboratory of Optics

17. listopadu 50A, 772 07 Olomouc, Czech Republic

Tel: +420 58 563 1680

Mail: Pavel.Pavlicek@upol.cz

Iveta VILÍMOVÁ

EA6295 NMNS
Nanomédicaments
et Nanosondes

Développement de nanosondes pour la détection de miARN dans des fluides biologiques

Résumé

Ces travaux de thèse de doctorat décrivent la préparation de nanosondes magnétiques pour améliorer la détection des miARN quelle que soit la technique analytique. Les travaux sont organisés selon deux principaux objectifs : i) formulation et caractérisation de nanosondes conçues pour capter des miARN cibles : TmiR-155, un biomarqueur du cancer du sein et TmiR-484, un biomarqueur du cancer colorectal, et ii) validation des protocoles de capture médiée par les nanosondes de TmiR-484 dans des échantillons biologiques. Les nanosondes sont à base de nanoparticules d'oxyde de fer superparamagnétiques - SPIONs, avec une couche de polyéthylène glycol (PEG) liée de façon covalente et portant à leur extrémité un groupement biotine. Par l'utilisation de SPIONs PEGylées comme précurseur, les nanosondes ont été formulées en deux étapes : i) modification de la surface des SPIONs PEGylées avec de la streptavidine, et ii) fonctionnalisation avec une séquence de nucléotides biotinylés, CmiR-155 ou cDNA-484, qui sont complémentaires aux miRs cibles, TmiR-155 ou TmiR-484 respectivement. Le tri magnétique a été utilisé comme méthode de purification, séparant les nanosondes de divers milieux et permettant leur reconcentration. La stabilité colloïdale a été évaluée en mesurant leur diamètre hydrodynamique (DH) et leur potentiel zêta (ZP). La principale méthode d'analyse utilisée pour suivre les étapes de formulation et la concentration de miR greffé est la chromatographie liquide haute performance par exclusion de taille (SE HPLC). Le nombre estimé de séquences nucléotidiques greffées par nanosonde est de 22 pour CmiR-155 et de 17 pour l'ADNc-484. Les nanosondes résultantes ont une taille d'environ 70 nm et un ZP proche de la neutralité. Les nanosondes sont restées colloïdalement stables après incubation dans des échantillons de sérum humain pendant 12 heures. Les nanosondes ont été testées pour leur efficacité de capture des deux TmiR dans une solution modèle à différentes concentrations, et le TmiR-484 a également été capté dans des échantillons de sérum humain de volontaires adultes sains, résultats confirmés par une analyse qRT-PCR. Dans l'ensemble, le potentiel de capture des miARN cibles dans des échantillons biologiques encourage l'utilisation future des nanosondes pour améliorer la détection d'une expression dérégulée des miARN.

Mots clés: nanosondes, miARN, conjugaison, fonctionnalisation, isolation de miR, sérum humain

Abstract

This PhD thesis addresses the sample preparation of magnetic nanoprobes that would enable the improvement of miRNA detection by any analytical technique. The work is organized following the two main objectives: i) formulation and characterization of nanoprobes designed to capture target miRNA, TmiR-155, a biomarker of breast cancer, and TmiR-484, a biomarker for colorectal cancer, and ii) validation of protocols for nanoprobes-mediated capture of TmiR-484 in biological samples. The nanoprobes were based on Superparamagnetic Iron Oxide Nanoparticles - SPIONs, with a shell of covalently bound polyethylene glycol (PEG) carrying biotin at the opposite terminal group. Using the PEGylated SPIONs as a precursor, the nanoprobes were formulated in two steps: i) surface modification of the PEGylated SPIONs with streptavidin, and ii) functionalization with a biotinylated nucleotide sequence, either CmiR-155 or cDNA-484, which are complementary to the target miR, TmiR-155 or TmiR-484 respectively. Magnetic sorting was used as a purification method, separating nanoprobes from various media and allowing their reconcentration. The colloidal stability was assessed by measuring their hydrodynamic diameter (DH) and zeta potential (ZP). The main analytical method used for monitoring the formulation steps and the miR concentration was Size Exclusion High-Performance Liquid Chromatography (SE HPLC). The estimated number of nucleotide sequences grafted per nanoprobe was 22 for CmiR-155, and 17 for cDNA-184. The resulting nanoprobes had a size of about 70 nm and nearly neutral ZP. The nanoprobes remained colloidally stable after incubation in human serum samples for 12 hours. The nanoprobes were tested for their capture efficiency of both TmiRs in model solution at different concentrations, and TmiR-484 was also captured in human serum samples from healthy adult volunteers, which was confirmed by qRT-PCR analysis. Altogether, the potential to capture target miRNA in biological samples is encouraging the future use of nanoprobes to enhance the sensing of dysregulated levels of miRNA expression.

Keywords: nanoprobes, miRNA, conjugation, functionalization, miR isolation, human serum